Targeting the Microbiome by NLRP6 Deletion and the Development of Murine Alzheimer's Disease

Doctoral thesis

to obtain a doctorate (PhD)

from the Faculty of Medicine

of the University of Bonn

Tobias Dierkes

from Münster, Germany

2022

Written with authorization of

the Faculty of Medicine of the University of Bonn

First reviewer: Prof. Dr. Eicke Latz

Second reviewer: Prof. Dr. Michael Pankratz

Day of oral examination: 30. June 2022

From the Institute of Innate Immunity

Director: Prof. Dr. Eicke Latz

Table of Contents

List of Abbreviations

Abbreviation	
AD	Alzheimer's disease
Aim2	absent in melanoma 2
ALRs	(AIM2)-like receptors
ALS	amyotrophic lateral sclerosis
AMPs	antimicrobial peptides
APP	amyloid precursor protein
ASC	associated speck like proteins
ASV	amplicon sequence variant
Aβ	amyloid beta
BBB	blood-brain barrier
bp	base pare
CD	chow Diet
CLRs	C-type lectin-like receptors
CNS	central nervous system
CSF	cerebrospinal fluid
DAMPs	damage-associated molecular patterns
DE	differential expressed
DSS	dextran sulphate sodium
FA	formic acid
FACS	fluorescence-activated cell sorting
GSDMD	gasdermin D
HAMPs	homeostasis-altering molecular processes
HET	Haus für Experimentelle Therapie
IEC	intestinal epithelial cells
IL	interleukin
LPS	lipopolysaccharide
LRR	leucine-rich repeat
LTA	lipoteichoic acid

MAMPs	microbe-associated molecular pattern
MeX04^{+}	methoxy
MWM	Morris water maze
NBD	nucleotide-binding domain
Nf-kb	nuclear factor ’kappa-light-chain-enhancer’ of activated B cell
NFTs	neurofibrillary tangles
NLRs	(NOD)-like receptors
NOD	nucleotide-binding oligomerization domain
PAMPs	pathogen-associated molecular patterns
PCoA	principal coordinate analysis
PCR	polymerase chain reaction
PD	Parkinson’s disease
PFA	paraformaldehyde
PRRs	pathogen-recognition receptors
Pyd	pyrin domain
RIG-I	retinoic acid-inducible gene-I
RlRs	(RIG-I)-like receptors
RT-qPCR	transcriptase quantitative polymerase chain reaction
SEM	standard error of the mean
TLRs	toll-like receptors
WD	western diet
WT	wild-type

1 Introduction

1.1 Innate Immunity

In life humans and every other vertebrate, encounter multiple forms of organisms, including viruses, bacteria and fungi (Pradeu, 2020). Interactions can be neutral or even beneficial (Dethlefsen et al., 2007). However, if certain organisms spread and reproduce, the host can be threatened (Méthot and Alizon, 2014). The immune system is a network of biological processes and its primary focus is to interact with the surrounding and react accordingly. Risks can also arise from noninfectious, stress-induced tissue damage or tumorigenesis (Medzhitov, 2007). The immune system has multiple and highly effective mechanisms in place to prevent damage.

The most visible layer of defense is the physical and chemical barrier. It includes the skin and mucous membranes which create a mechanical barrier and forms a surface rendered unfavorable for microorganisms by the presence of antimicrobial peptides, lysozyme and other defense molecules. Furthermore, commensal microorganisms promote protection by competing against potential pathogens (Peterson and Artis, 2014; Spadoni et al., 2017). If the outer layer is breached cells of the innate immune system take over. Its specialized cells, such as macrophages, dendritic cells, monocytes, granulocytes and mast cells circulate within the body and recognize potential threats, resulting in clearance or an inflammatory response (Chaplin, 2010). Adding to the cells of the innate immune system are multiple other cell types in blood plasma as well as in interstitial fluids, that contribute to constitutive innate immune mechanisms (Paludan et al., 2020).

The variety of signals recognized by the innate immune system can be distinguished in three groups. First, pathogen-associated molecular patterns (PAMPs) including microbial-derived molecules that are highly conserved components of microorganisms and absent from host cells (Janeway, 1989). PAMP signals can be triggered by bacteria, fungi, parasites, self-antigens and viruses. A second class of signals are damage-

associated molecular patterns (DAMPs), structures that are only exposed for recognition as a result of tissue damage or infection (Gong et al., 2019). These structures cover a vast type of ligands, e.g. glycan structures, such as fucose, mannose, β-glucan and galactose. And lastly, homeostasis-altering molecular processes (HAMPs) are recognized. HAMPs refer to abnormally high or low rates of biological processes that might point to an infection. It is generally believed that the information about disrupted homeostasis is transmitted to the HAMP sensors through post-translational modifications (Liston and Masters, 2017).

Responsible for translating PAMPs, DAMPs and HAMPs into an intracellular signal are germ-line encoded pathogen-recognition receptors (PRRs). There are Toll-like receptors (TLRs), nucleotide-binding oligomerization domain (NOD)-like receptors (NLRs), retinoic acid-inducible gene-I (RIG-I)-like receptors (RLRs), C-type lectin-like receptors (CLRs), and absent in melanoma 2 (AIM2)-like receptors (ALRs) (Takeuchi and Akira, 2010). The activation of PRRs results in a protective inflammatory response releasing antimicrobial peptides and inflammatory mediators. Antimicrobial peptides act directly against extracellular microbes. Inflammatory mediators such as cytokines and chemokines recruit further immune cells that will contribute to the inflammatory response, a process known as inflammation (Jakubzick et al., 2017). However, if the pathogen is within the cell, intracellular killing pathways are in place to neutralize the threat e.g. by degradation in lysosomes (R. Medzhitov 2008). As last resort, cells can self-destruct by programmed cells death as an innate immune mechanism (Man et al., 2017). Following PRR activation and the inflammatory response is a resolution phase resulting in a homeostasis (Netea et al., 2017).

It can become problematic for the organism if the resolution phase is inhibited by unremovable danger signals or innate immune components that remain activated. Consequently, tissue disruption and malfunction are promoted and the immune response is no longer beneficial for the host. This state is known as chronic inflammation and has been associated with multiple non-communicable diseases such as Alzheimer's Disease, cardiovascular diseases, cancer, osteoporosis, arthritis, colitis or asthma (Schett and Neurath, 2018). The immune system is not only associated with

infections of foreign microorganisms, it also plays an important role in multiple physiological processes such as developmental and regeneration processes as well as the clearance of dead cells, (Pradeu, 2020). Furthermore, components of the host can be targeted which may lead to autoinflammatory (Dinarello, 2009) and autoimmune pathologies (Rosenblum et al., 2015).

1.1.1 Inflammasomes

As mentioned, the activation of PRRs results in inflammation. The discovery of an innate-immune receptor protein from the NLRP protein family and the adaptor protein ASC, assembled into an intracellular protein-complex that recruits and activates caspase 1, was made in 2002 (Martinon F. et al., 2002). This discovery of a macromolecular complex that senses PRRs and initiates the inflammatory response is a key finding in the field of innate immunity and cell death (Broz and Dixit, 2016). Similar to other innate immune signalling receptors, the inflammasome detects and responds to microorganisms and tissue damage (Newton and Dixit, 2012). So far, the NLRP3 inflammasome has been the main focus of the scientific community which is mainly studied in immune cells of the innate immune system. Recently, however, more and more studies focus on additional inflammasomes. For example, NLRP6, a comparatively less well understood inflammasome, detects microbial metabolites such as lipopolysaccharide (LPS) which is the major component of gram-negative bacteria cell walls (Zhao Y. & Shao F., 2015).

1.1.2 The NLRP6 Inflammasome

NLRP6 is a member of the NOD-like receptor family, originally termed PYPAF5. Functioning as a cytosolic innate immune sensor it can detect microbe-associated molecular patterns and activate the NLRP6 inflammasome. This inflammasome consists of associated speck like proteins (ASC) and the inflammatory caspase-1 or caspase-11. Inflammasome activation triggers the maturation and secretion of pro-

inflammatory cytokines IL-18 and IL-1b (Kayagaki N. et al., 2011). NLRP6 activity is crucial to maintain tissue homeostasis. Chronic and unbalanced activation can lead to multiple pathologies, especially gastrointestinal inflammatory, infectious and neoplastic diseases. It is assumed that NLRP6 acts within intestinal epithelial cells and thereby potentially influences the microbiome composition. However, the exact mechanism of NLRP6 activity and its contributions to health and disease have not been fully elucidated to date. (Kayagaki N. et al., 2011)

1.1.3 NLRP6 Inflammasome Assembly

The NLRP6 inflammasome consists of three domains. Considered to be the most important element for the inflammasome assembly is the N-terminus which is composed of a pyrin domain (PYD) that interacts with ASC (Shen C. el al., 2019). The central element of NLRP6 is the nucleotide-binding domain (NBD) which is followed by the C-terminal leucine-rich repeat (LRR) domain (Lamkanfi M. et al., 2014). The LLR domain interacts with DAMPs and Microbe-associated molecular pattern (MAMPs). Howeverm these MAMPs and DAMPs remain mostly unidentified to date (Elliott EI. et al., 2015).

Microbial and metabolic stimuli, Tumor necrosis factor-a (TNF-a) and viruses can activate the transcription of NLRP6 (Wang P. et al., 2015). However, miRNAs, such as the miRNA-331-3p, can inhibit translation after transcription (Nie H. et al., 2020). In the absence of inhibitory miRNAs, the mRNA is translated and the PYD domain forms filamentous structures through self-assembly. Conformational changes follow and enable the recruitment of ASC via PYD_PYD binding. The NBD domain of NLRP6 is most likely strengthening this process (Shen C. et al., 2019). A complex consisting of caspase-1 and nuclear factor ’kappa-light-chain-enhancer’ of activated B cell (NF-kB) becomes activated and the inflammasome response is triggered via the caspase-1-dependent cleavage of proIL-1ß and proIL-18 into their mature forms. However, only specific triggers can induce an assembly and the activation of the NLRP6 inflammasome (Grenier J.M. et al., 2002). Different activators, inhibitors and even

bacteria of different taxa were shown to regulate the NLRP6 formation (Hara H. et al., 2018). Especially microbial ligands such as lipopolysaccharide (LPS), MDP, iE-DAP, Pam3CSK4 and microbial metabolites, e.g. taurine, histamine and spermine seem to have an impact on NLRP6 assembly and activation (Lu W.L. et al., 2019 & Levy M. et al., 2015). Beyond bacterial products, NLRP6 also functions as a sensor for gram positive bacteria and viruses (Wang P. et al., 2015).

The NLRP6 proteins can be detected in the lung, kidney and liver. However, the highest expression is found in the gastrointestinal tract (Elinav E. et al., 2011 & Lech M. et al., 2010). Consequently, studies focus on the intestine to investigate NLRP6 functions in health and disease. Of note, studies have shown that NLRP6 can also impact the homeostasis of the oral cavity (Lu W.L. et al., 2019).

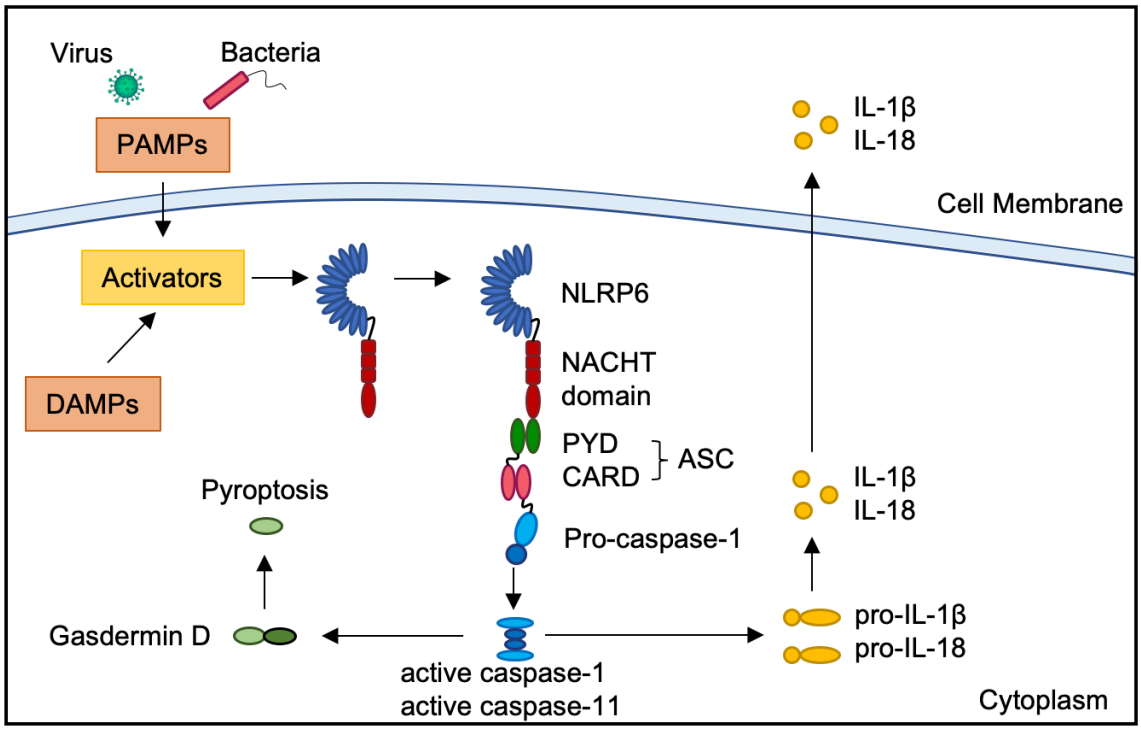

Figure 1.1 - NLRP6 Inflammasome Activation. Specific DAMPs and PAMPs including viruses and bacteria can induce the transcription and oligomerization of the different NLRP6 inflammasome sensor proteins. The adaptor ASC protein, consisting of a PYD and CARD domain, oligomerizes within the inflammasome and recruits pro-caspase-1. The active caspase-1 or caspase-11 cleaves the precursors of the pro-inflammatory cytokines IL-1ß and IL-18. Gasdermin D (GSDMD) can also be cleaved, which can produce pores in the plasma membrane. The active pro-inflammatory cytokines are released through those GSDMD pores. However, increased formation of GSDMD pores can induce cell swelling and pyroptotic cell death. Danping Zheng et al., 2020

1.2 NLRP6 in the Intestine

The mammalian intestine contains trillions of microorganisms, including bacteria, fungi, virus and parasites, collectively termed the microbiome. It mainly inhabits the mammalian intestinal mucosa and lumen and coevolved with the host. The symbiosis between host and the microbiome is critical. It is a fine and tightly regulated line between enabling critical functions conferred by the microbes and pathogenic events

such as an invasion of pathogens into the sterile host or uncontrolled inflammation directed against non-invading resident microbes. In steady state the immune system tolerates innocuous stimuli. However, invading pathogens can induce a potent immune response (Chu H. el al., 2013). Mammalian intestinal epithelial cells (IEC), including enterocytes and goblet cells, express high amounts of NLRP6 and therefore act as potential mediators between the host and the microbiome (Elinav E. et al., 2011). This has been shown in mice with Nlrp6 deletion which led to shifts within stool samples towards higher abundance of the bacterial family Prevotellaceae and phyla TM7 (Elinav E. et al., 2011). In addition, transferring this altered fecal microbiota to wild-type (WT) mice, in combination with higher susceptibility to dextran sulphate sodium (DSS), induced colitis (Elinav E. et al., 2011). Furthermore, the dysbiosis in Nlrp6 inflammasome-deficient mice also increases the susceptibility to colitis-induced carcinogenesis through the activation of IL-6 signaling in IEC (Hu B. et al., 2013).

Research is still in the early stages of revealing the molecular mechanism by which NLRP6-associated signaling modulates the gut microbiome. Currently available data suggest that the gut epithelial NLRP6 inflammasome and IL-18 secretion are modulated by commensal-derived metabolites. The downstream expression of antimicrobial peptides (AMPs) genes in the gut then shapes the host-microbiome (Levy M. et al., 2015). Metabolite-induced morphological alterations of intracellular connections might be involved during this modulation (Grosheva I. et al., 2020). Also, it has been shown that NLRP6 can bind to lipoteichoic acid (LTA) derived from Gram-positive bacteria and become activated (Hara H. et al., 2018). This sensing triggers caspase-1 and caspase-11 via ASC and subsequently leads to IL-1b and IL-18 maturation. NLRP6 monomers can also bind directly to LPS, a ligand typical for Gram-negative bacteria, resulting in NLRP6 oligomerization, the recruitment of ASC and the NLRP6 inflammasome assembly (Leng F. el al., 2020). Suggesting NLRP6 to be a potential LPS sensor after Gram-positive pathogen infection in vivo.

An additional cell type expressing NLRP6 are goblet cells within the intestine. NLRP6 might impact the mucus secretion in goblet cells via autophagy. This has been seen in Nlrp6-deficient mice, which showed impaired autophagy within the intestine and altered

secretion of mucus granules in goblet cells (Wlodarska M. et al., 2014). Furthermore, goblet cells located at the entrance to the colonic crypt may sense non-specific TLR ligands and activate NLRP6 intracellularly, leading to exocytosis and expelling bacteria. Again, this NLRP6 goblet cell function depends on an excessive administration of LPS (Birchenough GM. et al., 2016). Adding to the list of intestinal cell types expressing NLRP6 and thereby to the potential mediators of NLRP6 impacts on intestinal homeostasis are monocytes. DSS-induced injuries increase Nlrp6 expression in Ly6Chi inflammatory monocytes which induce IL-18 and TNF-a, hence controlling bacteria-driven inflammation (Seregin SS. et al., 2017). Other NLRP6 expressing cell types are colonic myofibroblasts and hematopoietic cells, which seem to support epithelial proliferation and self-renewal upon chronic injury (Normand S. et al., 2011 & Chen GY. et al., 2011).

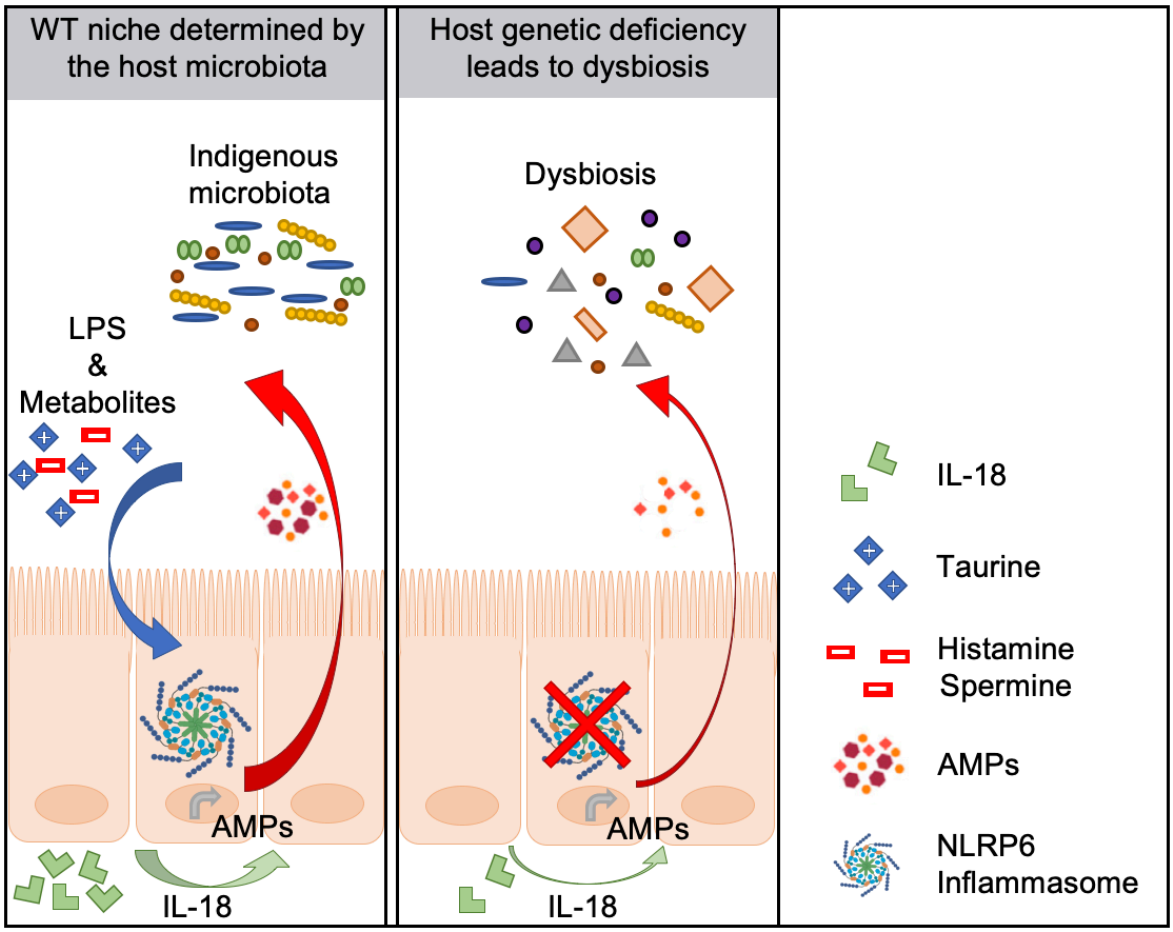

Figure 1.1.2 - NLRP6 in the Intestine. We suggest that NLRP6 in the gut can be modulated by commensal-derived metabolites (e.g. taurine, spermine and histamine). This leads to the production of mature IL-18 and unique antimicrobial peptide repertoires. This axis determines the host indigenous microbiome profile and vulnerability to intestinal inflammation. Adapted from Maayan Levy et al., 2015

1.2.1 Shaping the gut microbiome

As mentioned, the NLRP6 inflammasome might influence microbiome compositions within the host and a dysregulation of NLRP6 may cause dysbiosis (Elinav E. et al., 2011). However, not only the host genotype shapes the microbiome. Even more important for the modulation of gut microbial composition are environmental factors. Because the human gut microbiota has been linked to important determinants of health and disease, e.g. metabolism, immunity, development, behavior, it is necessary to understand the dynamic crosstalk between host and microbiome (Bäckhed F. et al.,

2015). This task is challenging since the human gut microbiota comprises ten times more cells than the human body and includes thousands of species of bacteria, viruses, fungi and protozoa. Moreover, the composition can vary significantly from person to person and can shift to some degree over time. For example, the microbiome can vary significantly when comparing populations from different continents. (De Filippo C. et al., 2010).

Environmental Factors:

Microbes can respond to various external stimuli according to their natural habitats, by sensing oxygen, thermal differences, virulence factors and metabolic machineries. Furthermore, microbial populations are under the various selection force from other microbes. Multiple studies have shown a role of diet and pharmacological factors, as well as contributions of many other external stimuli in shaping the gut microbiome (CS Chang et al., 2019). Some examples: the mother's microbiome is the foundation for an individual's microbiome as it is acquired during development and birth. Even a vaginal versus C-section delivery can have significantly different outcomes (Iizumi T. et al., 2017). Later in life, dietary habits can strongly influence the activities and composition of the gut microbiome (David LA, et al., 2014). Pharmacological factors, most prominently antibiotics, can affect the microbiome community depending on the class, dose, and length of exposure (Iizumi T. et al., 2017). Even social contacts can have effects (Tung J. et al., 2015). In general, the interaction with environmental factors can help to develop a healthy microbiome but on the other hand, they can also increase the risk for immune-mediated diseases.

Host Factors:

Host genetic factors might not be as important in the modulation of the gut microbiome as environmental factors, but the knowledge as to how host factors shape the gut microbiota could still provide opportunities to manipulate gut microbes and find potential applications to treat microbiome-related dieses.

For example, a strong indication for the relevance of host factors are derived from studies with twins. They showed that the microbiome of monozygotic twins is much more similar than the microbiome of genetically unrelated individuals (Zoetendal EG. et al., 2001). To date, multiple host genes have been identified as being associated with shaping the microbiome (Goodrich JK. et al., 2016), both in humans and mice (Benson AK. et al., 2010), e.g. NLRP6. Also, the innate immune system, in particular the epithelium associated factors, contributes to shaping the microbiome (Kurilshikov A. et al., 20017). The gut is an organ composed of multiple layers of tissue, containing epithelia which interact directly or indirectly with the gut microbiome. However, how host genes modulate the gut microbiota remains largely unknown (Koch L., 2015). Evidence in mouse models, supported by human data, suggests an involvement of the Nlrp6 inflammasome. Moreover, Nlrp6-dependent modulation of the microbiome may contribute to the initiation or progression of disease, possibly even of neurodegenerative disease. This makes NLRP6 a potential interesting target.

1.3 Bacterial infections of the Central Nervous System

The central nervous system (CNS) is a network of cells, forming the spinal cord and the brain. Some of the fundamental roles in bodily functions are for example the sensory input, information processing, motor outputs, awareness, behavior and memory. One of the most prominent brain disorders is Parkinson's disease (PD), discovered by James Parkinson in 1817. Patients with PD suffer from shaking, stiffness, difficulties with walking, balance and coordination (S. Sveinbiornsdottir et al., 2016). Back in the day, Parkinson dosed a patient with a laxative and noticed, after the bowels were empty, less symptoms of PD (C. Willyard, 2021). Much later, in 2006, Jane Foster noticed a changed behavior of mice without gut bacteria, compared to mice with a healthy selection of microorganisms (K. M. Neufeld et al., 2011). And in 2013 the first connections have been made between dysbiosis and autism (Hsiao et al., 2013), also antibodies again perodonal bacteria seem to be elevated in Alzheimer's disease (AD) patients when compared to age matched controls (Naseer et al., 2013).

Since then, functions of the gut microbiome are increasingly investigated in association with the CNS. For example, researchers have been trying to identify specific microbes associated with brain function, and to map out pathways that connect them to the brain.

1.3.1 The Gut-Brain Link

One of the major questions is still, how gut microbes interact with the brain in a direct or indirect manner. The CNS is surrounded by the blood-brain barrier, a highly selective semipermeable border of endothelial cells. Only selected solutes that circulate in the blood can cross into the extracellular fluid of the CNS (R. Daneman et al., 2015). Still, research in humans and mice has shown connections between the gut and the brain. The vagus nerve, the longest nerve of the twelve cranial nerves, connects the brain with the rest of the body and might be one point of entrance. For example, injecting misfolded α-synuclein into the gut of mice resulted in a higher α-synuclein accumulation in the animals' brains. When the vagus nerve is removed, α-sunuclein can no longer be detected in the brain (S. Kim et al., 2019). Another connection could be spawned by bacterial metabolites. Small molecules, produced by bacteria can enter the bloodstream. It is believed that at least half of the metabolites in the blood are made or transformed by microbes. One example is vitamin B3 (nicotinamide), because it can pass through the blood brain barrier and has been associated with amyotrophic lateral sclerosis (ALS) (E. Blacher et al., 2019). In addition, specific microbes, such as *Chlamydia pneumonia*, seem to be able to cross the blood brain barrier by infecting monocytes (MacIntyre A. et al., 2002). Furthermore, microbes affecting the brain could even pass from one generation to the next. For example, bacterial infections in a mother during pregnancy appear to increase the risk of autism spectrum disorder, a condition related to the development of the brain, in her child (B.J.S. al-Haddad et al., 2019).

1.3.2 Bacteria associated with Alzheimer's Disease

Alzheimer's Disease (AD), the most prevalent neurodegenerative disorder, has been associated with a number of bacterial pathogens as well, either directly or indirectly. Once inside the central nervous system (CNS), microbes can infect neurons, microglia and astrocytes. Such infected cells, containing metabolically active pathogens, were detected in AD pathology (HC Gérald et al., 2006).

The following microbes were found to be associated with AD:

Bacteria	Information	Citation
Chlamydia pneumonia	Gram-negative	BJ. Balin, et al. 1998
Heliobacter pylori	Gram-negative	T. Shindler-Itskovitch, et al. 2016
Treponema	Gram-negative	GR. Riviere, et al. 2002
Porphyromonas gingivalis	Gram-negative	S. Poole, et al. 2013
Borrelia burgdorferi	Gram-negative	J. Miklossy, et al. 2004
Spirochete	Gram-negative	P. Maheshwari, et al.2015

1.4 Alzheimer's Disease

AD is the most prominent form of dementia, a neurodegenerative disorder associated with a decline in memory and other cognitive deficits. An estimated 44 million people worldwide suffer from dementia and calculations predict an increase up to 135 million cases in 2050 (Prince M. et al., 2014). Of all dementia patients, 60% - 80% are diagnosed with AD (Brookmeyer et al., 2007). Furthermore, in 2050 the population of individuals over 60 will double and AD is an age-related disease. Consequently, expectations suggest that elderly would spend more of their later years in an overall ill health (Christensen el al., 2010). Hence, researchers around the world are trying to find ways to prevent or slow down disease progression.

For a long time, the brain was considered an immune-privileged organ that would be provoked by inflammation only through direct infection or infiltration of peripheral immune cells after the blood-brain barrier (BBB) was damaged (Heneka MT. et al., 2014). However, now it is widely accepted that systemic infections, aging and neurodegenerative diseases can induce an immune response in the CNS (Gyoneva S., et al. 2014), potentially followed by neuroinflammation (Venegas C. et al., 2017). Neuroinflammation and neuronal damage can be aggravated by overly active and dysregulated microglia, the resident innate immune cells of the brain (Block ML. et al., 2007). And indeed, a growing number of studies have shown an association between AD progression and microglia-mediated immune response (Sims R. et al., 2017). In AD, microglia are activated by danger signals. Considered to be one danger signal are intraneuronal formations of neurofibrillary tangles (NFTs), which consist of hyperphosphorylated tau proteins (Morales I. et al., 2013). Another, and for this thesis more relevant, danger signal is the accumulation and deposition of amyloid beta (Aβ) (Halle A. et al., 2008).

1.4.1 Amyloid beta

Amyloid beta (Aβ) is a fragment of a protein, which is excised from a larger protein called amyloid precursor protein (APP). Throughout life the β-and γ-secretase cut APP by proteolytic cleavage at three possible amino acid residues: 38, 40 and 42 (Goedert and Spillantini, 2006). In a healthy brain, these fragments are decomposed from the brain by microglia or transported into the cerebrospinal fluid (CSF), a body fluid found within the tissue that surrounds the brain and spinal cord. However, in Alzheimer's disease they accumulate in the extracellular space (Heneka M.T. et al., 2015). As soon as Aβ reaches a certain critical concentration it can self-associate and form soluble oligomers, protofibrils and fibrils, which aggregate to form hard and insoluble plaques (Selkoe and Hardy, 2016). Especially the oligomeric and fibrillar forms of Aβ act as a DAMP and are able to cause inflammasome activation. The first report on microglial inflammasome activation upon fibrillar Aβ exposure was in 2008 and showed that

fibrillar Aβ induced IL-1β release from microglia in an NLRP3- and ASC-dependent manner (Halle A. et al., 2008).

1.4.2 Microglia, Immune Cells of the Brain

The major principal cellular component of the immune system in the brain are microglia, representing about 10% of all cells in the CNS (Ginhoux F., et al., 2010). They survey the white and grey matter and are the first line of defence against invading pathogens, cell debris or injuries (Hughes V., 2012).

In addition, microglia play a key role in maintaining homeostasis in the CNS (Davalos D. et al., 2005). Microglia are also involved during the formation and control of synaptic plasticity (Tremblay M-É. et al., 2010) and learning (Parkhurst CN. et al., 2013). These findings suggest an intimate role of microglia in maintaining neuronal networks, hence, influencing learning and memory processes in the adult brain. Furthermore, the immune reaction of microglia occurs usually at a very early stage in response to acute brain injuries (d'Avila J.C. et al., 2012), neurodegenerative diseases (Lucin K.M. et al., 2013), ageing (Baron R. et al., 2014) and systemic inflammation (Gyoneva S. et al., 2014), e.g. obesity (Erion J.R. et al., 2014). The response can be induced by a variety of changes in the brain, including very subtle alterations in the microenvironment, such as imbalances of ion homeostasis (Kreutzberg G.W., 1995). Furthermore, microglia can detect e.g. neurotransmitters, neurohormones, neuromodulators, cytokines and chemokines. Also, they carry pattern recognition receptors. Together, this complex network of transporters, channels and receptors on the cell surface of microglia is referred to as the microglia sensome (Hickman SE. et al., 2013).

1.4.3 Pro-inflammatory Cytokines in the Brain

TNF-α and IL-1β are cytokines, small proteins ranging from 8000 to 40 000 Da and can be secreted by any immune or non-immune cell. (Dinarello C.A., 1997). They are part of the inflammatory response as discussed above. However, cytokines have additional biological effects: cytotoxicity, stimulation or inhibition of cell proliferation, antiviral activity, cell growth and differentiation. Because cytokines have so many functions in the CNS, it can be expected that cytokine levels vary in neurodegeneration. For example, in AD, cytokine levels of IL-1, TNF-α and IL-6 are increased and considered pro-inflammatory (Akiyama H. et al., 2000).

In neurodegeneration, pro-inflammatory cytokines can occur in the brain and, interestingly, even systemically. For example, a high incidence of cognitive decline and delirium was reported in patients which suffer from systemic inflammation with increased pro-inflammatory cytokine levels in the system. This could indicate a connection between the peripheral immune system and the brain (Mélik-Parsadaniantz S. et al., 2008), which could be mediated by pro-inflammatory cytokines. In addition, the outer membrane of gram-negative bacteria (LPS), injected in the periphery of mice, triggered neurodegeneration and neuroinflammation in the brain (Walter K.A. et al., 2017). Again, pro-inflammatory cytokines were detected in the brain and in serum from the periphery. Such observations led to the hypothesis that systemic inflammation can chronically activate microglia and contribute to the initiation or progression of neurodegeneration (Qin L. et al., 2007). This might also explain, why elderly patients show neurobehavioral manifestations even after they recovered from sepsis and cytokine levels dropped (Widmann C.N. et al., 2014). This idea of systemic infection driving neurodegeneration, such as AD, places microglia as a key player in neuro inflammation and makes them an interesting target in treating neurodegeneration.

1.4.4 NLRP3 in Alzheimer's Disease

The first involvement of NLRP3 inflammasome signalling in AD was reported in 2008 (Halle A. et al., 2008). Since then it has been shown that amyloid-β deposition can be recognized by the NLRP3 inflammasome. Even more, NLRP3 deficiency can largely protect from AD disease development in APP/PS1-transgenic mouse models (M. T. Heneka et al., 2013). This breakthrough proved again a pathogenetic nature of aggregated substances that are found in the brains of AD patients, such as Aβ plaques. It is suggested that microglia detect Aβ via the sensome. CD36, a co-receptor of TLR4, and CD14, is activated by aggregated Aβ. This results in the dimerization of TLR4 and TLR6, forming a TLR4-TLR6 heterodimer, followed by the recruitment of the adaptor protein "myeloid differentiation protein 88" (MyD88). MyD88 then activates the nuclear factor-κB (NF-κB). NF-κB induces the transcription and expression of tumor necrosis factor alpha (TNF-α) and interleukin-1β (IL-1β), which are components of an acute immune response (Rubio-Perez J.M. et al., 2012). Of particular relevance to this thesis, the NLRP3 inflammasome requires a priming step in order to be activated. NLRP3 can be triggered by crystalline materials or aggregated substances, such as Aβ. However, LPS or bacterial DNA and other pro inflammatory factors, such as cytokines, can also induce the priming step of the NLRP3 inflammasome (Henao-Mejia J. et al., 2012). Again, this finding makes NLRP6 mediated dysbiosis interesting, because it is assumed that TLR stimuli are translocated into the circulation in NLRP6 deficient mice (Henao-Mejia J. et al., 2012). Hence, microbiomes could also contribute to brain and systemic inflammation in AD pathology.

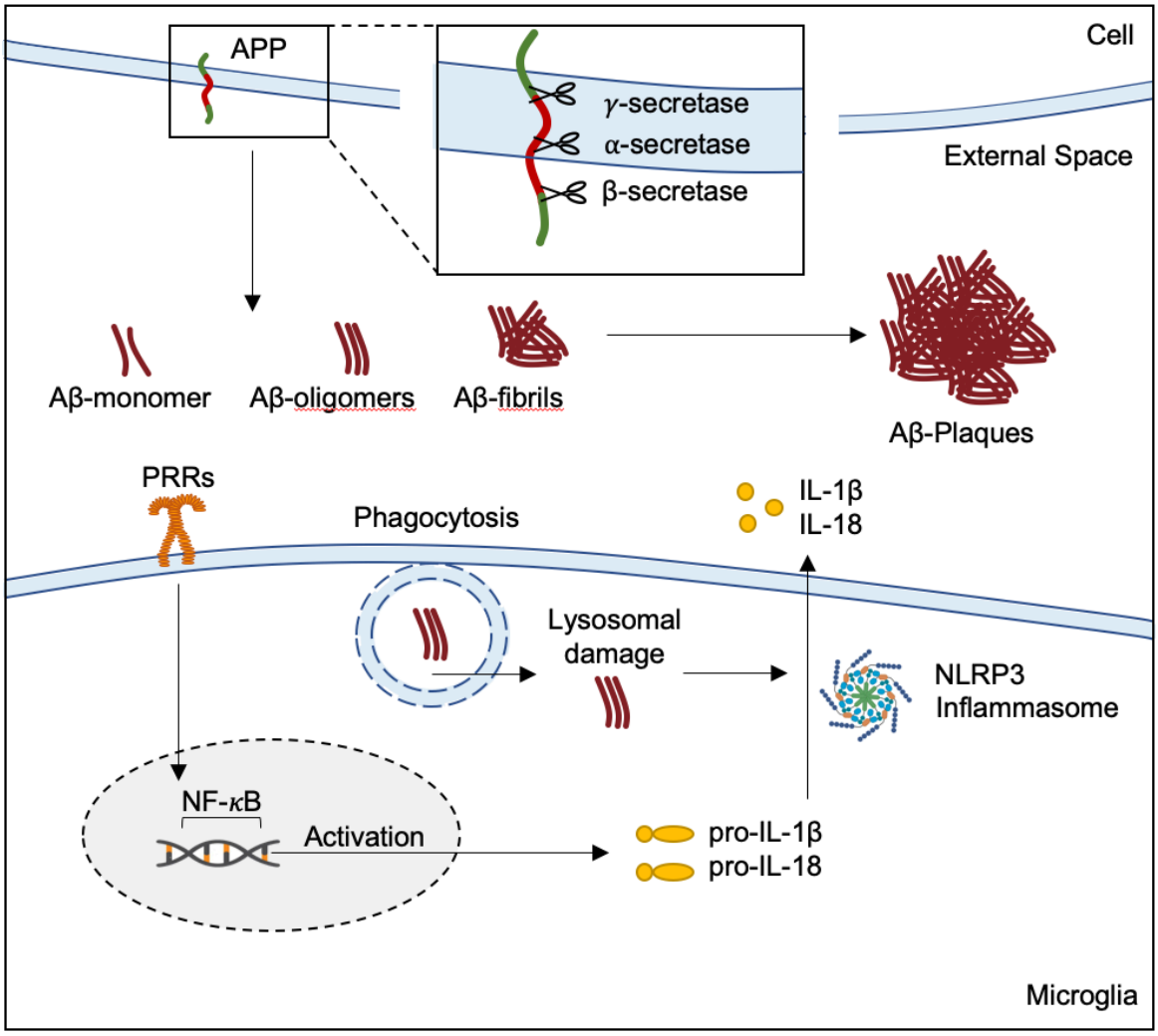

Figure 1.3 – Microglia-Sensome and Microglia Activation. The amyloidogenic pathway can process the trans membrane amyloid precursor protein (APP) by □-, β-, and □-secretase. Aβ peptides can form monomers, oligomers and fibrils which potentially cluster together and form Aβ-plaques. Pattern recognition receptors (PRRs), can be triggered by fibrillar and aggregated Aβ, LPS or bacterial DNA and other pro inflammatory factors to induce an innate immune response. The NF-κB transcription factor leads to the transcriptional induction of genes encoding components of the NLRP3 inflammasome, pro-IL-1b and pro-IL-18 (priming step). Additional signals are required for the activation of NLRP3, including deubiquitination of NLRP3 (licensing step). Microglia can take up Aβ by phagocytosis, which potentially causes lysosomal damage. The NLRP3 inflammasome assembles and caspase-1 activates (activation step). Hence, IL-1β and IL-18 are processed and released in their bioactive form. The inflammatory response generated by microglia activation can cause neuronal damage. Adapted from M. T. Heneka, 2015

1.5 Aim of Study

Alzheimer's disease is the world's most common neurodegenerative disease and to date there is no sufficient cure or strategy to prevent disease progression. For patients and society, it is crucial to further investigate AD. We do assume that AD is induced by the deposition of amyloid-β peptides and the appearance of hyperphosphorylated Tau proteins, driving neuroinflammation. Moreover, we suspect pathogen-associated molecules as well as endogenous danger signals to trigger innate immune signaling receptors leading to inflammatory processes in the brain. In addition, the microbiota has emerged as a major component of human physiology and pathology, integrating influences from both host genetics and environmental impact. The aim of this study was to profile the gut microbiome and its impact on inflammatory processes involved in AD, characterizing dysbiosis development during AD and how innate immune control of the microbiota impacts disease progression, using NLRP6-deficient mice as a dysbiosis model and APP/PS1 mice as AD model. Characterizing the role of the microbiota in AD might open up new avenues to the design of therapies for this devastating cureless disease.

2 Materials and Methods

2.1 Special Materials

2.1.1 Devices

Name	Supplier
Bruker 600 mhz spectrometer	Bruker biospin
Octomacs	Milteny biotec
Hiseq2500	Illumina
Bd facscanto ii	Dako, denmark
Meso quickplex sq 120	Meso scale discovery
Wes	Simple westerntm
Cryotome	Thermo fisher
Axio scan.z1	Zeiss

2.1.2 Reagents and Kits

Name	Supplier
Nucleotype mouse pcr 743200.5	Macherey-nagel
Power soil kit	Mobio
Neural tissue dissociating (p)	Milteny Biotec
Myelin removal beads ii	Milteny Biotec
Cd11b (microglia) microbeads	Milteny Biotec
Rneasy micro kit	Qiagen
Intrastein reagent a	Dako, denmark
Intrastain reagent b	Dako, denmark
Bca protein assay kit	Thermo scientific piercetm

V-plex® and v-plex plus proinflammatory panel 1 (mouse)	Meso scale discovery
V-plex® and v-plex plus aβ peptide panel 1 (6e10) kit	Meso scale discovery

2.2 Mouse Models

2.2.1 Dysbiosis and Alzheimer's Disease Mouse Model

To determine the impact of the microbiota on AD development, this study used four groups of age-matched mouse models in a genetic BC57/Bl6 background: Wild Type (WT), APP/PS1, Nlrp6$^{-/-}$ and APP/PS1/Nlrp6$^{-/-}$. The Nlrp6 knockout mouse (Nlrp6$^{-/-}$) was generated by replacing exon 1 and 2 with a neomycin resistance cassette (IRESnlslacZ / MC1neo). This results in a shortening of the gene due to the lack of the start codon and the pyrin coding region (E. Elinav et al., 2011). The hemizygous double transgenic mouse model APP/PS1 is a well-established model system for human Alzheimer's disease in which the chimeric mouse/human amyloid precursor protein and a human PS1 Δexon 9 mutation is expressed (Jankowsky et al., 2001). The heterozygous APP/PS1 mice have already been examined neuropathologically and show an accumulation of Aβ peptide and an associated chronic inflammatory component, as well as a deterioration in spatial memory. The animals have spontaneous, non-convulsive epileptic activity in cortical and hippocampal networks (Palop et al., 2007). The mice were maintained at a temperature of 22°C and a 12 h/12 h light/dark cycle, housed in groups and given free access to food and water. All mice were bred for planned experiments and randomized to experimental groups while visibly sick animals were excluded before data collection. All mice were handled identical across experiments. All experiments performed were authorized by the LANUV NRW, Germany.

All mice grew up in the “Haus für Experimentelle Therapie 1” (HET 1) to an age of one year. Three independent cohorts were bred and analyzed separately. Thereafter, only cohort one and two were transferred to the “Haus für Experimentelle Therapie 3” (HET 3), for the behavior studies and the take-down. Both animal facilities have the same living conditions, only the degree of exposure to other organisms has been reported to be different: **Table 2.1**. The Animal Health Reports suggest a more diverse micro environment in the HET3. The third cohort could not be moved to the HET 3 because of COVID-19 regulations in 2021.

Table 2.2 – Animal Health Report June 2020

Haus für Experimentelle Therapie (HET) 1 & 3, Bonn Germany

Viruses	Test Method	HET 1	HET 3
Mouse Hepatitis Virus (MHV)	MIA	0/4	0/1
Mouse Rotavirus (EDIM)	MIA	0/4	0/1
Murine Norovirus (MNV)	MIA	1/4	1/1
Minute Virus Of Mice (MVM)	MIA	0/4	0/1
Mouse Parvovirus (MPV)	MIA	0/4	0/1
Gdvii (Theiler´S) Virus (TMEV)	MIA	0/4	0/1
Lymphocytic Choriomeningitis (LCMV)	MIA	0/4	0/1
Mouse Adenovirus Type1 (MAD1)	MIA	0/4	0/1
Mouse Adenovirus Type2 (MAD2)	MIA	0/4	0/1
Mousepox (Ectromelia) Virus (ECT)	MIA	0/4	0/1
Pneumonia Virus Of Mice (PVM)	MIA	0/4	0/1
Reovirus Type 3 (REO3)	MIA	0/4	0/1
Sendai Virus (SEN)	MIA	0/4	0/1

Bacteria & Mycoplasma	Test Method	HET 1	HET 3
Helicobacter spp.	PCR	0/4	1/1
Pasteurella pneumotropica	Culture	0/4	0/1
STREPTOCOCCI ß-HAEMOLYTIC	Culture	0/4	0/1
Streptococcus pneumoniae	Culture	0/4	0/1
Corynebacterium kutscheri	Culture	0/4	0/1
Samonella spp.	Culture	0/4	0/1
Citrobacter rodentium	Culture	0/4	0/1
Mycoplasma pulmonis	MIA	0/4	0/1

Clostridium piliforme	MIA	0/4	0/1
Streptobacillus moniliformis	Culture	0/4	0/1
Endoparasites	Test Method	HET 1	HET 3
Trichomonas spp.	PCR	0/4	0/1
Entamoeba spp.	PCR	0/4	1/1
Giardia spp.	PCR	0/4	0/1
Hexaminta/Spironucleus muris	PCR	0/4	0/1
Aspiculuris tetraptera	PCR	0/4	0/1
Syphacia obvelata	PCR	0/4	0/1
Chilomastix spp.	PCR	1/4	0/1
Eimeria spp.	PCR	0/4	0/1
Ectoprasites	Microscopy	0/4	0/1
Pathology	Test Method	HET 1	HET 3
Lesions	Observation	0/4	0/1

2.2.2 Western Diet Study

To induce hypercholesterolemia in mice, a Western diet (Teklad 88137) consisting of 17.3% protein, 21.2% fat (saturated fat 12.8%, monounsaturated fat 5.6%, polyunsaturated fat 1%) and 48.5% carbohydrates was fed. As control, the chow diet (Prolab Isopro RMH 30; LabDiet) consisting of 25% protein, 14% fat (ether extract) and 60% carbohydrates was used to study diet effects on long-term reprogramming of microglia. Female mice were fed a WD for 4 weeks, and subsequently subjected to regular chow diet for additional 4 weeks. $Ldlr^{-/-}$ mice were originally purchased from The Jackson Laboratory and kept in house at the university of Massachusetts, Boston, USA. All mice were previously backcrossed over ten generations to the C57Bl6/J background.

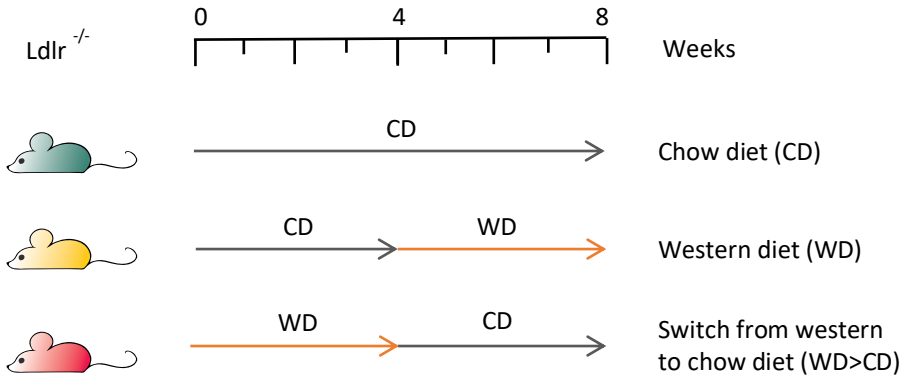

Figure 2.1 - **Dietary Plan.** Female Ldlr$^{-/-}$ Mice were on different dietary plans for a time period of 8 weeks. The first group was only fed with a chow diet (CD), the second group received a chow diet for four weeks followed by a four-week western diet (WD). The third group was put on a four-week western diet before switching the diet back to chow for four weeks.

2.2.3 Mouse Genotyping

Ear punches were performed on all mice to ID the animals and to collect the tissue for genotyping. The ear tissue was then lysed with the NucleoType Mouse PCR 743200.5 kit by MACHEREY-NAGEL and 1µl was used for the polymerase chain reaction (PCR). The PCR product was then separated in a 2% agarose gel with 120 Volt for 30-45 min. UV light visualized the PCR products and their base pare (bp) length to identify the genotype.

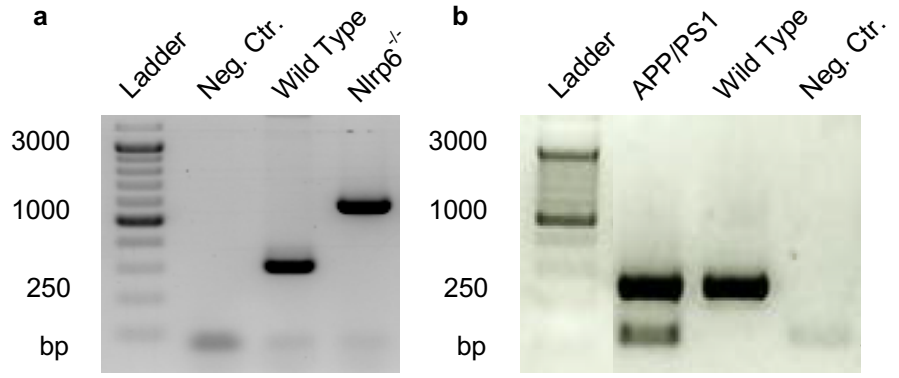

Figure 2.2 – Genotyping agarose gel. Visualization of a) Nlrp6$^{-/-}$ and b) APP/PS1 bands on 2% agarose gels. Genotyping was performed by Maximilian Rothe.

APP/PS1 Primers

APP/PS1 Wildtype	GTGTGATCCATTCCATCAGC
APP/PS1 Common	GGATCTCTGAGGGGTCCAGT
APP/PS1 Mutation	ATGGTAGAGTAAGCGAGAACACG
Result	APP/PS1 Mutant: 142 bp Wildtype: 265 bp

Nlrp6$^{-/-}$ (Pyrin_9) Primers

Nlrp6, MIL060-21	TCAAGCCCATCTTCTATGTC
Nlrp6, MIL060-22	CATGGTTAGTCTTTCTGCGTCTTT
Nlrp6, MIL060-23	TGATCTTCACAGAGCGAGCATTCC
NEO	GCTGACCGCTTCCTCGTGCTTTAC
Result	Wildtyp: 296 bp Knockout: 524 bp

Ldlr$^{-/-}$ Primers

Ldlr$^{-/-}$ Common	TATGCATCCCCAGTCTTTGG
Ldlr$^{-/-}$ Wildtype	CTACCCAACCAGCCCCTTAC
Ldlr$^{-/-}$ Mutation	ATAGATTCGCCCTTGTGTCC
Result	Wildtyp: 351 bp Knockout: 179 bp

PCR Protocol

Reagent	Volume in µl
H_2O	3,940
Macherey-Nagel™ Nucleotype™ Mouse PCR 2x	5,000
Each Primer (100µm)	0,020
DNA	1,00

PCR program

Cycles	Temperature in °c	Time
1	95	2 min
40	95	30 sec
	61	30 sec
	72	30 sec
1	72	5 min
1	20	10 sec

2.3 Stool Sample collection

Different time points were chosen to reflect the age effect on the microbiome in all groups: WT, APP/PS, Nlrp6$^{-/-}$ and APP/PS1/Nlrp6$^{-/-}$. Stool samples were taken every month of a selected group of each genotype. After 12 months stool samples were taken from all animals. The samples were collected directly after excretion and immediately snap frozen in liquid nitrogen. **Figure 1.2** shows the timepoints that were selected for 16S RNA sequencing.

Figure 2.3 - Stool Collection Timeline. Samples taken at age 2,4,7,9 and 12 months were chosen to be analysed by 16S RNA sequencing.

Stool samples for the Western Diet study were collected after the 8-week diet plan.

2.3.1 Microbiome Sequencing

Sequencing and bioinformatical analysis were performed by Dr. Timur Liwinski in the Eran Elinav lab. The DNA was extracted and processed for DNA isolation using a Power Soil kit (MoBio) (Turnbaugh et al., 2009). 515F/806R primers were used to amplify the 16S V4 region and sequenced using 2 x 250 base paired-end sequencing (Illumina MiSeq). Sequences were analysed using the Qiime (Quantitative Insights into Microbial Ecology, http://www.qiime.org) analysis pipeline (Caporaso et al., 2010).

2.4 Serum Metabolomics

At sacrifice, mice were anesthetized with isoflurane, and subsequently by cardiac puncture. The thorax was opened with a surgical scissor to approach the left ventricle of the heart. To take the blood, a syringe with a 27G needle was used. The needle was inserted into the left ventricle, penetrating 2–4 mm into the lumen while keeping the bevel of the needle face upwards. The blood was then stored on ice for 2-3 hours and subsequently spun down at maximal speed for 5 minutes. Serum on top was collected and stored at -80°C.

At the Eran Elinav lab the serum was thawed and centrifuged at 4°C at 12000 × g for 5 minutes. 90µL of plasma buffer (0.075 M NaH_2PO_4) was added to 90µL of the resulting supernatant and transferred to a 3 mm NMR tube. Subsequently, 4mL of D_2O containing 80 mg of 3-(trimethylsilyl) propionic-2,2,3,3-d_4 acid sodium salt (TSP) (Millipore-Sigma) and 40 mg of NaN_3 was added and mixed by shaking and sonication (pH 7.4). Metabolites were recorded on a Bruker 600 MHz spectrometer (Bruker Biospin) set at a constant temperature of 310K (Dona et al., 2014). For each sample a 1D nuclear Overhauser enhancement spectroscopy (NOSEY) experiment and a 2D J-resolved experiment were performed. 32 scans were acquired and the spectral data was collected into 64K data points. Topspin 3.1 (Bruker Biospin) automatically corrected the phasing, spectral calibration and baseline.

2.5 Tabula Muris

The “Tabula Muris” is a collection of single cell transcriptome data from mice (*Mus musculus*). It contains nearly 100,000 cells from 20 organs and tissue. For a higher sensitivity and coverage of the data, the full-length transcripts were analyzed. Therefore, the data provides information on gene expression in different tissues and cell types, e.g. the brain and microglia cells. https://tabula-muris.ds.czbiohub.org (the tabula Muris consortium, 2018).

2.6 Morris Water Maze

The Morris water-maze, a spatial memory test, was performed for behavior phenotyping. All experiments were carried out by the same experimenter at the same time of the day. The experiment was conducted in a circular Ø 1m pool filled with opacified water at 24°C. The basin was dimly lit, surrounded by a white curtain and three extra maze cues as spatial references. For analysis the circular pool was virtually divided into four quadrants, with one containing a hidden platform (15.315 cm) 1.5 cm below the water surface. For training purposes, the mice were placed on the platform and placed into the water in a quasi-random fashion to prevent strategy learning. If the mice did not find the platform after 40 seconds, they were placed on it manually for 15 seconds. Each animal went through 4 trials every day for eight consecutive days. 24h after the last day of training a special probe trial was performed. The platform was removed and the mice had 40 seconds within the pool. Time spent in each quadrant can be analyzed, especially the quadrant where the platform had been located. After the first probe run, a platform with a visual cue was reintroduced to the water maze, but at a different position, for four runs, each 40 seconds. All mouse movements were recorded by a computerized tracking system that calculated distances moved and latencies required for reaching the platform (Noldus, Ethovision 3.1)

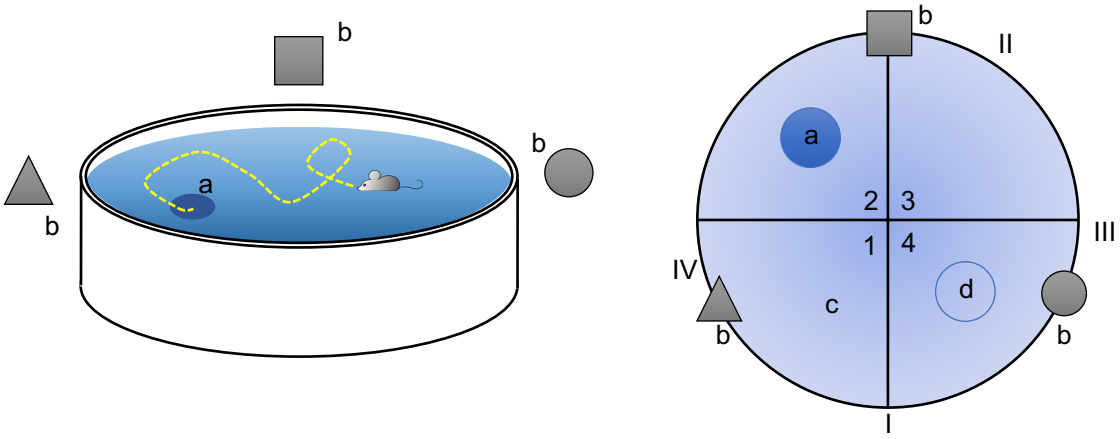

Figure 2.4 – Morris Water Maze Setup. left, schematic side view of the Morris Water Maze Setup. a) hidden platform, b) three extra maze cues as spatial references around the pool. Right, schematic top view on the Platform. c) one of four quadrants (1-4), d) flagged Platform for visual cued test (only during visual cued test, I - IV) start positions for each trial every day.

2.7 Tissue Processing

At the age of 12 months and three hours before surgery the animals were injected with 10 mg/kg methoxy-X04 (5 mg/mL in 50 % DMSO; 50 % NaCl (0.9% physiological solution), pH12) (Bolmont et al., 2008). Fur surgery the mice were anesthetized, followed by bleeding through cardiac puncture (via the left ventricle) and then transcardially perfused with ice-cold 1x PBS shortly prior harvesting the organs. The brain was taken, the cerebellum discarded and the hemispheres separated. One hemisphere was fixed in 4% PFA in PBS for 24h and then stored at 4°C, assigned for immunohistochemical staining. The other hemisphere was dissected by separating the frontal cortex. The frontal cortex was used for protein analysis and the rest was used for microglia isolation. Samples for protein were stored at -80°C. Samples for microglia were kept on ice and processed after the surgery.

2.8 Microglia Isolation

After dissecting the brains from adult mice, the tissue was enzymatically digested using a Neural Tissue Dissociating Kit (P) and the Milteny Biotec OctoMACS. Subsequently the cells were incubated for 15 minutes with Myelin Removal Beads II (Milteny Biotec) and separated from myelin in a magnetic field using LS columns (Milteny Biotec). The supernatant was then incubated with CD11b (Microglia) Micro-Beads (Milteny Biotec) for 15 minutes. CD11b positive cells were separated in a magnetic field using MS columns (Milteny Biotec). After the enzymatic digestion the samples were kept on ice and at 4°C and everything was done in accordance with the Milteny Biotec manufacturer's guidelines.

2.8.1 Microglia RNA Sequencing

Microglia were lyzed in 700 µl Trizol. Isolation of bulk RNA was performed with the RNeasy Micro Kit (Qiagen). The library production for 3'-mRNA sequencing was performed with up to 125 ng purified RNA according to the manufacturers' protocol and sequenced on a HiSeq2500 (Illumina) at the NGS Core Facility (University Hospital, Bonn, Germany). Reads were aligned with STAR (v2.5.3a) against the murine reference genome mm10. Transcripts were quantified with the Partek E/M algorithm and further DEseq2 normalized. Differentially expressed genes were determined for chow diet in comparison to high fat diet microglia by ANOVA analysis (fold-change |1.5|, FDR-adjusted p-value ≤0.05). Data visualization and biological interpretation were performed with the Partek Genomics Suite and R (v3.5.0).

2.8.2 Microglia FACS

To label the surface, each sample was incubated in 50 mL FACS buffer, containing the antibodies, 1:100 diluted, as listed down below, at room temperature for 15 minutes. To fix the sample, 50 mL / sample of IntraStein Reagent A (Dako, Denmark) was used

for 15 minutes at room temperature and in the dark. Subsequently, samples were washed twice with FACS buffer, centrifuged at 1200 rpm for 5 minutes, and permeabilized with 50 mL / sample of IntraStain Reagent B (Dako, Denmark) including the intracellular antibodies, diluted at 1:50. After a 15-minute incubation time in the dark, the cells were washed twice with FACS buffer and centrifuged at 1200 rpm for 5 minutes. The appropriate compensation controls and fluorescence minus one (FMO) controls were also prepared during this time.

Flow cytometric analysis was performed on a BD FACSCanto II, and data were acquired using Summit software (Dako, Denmark). The results were analyzed using FlowJo software (Tree Star, USA). Microglial cells were identified as being negative for LIVE/DEAD Fixable Aqua Dead Cell Stain, $CD45^+$, and $CD11b^+$. FSC vs SSC to remove debris and FSC-W vs FSC-A to remove cell doublets.

Table 2.3 - FACS Panel 1

(Laser) Filter	Channel	Fluorochrome	FACS Ab
(488) 530/30	FL1	FITC	TLR2
(488) 585/45	FL2	PE	TLR4
(488) 695-735	FL3	PerCP-Cy5.5	CX3CR1
(488) 780/60	FL4	PE-Cy7	CD11b
(633) 660/20	FL5	APC/A647	CD36
(633) 780/60	FL6	A780/APC-Cy7	Live/Dead
(405) 450/50	FL7	Brill Vio 421 / PacBlue	Methoxy
(405) 610/20	FL8	Brill Vio 605, BV650	CD45

Table 2.4 - FACS Panel 2

(Laser) Filter	Channel	Fluorochrome	FACS Ab
(488) 530/30	FL1	FITC	CD86
(488) 585/45	FL2	PE	I-A/I-E
(488) 695-735	FL3	PerCP-Cy5.5	CX3CR1
(488) 780/60	FL4	PE-Cy7	CD11b
(633) 660/20	FL5	APC/A647	CD40
(633) 780/60	FL6	A780/APC-Cy7	Live/Dead
(405) 450/50	FL7	Brill Vio 421 / PacBlue	Methoxy
(405) 610/20	FL8	Brill Vio 605, BV650	CD206 EL

2.9 Protein Extraction

The first step to extract protein from tissue is to homogenize the tissue. Keeping everything at 4 °C the samples were weighed first and 1 mL / 150 mg tissue (wet weight) of homogenization buffer + protease inhibitors were added (PBS, 5 mM NaF, 20 mM pyrophosphate, 1 mM AEBSF). A polytron homogenized the tissue at full speed for 15 seconds. Subsequently the protein was extracted by adding an equal volume of 2x RIPA (50 mM Tris pH 7.2, 150 mM NaCl, 2 % NP40, 1% NaDOC, 0.2% SDS). Samples were sonicated for 10 seconds (80% duty; 12% power) and incubated for 30 minutes on ice. Followed by a centrifugation at 100.000g for 30 minutes the supernatant was saved (RIPA fraction) und the pellet was extracted with 2% SDS-buffer (25 mM Tris-HCl pH 7.5 (RT), 2 % SDS), sonicated for 10 seconds (80% duty; 12% power), heated for 5 minutes at 90 °C and centrifuged at 100.000g for 30 minutes. The resulting supernatant (SDS fraction) was saved and the pellet was extracted with 70% formic acid (FA), sonicated for 10 seconds (80% duty; 12% power) and diluted 1:20 in 1M Tris buffer pH 11. All fractions were stored at -80 °C.

2.9.1 BCA protein assay

The protein from the snap-frozen tissue was extracted in RIPA, SDS und FA buffer as described above. Thermo Scientific PierceTM provides a commercial BCA protein assay kit (colorimetry-based) to estimate the protein concentration in a sample. The assay was performed as described by the manufacturer. BCA reagent A (sodium carbonate, sodium bicarbonate, BCA and sodium tartrate in 0.1 M sodium hydroxide) was combined with reagent B (4% cupric sulphate) in a ratio of 50:1. Following the standard assay procedure, BSA (2mg/ml) is used as a standard with 5 working standards (1–5µg). After incubation at 37°C for 30 min, the absorbance was measured at 562 nm against a reagent blank using a microplate reader (Beckman Coulter Co.). The sample concentrations were measured with reference to the standard curve. At the beginning the solution has a green color and turns violet over time if protein is present.

2.9.2 MSD Multi-Spot Assay

The cytokine and Aβ levels were determined on a multi-spot assay (Meso Scale Discovery). The RIPA fractions were used to measure cytokines (V-PLEX® and V-PLEX Plus Proinflammatory Panel 1 (mouse) Kit). The samples were diluted 1:1 onto the plate using reagent diluent 41 supplied with the kit. To measure Aβ peptides, the RIPA, SDS and FA fractions were diluted 1:1, 1:100 and 1:500, using diluent 35 supplied with the kit (V-PLEX® and V-PLEX Plus Aβ Peptide Panel 1 (6E10) Kit). For the rest of the steps the manufacturer's instructions were followed and the plates were measured on a MESO QuickPlex SQ 120. Measured cytokines: tumour-necrosis-factor-α (TNF-α), Keratinocyte chemoattractant (KC) / human growth-regulated oncogene (GRO), Interleukin 1 (IL-1), Interleukin 2 (IL-2), Interleukin 5 (IL-5) and Interleukin 6 (IL-6).

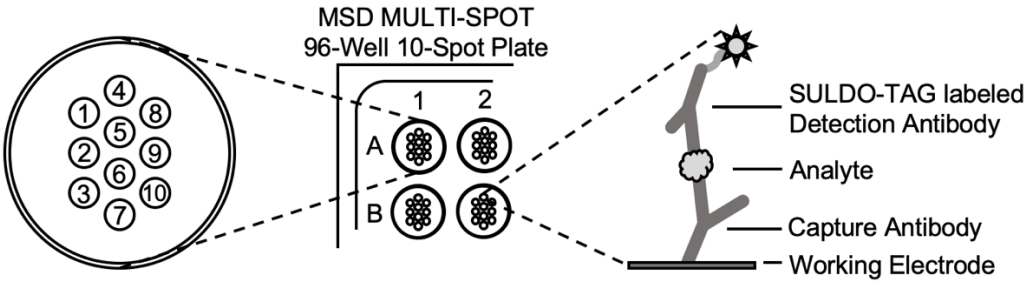

Figure 2.5 - MSD Mesoscale: 1.) Added samples and calibrators to an MSD plate coated with capture antibody (1-10). 2.) SULFO-TAG–conjugated detection antibody was added 3.) Plate can be analyzed an MSD instrument.

2.9.3 Western Blot by Simple WesternTM

Simple WesternTM provides a fully automated platform for traditional western blots. All RIPA fractions were diluted with 0.1X Sample Buffer, provided by Simple WesternTM, to a final concentration of 1.0 mg/mL of protein. The primary antibody was the Caspase 1 Monoclonal Antibody (5B10) by eBioscienceTM, 1:100 diluted. For all the following steps the manufacturer's instructions were followed.

Antibodies used for western blot analysis.

Antibody	Dilution	Manufacture	Cat. no. (RRID)
Mouse monoclonal anti-IL-1β	1:2000	1:2000 R&D Systems (Wiesbaden-Nordenstadt, Germany)	AB401-NA(AB_354347)

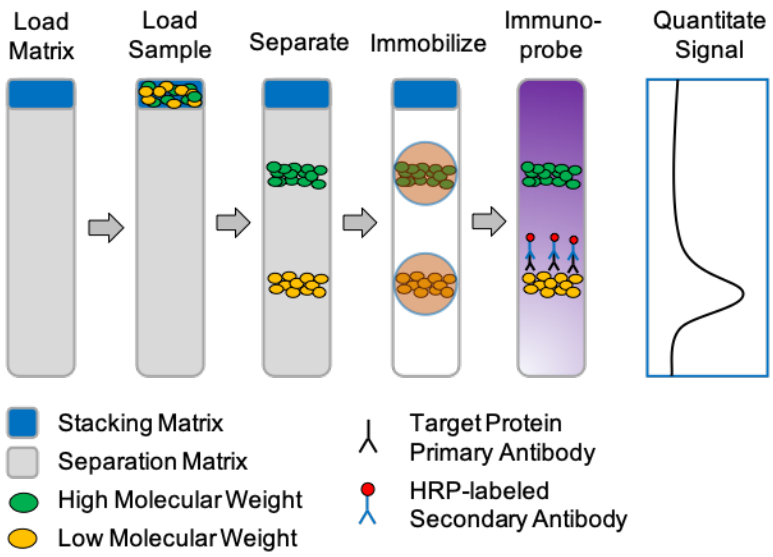

Figure 2.6 - Protein Simple *Wes:* Size based immunoassays take place in 25 capillary array single use cartridges. Proteins are automatically loaded into the capillary from the sample plate and separated by size as they migrate through a stacking and separation matrix. The separated proteins are then immobilized to the capillary wall via a proprietary, photoactivated capture chemistry. Target proteins are identified using a primary antibody and immunoprobed using an HRP-conjugated secondary antibody and chemiluminescent substrate. The resulting chemiluminescent signal is detected and quantitated. Adapted from Harris V.M. (2015) Protein Detection by Simple Western™ Analysis

2.10 Brain Histology, Imaging and Analysis

Paraformaldehyde (PFA) fixed brain hemispheres were sliced sagittally with a cryotome into 16µm thick slices and mounted on super frost slides surrounded with a barrier pen. After washing three times with PBS and blocking with 1% BSA in PBS for 1 hour at room temperature, 1:1000 DAPI dilution was added on top of the slices for 15 minutes and washed away with PBS. The injected methoxy stained Aβ plaques while animals were still alive.

Images were taken with a Zeiss Axio Scan.Z1 with a 20x objective Image analysis was performed in ImageJ using custom-written ImageJ plugins (Plugins by Jan Niklas Hansen). Each channel was analyzed separately. The DAPI channel was burred with a Gaussian Blur (sigma 20 px) and segmented into foreground and background pixels using the histogram threshold method Otsu (implemented in ImageJ). The Aβ plaque channel was segmented into foreground and background pixels using the histogram threshold method Triangle (implemented in ImageJ). Next, the remaining foreground particles in the segmented DAPI channel image were filtered for size: particles with a size below 1000 px were removed (corresponding pixels set to zero). Lastly the remaining foreground pixels in the DAPI channel and the remaining foreground pixels in the plaque channel were counted to determine the DAPI area and the plaque area.

2.11 Data Presentation

All graphs were generated using PRISM 9 and show means ± standard error of the mean (SEM) if not described otherwise. Also, each dot in a figure represent a biological replicate. Significances are indicated by *p value < 0.05, **p value < 0.01 and ***p value < 0.001. The normality of the data distribution was assessed using a Shapiro-Wilk test for all the statistical analyses. If the data followed the Gaussian distribution, parametric tests were used. Otherwise, a Grubbs' test (alpha of 0.05) was employed to identify and remove one outlier of the samples in order to reach the normality.

3 Results

3.1 Nlrp6 Expression in Mice

Before starting the study on how the Nlrp6 inflammasome possibly affects the development of Alzheimer's disease (AD), we had to establish the mouse breeding program. It had to be taken into consideration that all four genotypes had to be bred, aged and cohoused simultaneously in a cohort large enough to be statistically relevant. These precautions were meant to achieve a uniform microbiome, only challenged by the genetic modulation of the Nlrp6 inflammasome. While the mouse breeding was under way to increase the number of animals, we investigated Nlrp6 expression in mice. Back in 2017 Dr. Yonatan Herzig, former postdoctoral researcher at the institute of Innate Immunity, performed a number of experiments confirming that Nlrp6 is mainly expressed in the intestine, liver and kidney. Almost no expression was detected via reverse transcriptase quantitative polymerase chain reaction (RT-qPCR) and immunohistochemistry (data not published / shown). Adding to Dr. Herzigs findings, the Tabula Muris database allows a direct and controlled comparison of gene expression within all organs and cell types **(Figure 3.1)**. Sorting for *Nlrp6* expression in *Mus musculus* shows that the highest number of *Nlrp6* positive cells is detected in epithelial cells (74%) and enterocytes of the epithelium (66%) within the large intestine. The next highest numbers are found for hepatocytes in the liver (59%) and epithelial cells in the kidney (11%). The brain shows almost no *Nlrp6* positive cells: neurons (2%), oligodendrocytes (1%), astrocytes (0.5%) and microglia (0.1%). Given the very low expression of *Nlrp6* in the brain, these findings suggest that Nlrp6 has only an indirect influence on brain-related processes including neuroinflammation in mice.

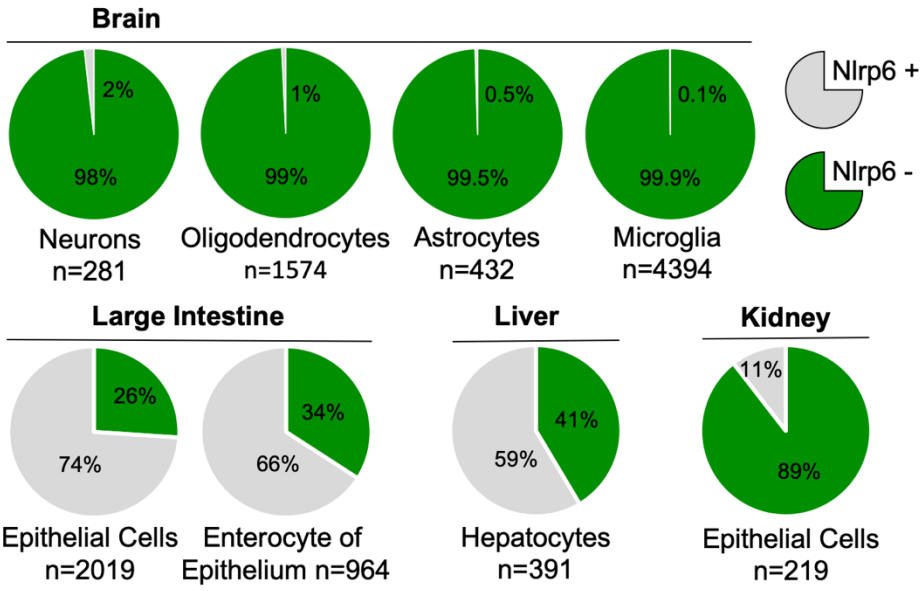

Figure 3.1 – Single cell transcriptome data from mice show almost no *Nlrp6* expression in the brain. Tabula Muris data represented as circle charts compare Nlrp6 gene expression in different tissues and cell types. [n] represents the number of measured cells and [%] the percentage of Nlrp6 positive [grey] and Nlrp6 negative [green] cells.

3.2 Impact of Nlrp6 on Learning and Memory Capabilities in APP/PS1 Mice

The first experimental approach after breeding suitable cohorts of one-year old wild type (WT), *Nlrp6* knock out (Nlrp6$^{-/-}$), APP/PS1 and APP/PS1 / Nlrp6$^{-/-}$ mice were the Morris water-maze trials. The Morris water-maze provides an impression on brain functionality by challenging learning and memory capabilities **(Figure 3.2)**. It has been shown that a decline in memory and learning in APP/PS1 mice is connected with Aβ deposition and neuroinflammation (e.g. Heneka et al., 2013). Hence, measuring the distance traveled (Figure 3.2b), overall time (Figure 3.2c) and time spent in quadrant 2 (Figure 3.2d), the quadrant with the hidden platform, over a time period of 8 days allowed to investigate the ability to learn and memorize spatial information in mice. Two independent Morris water-maze trials revealed that no statistical differences were

detected between APP/PS1 and APP/PS1 / Nlrp6$^{-/-}$ mice. This suggested that Nlrp6 has neither a protective nor an aggravating effect. Also, Nlrp6$^{-/-}$ mice showed similar values as WT mice. Furthermore, the search pattern for the platform is much more directed in WT and Nlrp6$^{-/-}$ mice. Whereas mice with APP/PS1 mostly swim in random circles, avoiding the middle of the water tank and, if so, finding the platform only by chance (Figure 3.2a). Search patterns can be another readout for altered behavior, learning and memory decline.

However, how can we find sufficient controls for a set up measuring behavior of mice. First of all, the observed learning and memory decline in mice with an APP/PS1 background has been published numerous times. Hence, it can be considered as control for a functional Morris water-maze set up. Additionally, on day 9, the probe trial with a visible platform, showed that all genotypes swam approximately the same distance (Figure 3.2e) and took almost the same time (Figure 3.2f) to reach the flagged platform. This indicated that the known instinct to avoid water and find solid ground was active in all mice, independent of their genetic background. Therefore, mice that were just floating around with no urge of finding the platform at all were excluded from the data analysis.

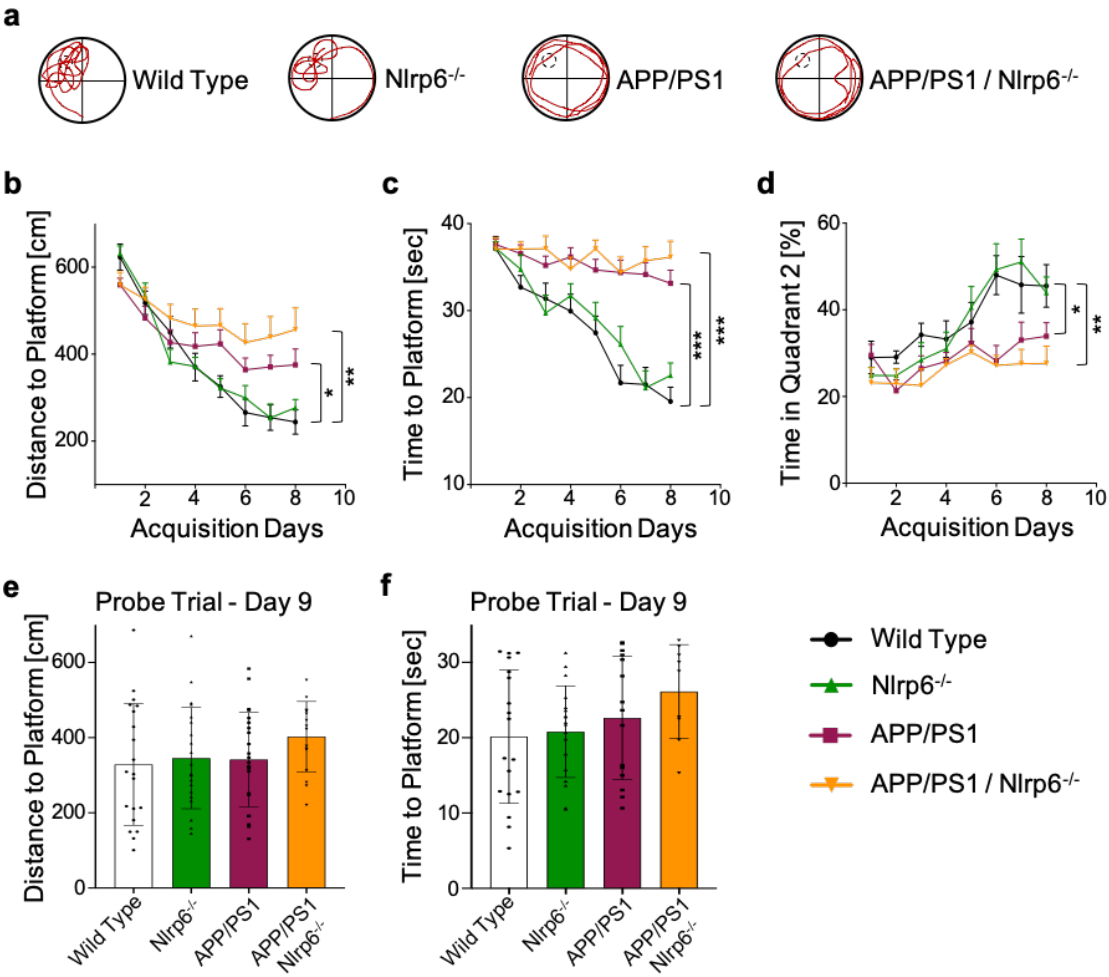

Figure 3.2 – Nlrp6 does not influence learning and memory capabilities in APP/PS1 mice. Morris water-maze trials were documented for 9 days with 4 runs per day, each run max. 40 seconds. (**a**) Representative run for each genotype, red line indicates swim pattern within 40 seconds. (**b**) Distance travelled [centimeters] to platform within 40 seconds, (**c**) Time [seconds] spend to reach the platform (**d**) Percentage of time spend in quadrant 2, containing the hidden platform. (**e**) Probe trial day 9. Distance [centimeters] travelled within 40 seconds and (**f**) Time [seconds] spend to reach flagged / visible platform. Graphs show mean and error bars show SEM of two independent Morris water-maze experiments. Each symbol represents an individual mouse. Significances are indicated by *p value < 0.05, **p value < 0.01 and ***p value < 0.001.

3.3 Gut Microbiome Sequencing in Nlrp6 deficient Mice

For the following data sets it is important to add that only the first and second cohort were relocated at an age of one year to the animal facility HET3, which was also the location of the water-maze setup. The animals spend one month within the HET3 to adjust to the new surroundings and for the Morris water-maze trials. As mentioned before, the HET3 facility is much more exposed to the outside environment and external microbes. Hence, the mice were exposed to a different and more diverse microbiome in the cages and especially in the MWM water tank **(Figure 3.3)**.

In order to monitor the potential drift in microbiome composition during aging and in presence or absence of Nlrp6. while breeding the first cohort we selected five mice of every genotype and collected stool samples every month until an age of one year. By deleting Nlrp6 we expected to create a dysbiosis as described in the introduction of this thesis. After the MWM-trials we collected additional stool samples of all animals in cohort one. Subsequently, the described stool samples were sent to the lab of Prof. Dr. Eran Elinav (Weizmann Institute of Science, Rehovot, Israel) for microbiome sequencing and analysis. Unfortunately, only a limited number of samples could be sequenced, namely time points 2, 4, 7 and 9 months of age (Figure 3.3a). Nevertheless, the first batch of data revealed a shift in microbiome diversity at all times in Nlrp6 knock out mice, compared to WT and APP/PS1 animals, hence, supporting the hypothesis of dysbiosis in Nlrp6$^{-/-}$ mice. However, age seemed to have only a minor impact on the diversity of microbiome sequences. The small number of animals, however, demands caution.

Later, the second and third cohort were processed. Stool samples of all one-year old mice were again sent to the Eran Elinav lab, and for comparison reasons both cohorts were sequenced and analyzed simultaneously (Figure 3.3b). Surprisingly, no genotype specific PCoA2 clusters for microbiome variance clusters were detected. This observation contradicted the first finding and argued against the Nlrp6$^{-/-}$ dysbiosis hypothesis. However, further analysis revealed that there were strong variations in microbiome variance between cohorts two and three (Figure 3.3c), suggesting an

independent analysis of each cohort. Indeed, only cohort 2 shows the previously detected difference in microbiome composition in Nlrp6 deficient mice, compared to WT and APP/PS1 (Figure 3.3d). Again, Nlrp6 alone, independent of APP/PS1, seems to have an impact on the microbiome composition (Figure 3.3e). Important to add, cohort three only had 19 animals (cohort two = 33 mice), reducing its statistical power. Overall, the data indicate that the Nlrp6 status has an effect on the microbiome without an additional detectable effect of APP / PS1 in cohorts one and two. Microbiome differences between all three cohorts need to be further discussed in the discussion part of this thesis. However, because of this finding, some of the following data sets show data for each cohort independently.

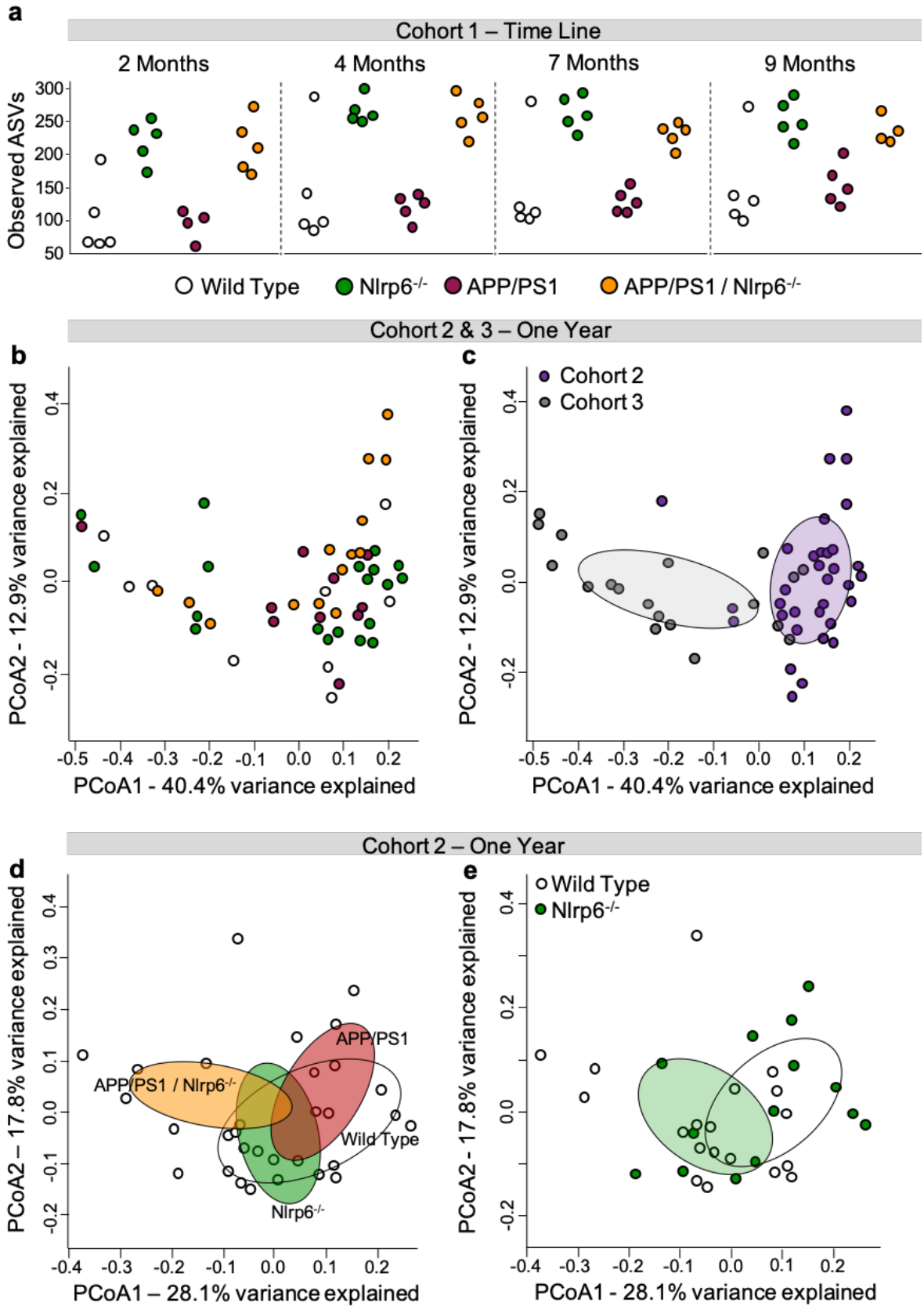
a
Cohort 1 – Time Line
2 Months
4 Months
7 Months
9 Months
Observed ASVs
300
250
200
150
100
50
Wild Type
Nlrp6-/-
APP/PS1
APP/PS1 / Nlrp6-/-
Cohort 2 & 3 – One Year
b
PCoA2 - 12.9% variance explained
0.4
0.2
0.0
-0.2
-0.5 -0.4 -0.3 -0.2 -0.1 0.0 0.1 0.2
PCoA1 - 40.4% variance explained
c
Cohort 2
Cohort 3
PCoA2 - 12.9% variance explained
PCoA1 - 40.4% variance explained
Cohort 2 – One Year
d
PCoA2 – 17.8% variance explained
0.4
0.3
0.2
0.1
0.0
-0.1
-0.2
-0.4 -0.3 -0.2 -0.1 0.0 0.1 0.2
PCoA1 – 28.1% variance explained
APP/PS1
APP/PS1 / Nlrp6-/-
Wild Type
Nlrp6-/-
e
Wild Type
Nlrp6-/-
PCoA2 - 17.8% variance explained
PCoA1 - 28.1% variance explained

Figure 3.3 – Microbiome sequencing reveals differences in microbiome variance between all three cohorts of mice. All cohorts grew up at different time periods but within the same housing facility and room. Only the first and second cohort of mice was moved after one year into a different facility for behavior analysis - Morris Water Maze (MWM). (**a**) First cohort: stool samples of selected mice were collected at different time periods and sequenced n = 5 per genotype. The ASV (Amplicon Sequence Variant) identifies single and exact sequences that are statistically significant. (**b**) To avoid sequencing batch effects, the second and third cohort were sequenced simultaneously. The principal coordinate analysis (PCoA) of one-year old mice shows no difference between genotypes. (**c**) Comparing cohort two and three with each other shows a very high variation. Indicating the significant impact of the MWM and breeding time. (**d**) Between cohort two and three only the second cohort shows a significant effect of the Nlrp6 deletion. (**e**) However, neither APP/PS1 alone nor in interaction with Nlrp6 deletion has an additional effect. Each dot represents an individual mouse.

3.3.1 Digestive Tract of Nlrp6 knock out and APP/PS1 Mice

While waiting for the microbiome sequencing data a further physical investigation of the cecum and colon in Nlrp6 deficient and APP/PS1 mice was initiated. Literature suggests a connection between the microbiome composition and the physical appearance of the digestive tract in mice, especially regarding the cecum and colon (Dodiya H.B. et al., 2020). Nlrp6 is mainly expressed in the intestine and might have an indirect or direct effect on the weight of the cecum and the length of the colon. Therefore, cecum and colon samples were collected of all genotypes **(Figure 3.3.1)**. However, no alterations were measured, suggesting that Nlrp6 and APP/PS1, independent of the cohort, have no effect on colon length (Figure 3.3.1b) or cecum weight (Figure 3.3.1c).

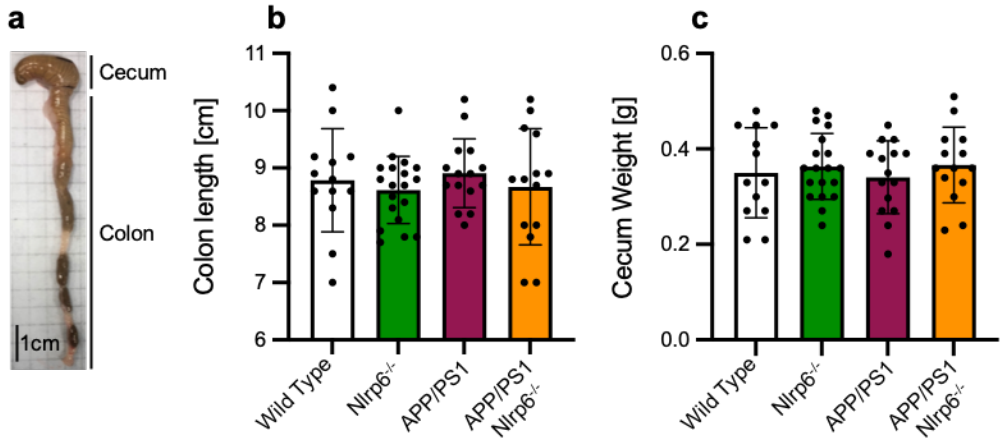

Figure 3.3.1 – Physical appearance of cecum and colon in Nlrp6 deficient and APP/PS1 mice show no alterations. (**a**) Example of a cecum and colon prepared for further investigations. Comparing Wild Type, Nlrp6$^{-/-}$, APP/PS1 and App/PS1 / Nlrp6$^{-/-}$ mice by measuring (**b**) colon length in [centimeters] and (**c**) cecum weight in [grams]. No difference between cohorts of animals (not shown). Graphs show mean and error bars show SEM. Each dot represents an individual mouse.

3.4 Metabolome Analysis in Nlrp6 deficient and APP/PS1 Mice

To examine the role of the gut microbiome in Alzheimer's Disease, we were interested in finding the connection between the microbiome within the digestive tract and the brain, the organ showing the most severe AD phenotype. Possibly the most informative could be the analysis of blood as it flows throw the entire organism, indirectly connecting all organs with each other. Specifically, metabolomic in serum samples derived from the genotypes of interest were analyzed **(Figure 3.4)**. As mentioned in the introduction, the microbiome and also the Nltp6 knock out phenotype impact metabolomes, potentially causing alterations in the brain. We divided the large field of metabolomics and small molecules in polar & semi polar metabolites (Figure 3.4a) and lipids (Figure 3.4b). However, blood serum of cohort two and three revealed no metabolomic changes. And again, because cohort three did not go through the MWM process, we had to compare the two groups with each other. No genotypic clusters were detected with the principal component analysis (PCA) (Figure 3.4c & d). The number of animals in cohort three was too low for a meaningful statistical analysis, but

not even a trend was visible. Further investigations of kidneys, liver and intestines, by measuring pro-inflammatory cytokines, did not reveal any genotype-specific phenotype either (Figure 3.4.1). The intestine of APP/PS1 / NLRP6$^{-/-}$ mice did show signs of inflammation with increased, albeit not significantly, IL-12p70 and KC/GRO cytokine levels.

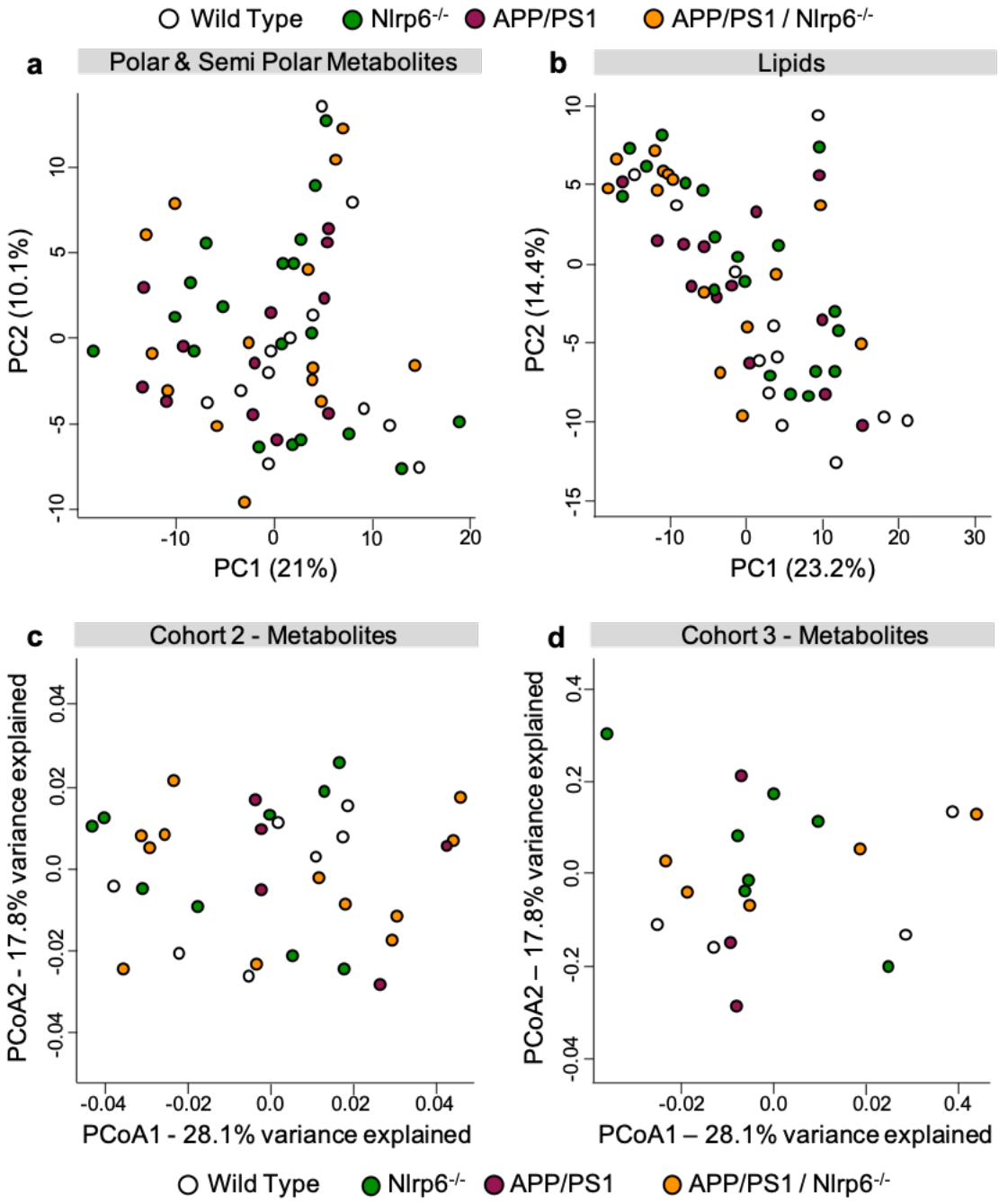

Figure 3.4 – Nlrp6$^{-/-}$ and APP/PS1 mice show similar metabolite profiles in serum. Serum was collected from mice cohorts two and three at the age of one year. Principal component analysis (PCA) of the measured metabolite profiles did not revealsignificant clusters when comparing (**a**) polar and semi polar metabolites (**b**) and lipids between all four genotypes. Again, cohort three did not go through the MWM tests. Hence, the comparison between cohort two and three (**c & d**), which did not show any metabolomic differences in the serum. Each dot represents an individual mouse.

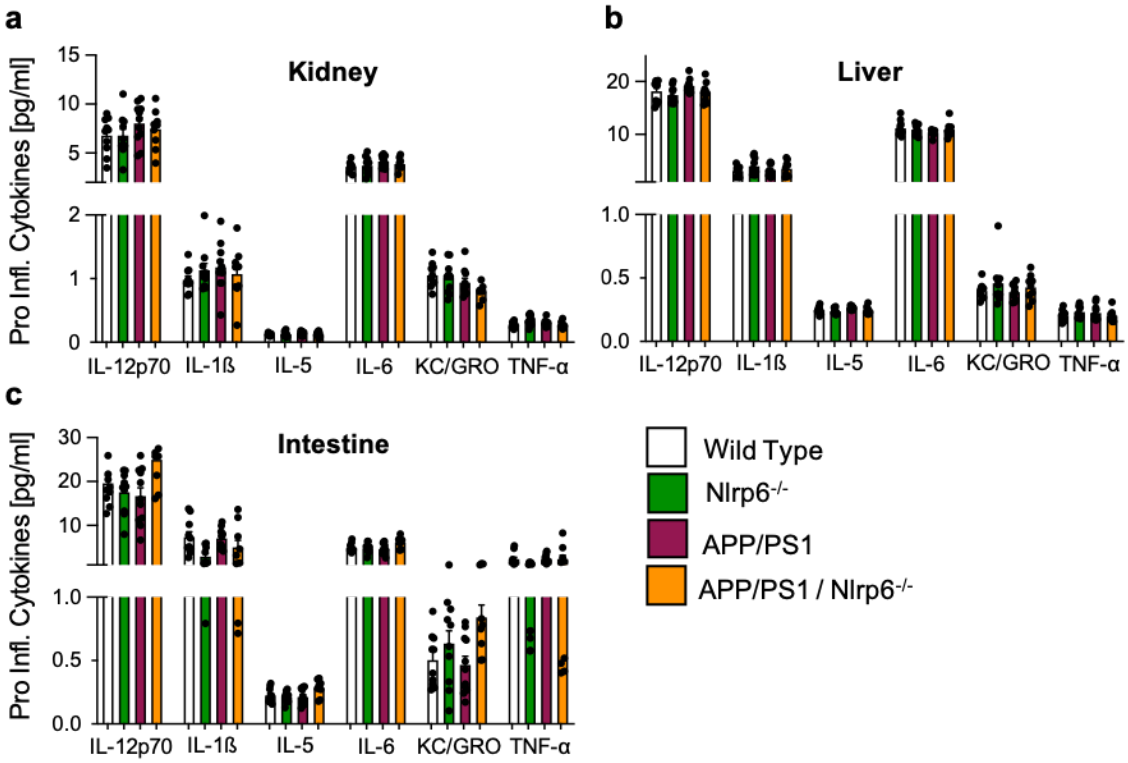

Figure 3.4.1 – Nlrp6 does not affect pro-inflammatory cytokines in kidney, liver and intestine. Organ homogenates measured for pro inflammatory cytokines in a mesoscale MSD multi-spot assay (mesoscale). Protein levels for IL-12p70, IL-1β, IL-5, IL-6, KC/GRO and TNF-α were sufficient to be measured by the assay. (**a**) No differences were detectable in the kidney for all four genotypes. (**b**) Also, liver samples did not show any significant difference in cytokine levels. (**c**) Only KC/GRO and IL-12p70 seems to be slightly increased in intestines of Nlrp6 deleted mice. Graphs show mean and error bars show SEM of two independent experiments / cohorts. Each dot represents an individual mouse.

3.5 Microglial response to Nlrp6 deletion in APP/PS1 Mice

Following the experimental sequence of events, we first analyzed the microbiome composition, metabolite profiles within the blood as well as learning and memory abilities. After sacrificing the animals, it was finally possible to address the main area of AD development, the brain. As mentioned, the brain is the center of the nervous system (CNS) and most prominently affected by AD. Of specific interest was one specific cell type, namely microglia, as they are the immune cells of the brain. They account for the first and main form of active immune defense in the CNS.

3.5.1 FACS Analysis of Microglia in Nlrp6$^{-/-}$ and APP/PS1 Mice

Via fluorescence-activated cell sorting (FACS) one can sort a heterogeneous mixture of biological and prelabeled cells. For this study multiple proteins were labeled, and the first steps were to check for viability and to select microglia specifically **(Figure 3.5.1)**. In the following, FACS data are separated into cohorts because of high variations within the FACS data and the observed microbiome differences. As only live cells were of interest, a live/dead near-IR staining was performed. This reactive dye labels all intracellular and extracellular amines, which are more exposed in dead cells (Figure 3.5.1b). The staining results showed that the isolation efficiency of live cells varies between cohorts but not between genotypes. Next, microglia cells were sorted by labeling CD11b and CD45. CD11b is a 165 kDa adhesion molecule which associates non-covalently with integrin beta-2 (CD18). CD11b is expressed on the surface of multiple cell types but is unique to microglia in the brain. However, macrophages of the blood might still be present in the cell suspension. Therefore, a combination of CD11b and CD45 labelling can be used to distinguish microglia from macrophages. Resting microglia are CD11b^{hi}, CD45^{low}, whereas macrophages are CD11b^{hi}, CD45^{hi} (Figure 3.5.1c). Again, differences were measured between cohorts and additionally cohort three had a significantly higher percentage of live microglia cells in mice with APP/PS1. This observation was made only in cohort three with a lower number of animals

compared to cohorts one and two. This and all the following deviations between cohorts will be discussed in the discussion of this thesis.

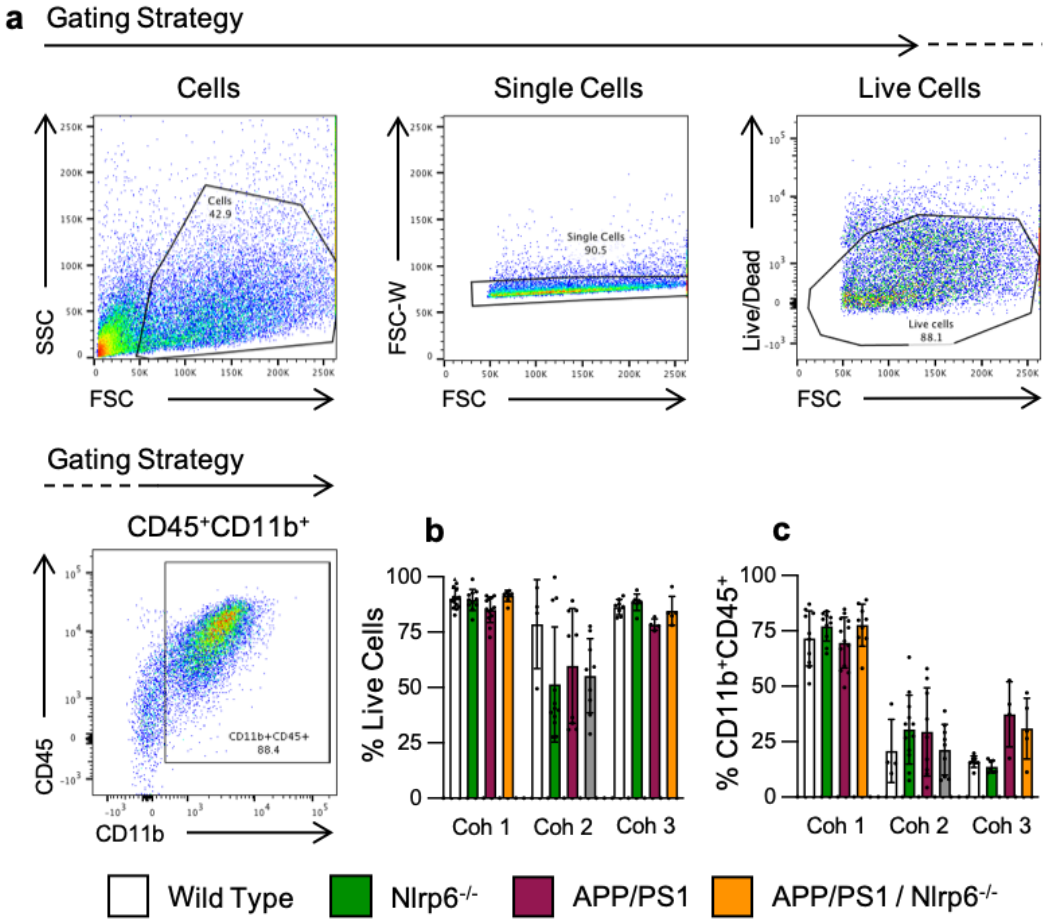

Figure 3.5.1 – Flow cytometry of microglia. Microglia were isolated from one-year old mice shortly after takedown, stained and measured. (**a**) Gating strategy on single cells, live cells and $CD45^{+}CD11^{+}$ cells revealed (**b**) the percentage [%] of live cells. The second cohort shows a reduced percentage of live cells. (**c**) Again, the percentage of live $CD45^{+}CD11^{+}$ cells varies between cohorts. Cohort two and three have a lower percentage of live $CD45^{+}CD11^{+}$ cells. Additionally, mice with APP/PS1 background in cohort three have an increased $CD45^{+}CD11^{+}$ percentage. Graphs show mean and error bars show SEM of three independent experiments and cell isolations. Each dot represents an individual mouse.

3.5.2 Toll-like Receptor 2 and 4 in Microglia of Nlrp6$^{-/-}$ and APP/PS1 Mice

Microglia, the immune cells of the brain, also express Toll-like receptors (TLR). As mentioned in the introduction, TLRs are transmembrane proteins and belong to the pattern recognition receptor family. Their activation triggers an intracellular signaling pathway and inflammatory cytokine production, hence inflammation in the brain. Two of the most prominent TLR immune receptors in microglia are TLR2 and TLR4. A higher expression of TLRs usually indicates an increased immune status. Therefore, we labeled TLR2 and TLR4 and compared the number of positive microglia cells in all four mouse lines **(Figure 3.5.2)**. For TLR4 expression in CD45^{+} and CD11b^{+} cells the FACS measurements showed different results within cohorts (Figure 3.5.2b). The general percentage of TLR4 positive cells was increased in cohort two. However, no differences between genotypes were detected, in contrast to cohort one and three. Cohort one showed an increased TLR4^{+} microglia quantity in WT and APP/PS1 animals. This observation was not reproduced in cohort three because only APP/PS1 / Nlrp6$^{-/-}$ animals had a decreased number of TLR4 positive microglia.

Regarding TLR2, cohort one and three clearly showed a higher percentage of CD11b^{+}CD45^{+}TLR2^{+} cells in APP/PS1 and APP/PS1 / Nlrp6$^{-/-}$ animals (Figure 3.5.2c). This result was not reproducible in cohort two. However, this might suggest that the analyzed microglia show an immune reaction against Aβ, only expressed in animals with APP/PS1 background. Furthermore, it seems like APP/PS1 / Nlrp6$^{-/-}$ mice have an even higher quantity of TLR2 positive microglia, compared to only APP/PS1 mice. This represents the first observed effect of Nlrp6 deletion in APP/PS1 animals within this study. Once microglia sense Aβ depositions as foreign substance, e.g. through TLR2, they try to clear it by phagocytosis. This finding raised the next question, i.e. whether microglia of Nlrp6$^{-/-}$ animals take up Aβ more efficiently then microglia of Nlrp6$^{+/+}$.

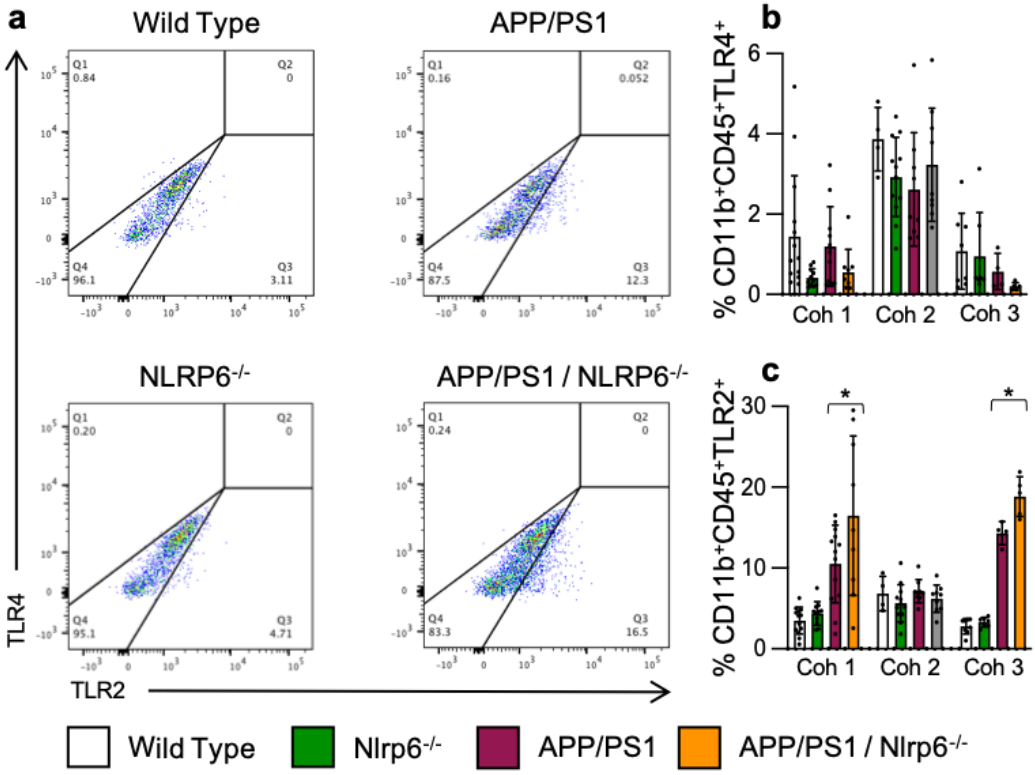

Figure 3.5.2 – TLR2 and TLR4 expression on microglia shows no Nlrp6-dependent phenotype. Flow cytometry analysis of live and $CD45^{+}CD11^{+}$ microglia from **Figure 3.6**. (**a**) Gating examples for TLR2 and TLR4 for each genotype. (**b**) Percentage [%] of TLR4 positive cells varies significantly between cohorts but not between genotypes. Cohort two showed the highest TLR4 expression. (**c**) Mice with APP/PS1 background in cohort one and three display a clearly increased percentage of TLR2 positive $CD45^{+}CD11^{+}$ cells. Graphs show mean and error bars show SEM of three independent experiments and cell isolations. Each dot represents an individual mouse. Significances are indicated by *p value < 0.05, **p value < 0.01 and ***p value < 0.001.

3.5.3 Microglia Phagocytosis of Aβ in Nlrp6$^{-/-}$ and APP/PS1 Mice

Phagocytosis is the process of ingesting and eliminating particles, including microorganisms, foreign substances and apoptotic cells. TLR2 and TLR4 receptors of the innate immune system are involved in the removal of unwanted residues as they activate a signaling cascade that stimulates phagocytosis. With Aβ being one of the

main drivers for neuro inflammation and degeneration in AD, it is interesting to see the efficiency of Aβ uptake by microglia (**Figure 3.5.3**). This applies especially after finding an increased TLR2^{+} microglia population in Nlrp6 deficient APP/PS1 mice. Indeed, the Aβ load is modulated in part by TLR2 and TLR4, and activation of TLR2 and TLR4 can increase the uptake of Aβ by microglial cells in the brains of mouse models of Alzheimer's disease (Serge Rivest, 2009)

The experimental approach was to inject the animals with 10 mg/kg of methoxy-X04 (Mex04), a dye selectively binding fibrillar β-sheet deposits with high affinity, hence detecting plaques, tangles and cerebrovascular amyloid in vivo. By selecting for CD11b^{+}CD45^{+} and Mex04^{+} cells we were able to compare microglia populations with Mex04 labeled Aβ. However, in this case no differences were detectable between APP/PS1 and APP/PS1 / Nlrp6$^{-/-}$ mice. WT and Nlrp6 knock out animals were used as negative control and showed almost no positive Mex04 cells (Figure 3.5.3b). Results are also comparable when divided by the normalized Mean Fluorescence Intensity (MFI) of the stained samples by the MFI of the negative control (figure 3.5.3c). These results suggest that Nlrp6 does not affect microglia activity in APP/PS1 animals at one year of age. To obtain more insight into what is happening within these cells, we changed the method and isolated mRNA.

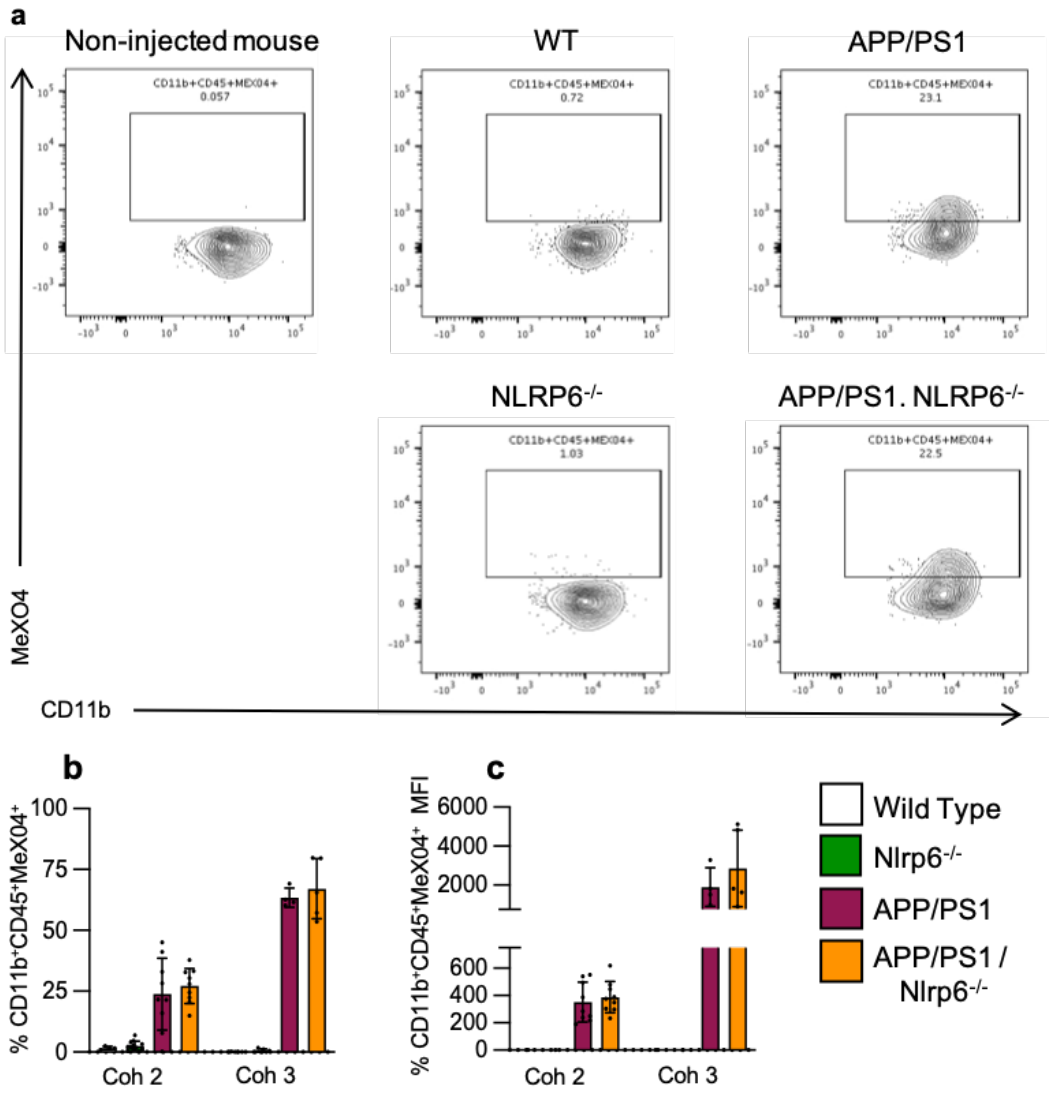

Figure 3.5.3 – Microglia uptake of methoxy labelled Aβ shows no Nlrp6 phenotype. Three hours before surgery, cohort two and there were injected with 10 mg/kg methoxy-X04 and subsequently microglia were isolated and analysed on the flow cytometry. (**a**) Gating on live cells, $CD45^{+}CD11^{+}$ and methoxy ($MeX04^{+}$) of non-injected mice (negative control) and all four genotypes of interest. (**b**) Only isolated cells from APP/PS1 and APP/PS1 / $Nlrp6^{-/-}$ animals in both cohorts show a positive signal for methoxy labelled Aβ. No visible difference was apparent when comparing APP/PS1 and APP/PS1 / $Nlrp6^{-/-}$. (**c**) Data is shown again as normalized Mean Fluorescence Intensity (MFI) by dividing the MFI of the stained sample by the MFI of the negative control. Again, no differences detectable between mice with APP/PS1 background. Graphs show mean and error bars show SEM of three independent experiments and cell isolations. Each dot represents an individual mouse.

3.5.4 Microglia mRNA Sequencing of Nlrp6$^{-/-}$ and APP/PS1 Mice

Performing mRNA sequencing reveals the presence and quantity of RNA in a biological sample at a fixed time point and gives an overview of the transcriptome. Hence, the obtained transcriptome data can be used to gain more insight into the physiological state of microglia in APP/PS1 and Nlrp6 knock out mice. Such information may in addition provide information on possible causes underlying the contradicting FACS data described above. Therefore, total microglia RNA was isolated from 3 male and 3 female mice of each genotype of the first cohort (**Figure 3.5.4**). After the reads were counted and normalized the alignment statistic showed an average over 92%. CPM normalization and the first clustering according to expression indicated one outlier in the female APP/PS1 group and had to be excluded. The calculation of presented genes with a cut off below two, as mean per group, resulted in 11.408 genes. However, the principal component analysis (PCA) of the mRNA sequences did not reveal any Nlrp6 related differences. Apparent are two clusters, microglia without an APP/PS1 background (WT & Nlrp6$^{-/-}$) and microglia with APP/PS1 (APP/PS1 & APP/PS1 / Nlrp6$^{-/-}$). This finding is not new to research and is connected with the amyloid precursor protein Aβ which is only produced in APP/PS1 animals. The amount of differential expressed (DE) genes were too low for further precise GO or pathway enrichment analyses. Hence, no further figures regarding the mRNA sequencing are displayed in this thesis. Furthermore, male and female mice seem to have different transcriptomes as well. Previous reports have shown that the sex can have an impact on microglia transcriptomics (Morgan et al., 2017). However, in this analysis the differences were not statistically significant, leading to the assumption that the number of mice might be too low for this statistic. Regarding the gender this prediction might be true, but not for the Nlrp6 phenotype because no trend is detectable.

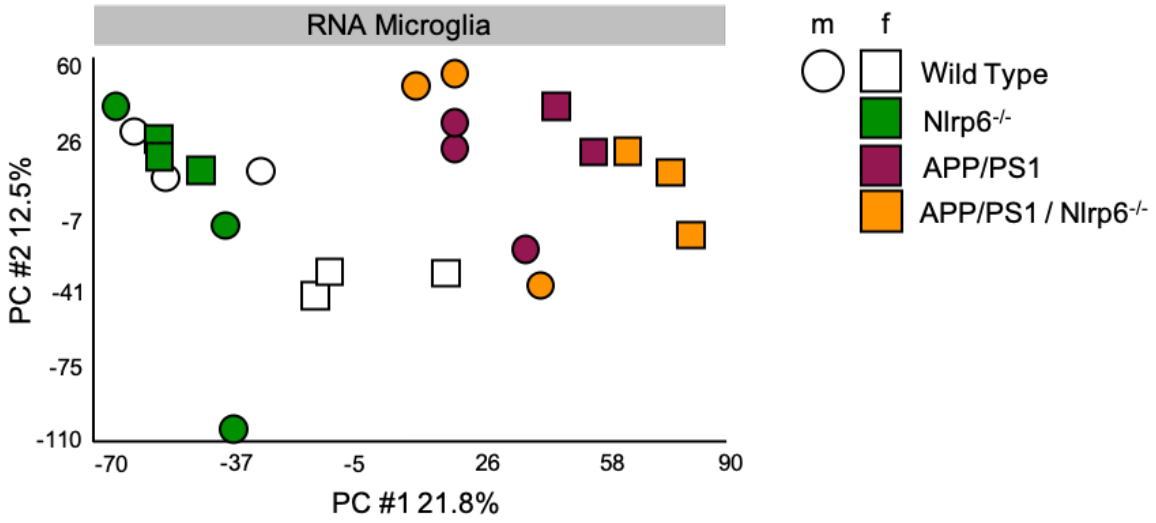

Figure 3.5.4 – RNA sequencing of microglia shows no Nlrp6 phenotype. Cohort one mice, three female and three males of each genotype, were selected for microglia mRNA sequencing. The principal component analysis (PCA) is a dimension reduction approach. It constructs linear combinations of gene expressions, called principal components (PCs). The PCs can effectively represent variation of gene expressions. To recognize is the cluster with APP/PS1 background and without. Within those clusters are no significant differences. Also, no statistical relevant difference comparing sexes. Each symbol represents one mouse.

3.6 Aβ Deposition in APP/PS1 / Nlrp6$^{-/-}$ Mice

Amyloid beta has been mentioned as the main driver of neuro inflammation and degeneration. It is found in the brain of APP/PS1 mice and AD patients. These depositions are largely responsible for the synaptic loss, memory impairment and neurotoxicity. A healthy brain is capable of internalizing excess Aβ or of promoting its transcytosis out of the brain. In contrast, when too many Aβ peptides accumulate, they become the main component of toxic Aβ plaques (Jarosz-Griffiths HH et al., 2015). At this point of the thesis, the Aβ uptake by microglia appeared to be similar between APP/PS1 and APP/PS1 / Nlrp6$^{-/-}$ mice (3.4.3). Therefore, it was crucial to take a closer look at Aβ plaques and the general Aβ concentrations in the brains of our mice of interest.

3.6.1 Aβ Plaques in the Brain of APP/PS1 / Nlrp6$^{-/-}$ Mice

Amyloid plaques are misfolded proteins that aggregate in the spaces between nerve cells. To visualize plaques, paraformaldehyde fixed mice brains were sliced sagittally into 16µm thick slices and imaged (**Figure 3.6.1**). All Aβ depositions were labelled by methoxy-X04, which was injected three hours before the brains were removed. Additionally, a 4',6-diamidino-2-phenylindole (DAPI) staining was performed. DAPI is a fluorescent stain that binds to adenine-thymine-rich regions in DNA and hence, revealing brain structures by staining all cells (Figure 3.6.1a). The images and the data showed that plaques mainly accumulate in the hippocampus and cortex. This corresponds with the AD phenotype. Usually, the areas of the brain affected first by plaques are concerned with memory and other cognitive functions, such as the hippocampus and the cortex. However, comparing the overall affected area covered by plaques, no differences were detected between APP/PS1 and APP/PS1 / Nlrp6 knock out mice (Figure 3.6.1b). The Aβ plaque area was very similar in both cohorts. Even combining cohort two and three with each other did not result in a statistically relevant Nlrp6 phenotype.

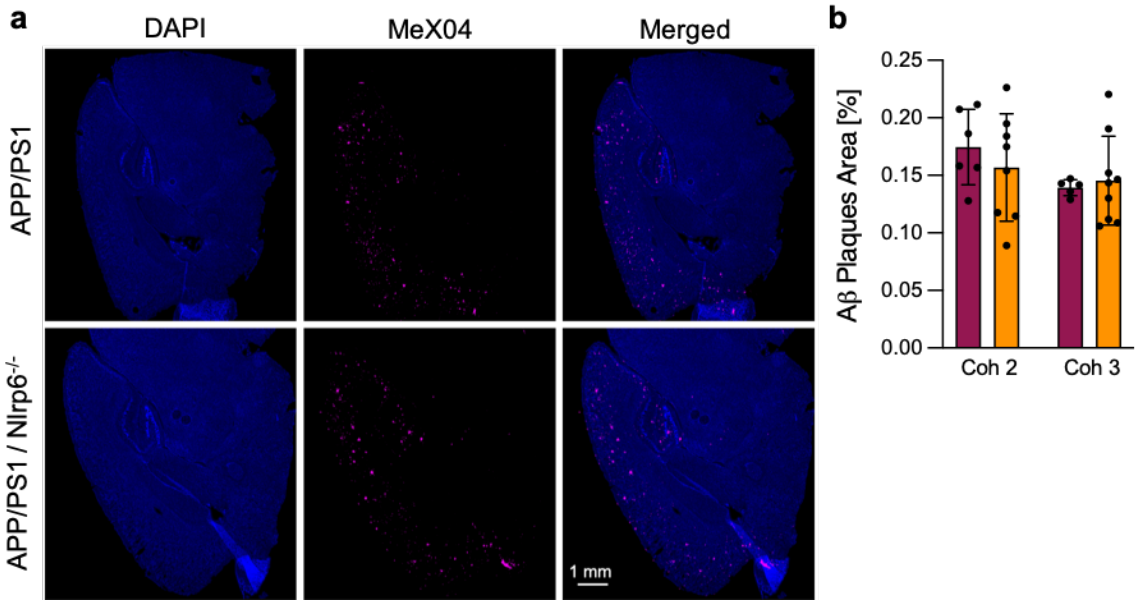

Figure 3.6.1 – Microscopy reveals similar amount of Aβ plaques in brain slices of Nlrp6$^{-/-}$ and APP/PS1 mice. Amyloid-β plaques were stained by methoxy (MeX04) injection. 16µm thick brains sagittal sliced were imaged on a Zeiss Axio scan for Aβ deposition. (**a**) DAPI was used to visualize the nuclei (blue) and MeX04 to visualize Aβ-deposition (violet). (**b**) Quantification of amyloid-β plaque given as area fraction [Aβ Plaques Area [%]. No difference in Aβ deposition between APP/PS1 and APP/PS1 / Nlrp6$^{-/-}$ mice brains. Animals with no APP/PS1 background (negative control) did not show any MeX04 staining (data not shown). Graph shows mean and error bars show SEM of cohort two and three as independent experiments. Each dot represents an individual mouse.

3.6.2 Overall Aβ Concentration in the Brain of APP/PS1 / Nlrp6$^{-/-}$ Mice

Imaging is one method to gain insight into a brain and its amyloid-β depositions. However, there are monomeric, oligomeric, or fibrillar forms of Aβ within the brain that have not been accumulated to plaques. Additionally, Aβ fibrils can occur in isoforms of different length. The 40-residue peptide (Aβ 40) is the most abundant isoform, while the 42-residue peptide (Aβ 42) increases with certain forms of AD (Schmidt et al., 2009). Another isoform is the 38-residue peptide (Aβ 38). Taking this into consideration, it was important to isolate all Aβ contained in the brain and then compare Aβ concentrations

between APP/PS1 and APP/PS1 / Nlrp6$^{-/-}$ mice. Isolating all Aβ residues is a three-step process and results in a RIPA fraction, SDS fraction and FA fraction. Each fraction was measured for Aβ 38, Aβ 40 and Aβ 42 on an MSD Multi-Spot Assay (**Figure 3.6.2**). However, no significant differences in Aβ concentration were detected. At most, cohort three seemed to show a higher signal for Aβ in some fractions and residues, e.g. Aβ 40. Nevertheless, cohort three has a lower number of animals and shows no statistical relevance and might just be a trend that can't be reproduced in cohort one and two. Additionally, the total Aβ 38, Aβ 40 and Aβ 42 amount in each fraction did not change in APP/PS1 / Nlrp6$^{-/-}$ mice brains.

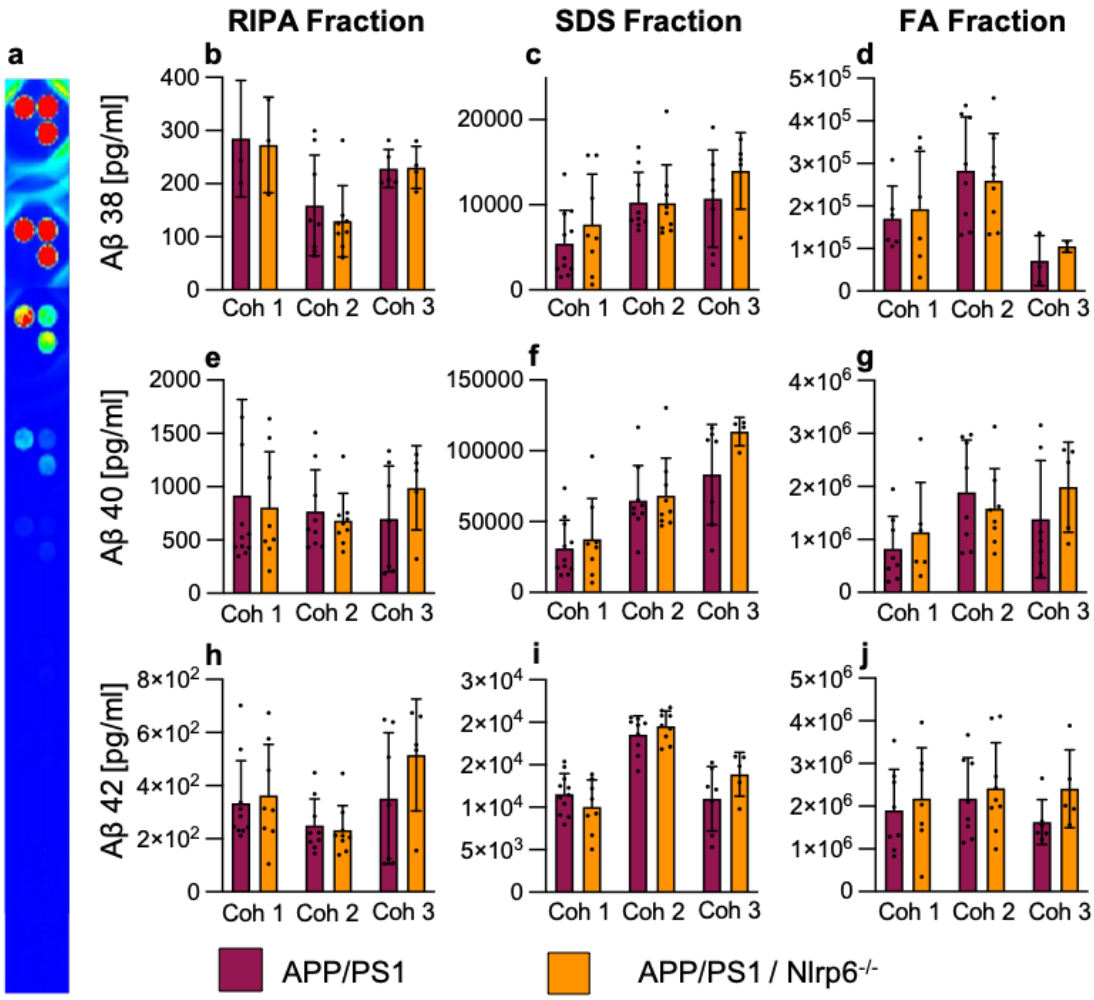

Figure 3.6.2 – Amyloid-β concentrations in brains of APP/PS1 mice differing in Nlrp6 function. (**a**) Example of signals on MSD multi-spot assay showing standard dilution from high concentration (top) to a low concentration (bottom). (**b**) Aβ 38 concentration [pg/ml] in brain homogenates after extracting the protein first with Radioimmunoprecipitation assay buffer (RIPA), then with (**c**) 2% sodium dodecyl sulfate buffer (SDS) and finally with (**d**) 70% formalic acid. Nlrp6 deletion has no effect on Amyloid-β 38 concentration. Only difference detected between cohorts. (**e,f,g**) Displaying the same protein extraction steps but only for Aβ 40. Again, only variation within cohorts but not genotypes. (**h,i,j**) No statistical difference in Aβ 42 concentration between genotypes after all three extractions. Graphs show mean and error bars show SEM of three independent experiments / cohorts. Each dot represents an individual mouse.

3.7 Pro-inflammatory Cytokines in Nlrp6 deficient and APP/PS1 Mouse Brains

Amyloid-ß challenges the innate immune system of the brain, triggering microglia receptors that have been found to regulate microglia activity. The response is a robust expression of genes that encode neuroinflammatory cytokines (Fawaz Alasmari, 2018). Cytokines are small proteins important in cell signalling, and as such, crucial for the immune response. There are pro-inflammatory and anti-inflammatory cytokines. Whereas pro-inflammatory cytokines are predominantly involved in the up-regulation of inflammatory reactions. To compare the activity status of the innate immune system in the brain of mice, we measured the following pro-inflammatory cytokines on an MSD Multi-Spot Assay: tumour-necrosis-factor-α (TNF-α), keratinocyte chemoattractant (KC) / human growth-regulated oncogene (GRO), interleukin 1 (IL-1), interleukin 2 (IL-2), interleukin 5 (IL-5) and interleukin 6 (IL-6) (**Figure 3.7**). Again, cytokine levels fluctuated between cohorts but the levels in WT, Nlrp6$^{-/-}$, APP/PS1 and APP/PS1 / Nlrp6$^{-/-}$ brains revealed no significant Nlrp6 phenotype. The main genotypic difference was between animals with APP/PS1 and those without, especially visible in the IL-1β measurements. This result can be explained because amyloid beta is solely expressed in mice with

APP/PS1. Nlrp6 seems to exert no additional effect in APP/PS1 or WT mice regarding pro-inflammatory cytokines in the brain.

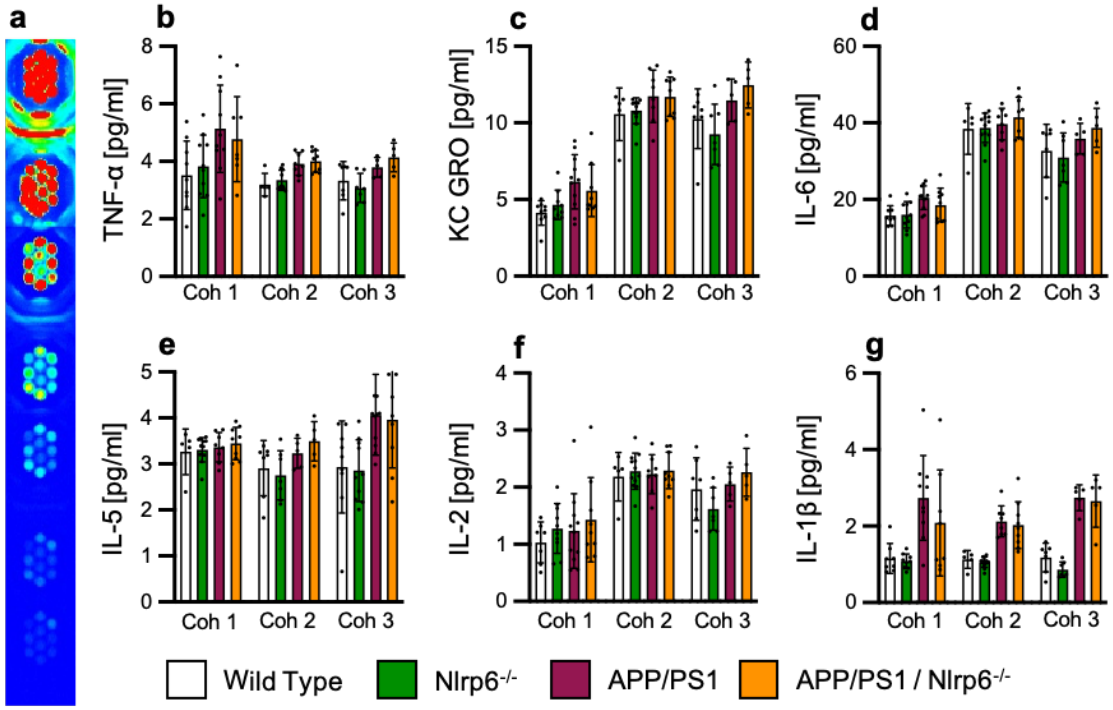

Figure 3.7 – Nlrp6 has no impact on pro inflammatory cytokines in the brain. Brain homogenates were analyzed for pro inflammatory cytokines in a mesoscale MSD multi-spot assay (mesoscale). (**a**) Example of signals on MSD multi-spot assay showing standard dilution from high concentration (top) to a low concentration (bottom). (**b**) Nlrp6 deletion does not affect TNF-α concentrations. Only mice with APP/PS1 appear to have slightly increased TNF-α. (**c**) KC GRO seems to show a trend for higher cytokine concentration in APP/PS1 and APP/PS / Nlrp6$^{-/-}$ mice. (**d**) IL-6 appears unaltered. (**e**) Lower IL-5 concentrations were measured in WT and Nlrp6$^{-/-}$ mice of cohort two and three. (**f**) Statistically IL-2 does not change within experiments. (**g**) The most severe differences have been seen in IL-1β concentrations. Animals with APP/PS1 have a significant higher concentration compared to WT and Nlrp6$^{-/-}$ mice. Represented data shows all detectable cytokines by the mesoscale assay. Graphs show mean and error bars show SEM of three independent experiments / cohorts. Each dot represents an individual mouse.

3.7.1 Caspase-1 Concentration in Nlrp6 deficient and APP/PS1 Mouse Brains

The final approach to compare the CNS's immune status in Nlrp6 deficient and APP/PS1 mouse brains was to measure the amount of caspase-1. Caspase-1 is an interleukin-1 converting enzyme and cleaves proteins, such as the precursors of pro inflammatory cytokines, into active and mature peptides. Additionally, it plays an essential role in programmed cell death, named pyroptosis. Hence, it is involved in the inflammatory neurodegenerative pathway associated with AD pathologies. To measure the amount of caspase-1, we ran the brain lysates of WT, Nlrp6$^{-/-}$, APP/PS1 and APP/PS1 / Nlrp6$^{-/-}$ mice through a size-based immunoassay (**Figure 3.7.1**). The results looked similar to the IL-1β measurements. Pro-caspase-1 levels seemed to be similar but the cleaved version was significantly increased in animals with APP/PS1. However, no Nlrp6 related phenotype was detectable. These findings suggest, that Nlrp6 has no effect on the amount of capase-1 or its cleavage.

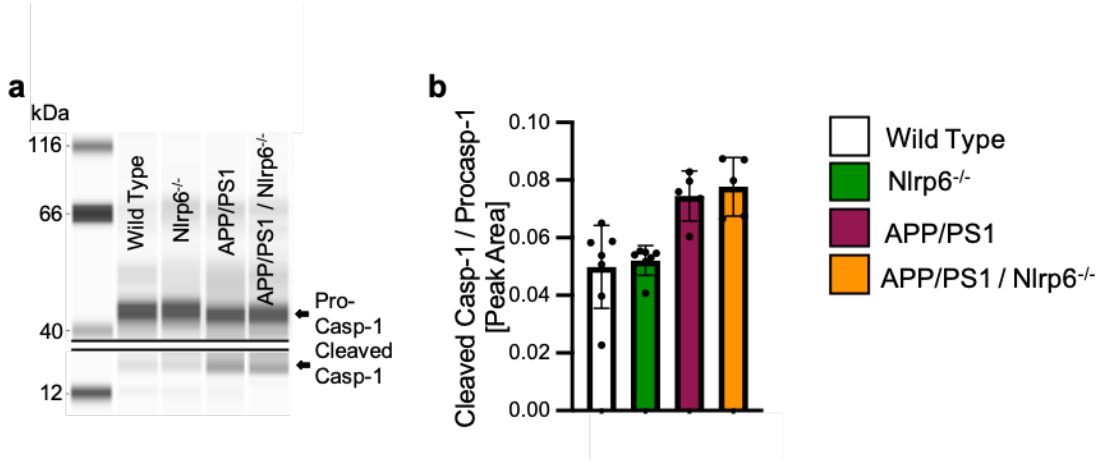

Figure 3.7.1 – Nlrp6 deletion does not affect Caspase-1 in mice brains. Simple WesternTM provides a fully automated platform for traditional western blots. (**a**) Image of capillaries showing Pro-Caspase-1 and cleaved Caspase-1 band for all four genotypes (n = 5 / genotype). (**b**) Quantification by peak area reveals an increased cleaved Caspase-1 concentration in APP/PS1 and APP/PS1 / Nlrp6$^{-/-}$ mice. Nlrp6 deletion has no detectable affect. Graphs show mean and error bars show SEM of two independent experiments. Each dot represents an individual mouse.

3.8 Western Diet induced Gut Microbiome in Ldl receptor deficient Mice

The first and overall idea of this study was to decipher individual compositional and functional microbiota variations as drivers of Alzheimer's disease. However, the Nlrp6 knock out model did not show dysbiosis in the gut microbiome, as expected. Nevertheless, there are other ways how to change the gut microbiome and consequently challenge the innate immune system. In 2018, Dr. Anette Christ performed a study on how western diet triggers the NLRP3-dependent innate immune reprogramming (Christ et al. 2018). Part of the study was to analyse stool samples of Ldl receptor knock out ($ldlr^{-/-}$) mice that were fed with a western diet (WD) or chow diet (CD) for four weeks and also included a cohort of $ldlr^{-/-}$ mice that switched back to a CD after receiving a WD for four weeks (WD>CD). Compared to the standard CD, the western diet is high in sugars, saturated fats and low in fibres. The data collected by Dr. Christ and her colleagues revealed that different dietary plans resulted in a significant change of the gut microbiome (**Figure 3.8.1**). The most prominent observation was the increased percentage of *p_Verrucimicrobia* and reduction of *p_Bacteroidetes* after a WD for four weeks. And the switch from WD back to CD seemed to restored a similar microbiome composition as the CD group. (Figure 2.8a)

Additionally, serum was collected and tested for associated lipopolysaccharide-binding proteins (LBP) (Figure 3.8b). LBP is a soluble acute-phase protein that binds to bacterial lipopolysaccharides and results in an immune response. It can be used as an indicator of bacterial infection in the blood. A four-week western diet led to a significantly increased concentration of LBP in the blood of $Ldlr^{-/-}$ mice. Hence, Microbial exposure can change levels of lipopolysaccharide-binding protein (LBP) in the serum, which has been associated with Overweight, obesity and metabolic syndromes. However, when switched back to a CD the LBP levels go back down.

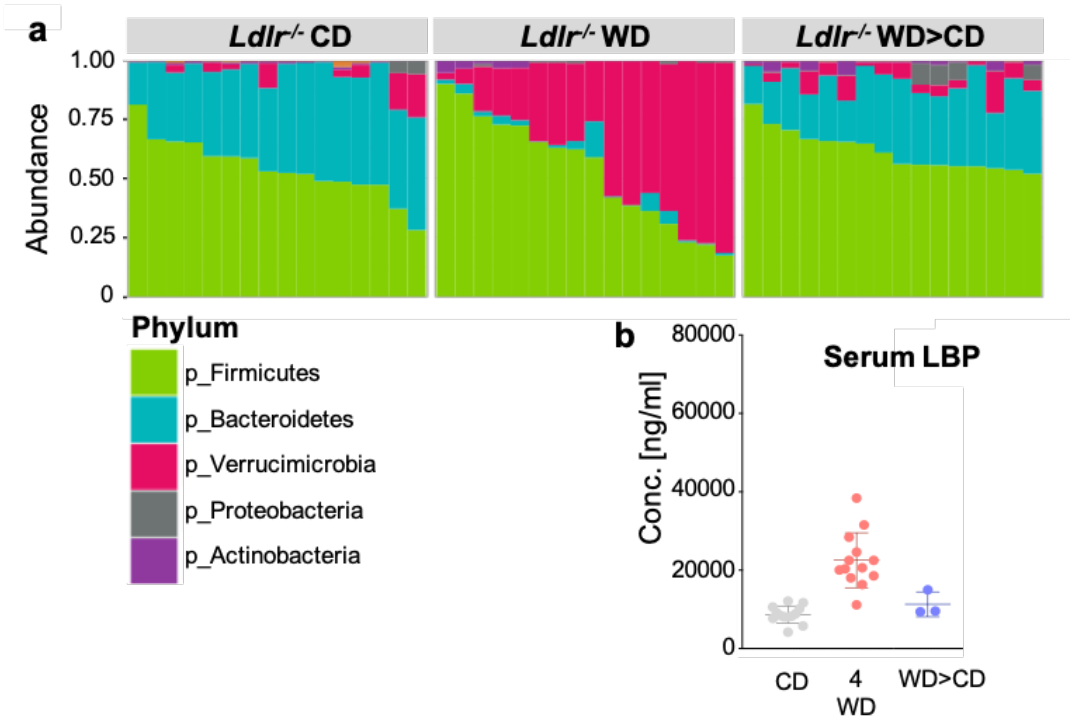

Figure 3.8.1 – Western diet induces transient changes in the gut microbiome. A western diet was fed for 4 weeks (WD) to induce hypercholesterolemia in Ldl receptor knock out mice. Additionally, a switch after 4 weeks of WD back to chow diet (CD) was performed (WD > CD). A continuous CD functions as control. Stool samples were collected after dietary plans and sequenced for microbiome. (**a**) Abundance shows how many percentages of the microbiome is made of a specific organism. To highlight, WD results in an increased percentage of p_Verrucimicrobia and reduction of p_Bacteroidetes. The switch from WD back to CD reverses most of the microbiome composition. (**b**) Concentrations of associated lipopolysaccharide-binding protein (LBP) in serum have been mesured and the concentration increases significantly after 4 weeks of WD. Graphs show mean and error bars show SEM of one experiment. Each dot represents an individual mouse.

3.9 Microglia mRNA Sequencing of Western Diet fed Ldl receptor deficient Mice

The change in diet led to alterations of the gut microbiome and increased levels of LBP. This observation enabled us to investigate how the innate immune system of the brain reacts to changes of the gut microbiome. To do so, we received isolated microglia from the same Ldlr$^{-/-}$ mice which were on different dietary plans: CD, WD or WD>CD. Thereafter, we isolated, sequenced and analyzed the mRNA sequences. The Principal

component analysis revealed clear clusters for each dietary plan, suggestion a transcriptional adjustment of microglia and reaction of the innate immune system of the brain (Figure 2.8a). Furthermore, switching from WD back to CD for four weeks resulted in an even higher mRNA variation in microglia: 1025 differentially expressed (DE) genes (Figure 2.8b & c). 379 genes were down-regulated and 646 genes up-regulated. Hence, WD seems to change the long-term expression of genes in microglia of $Ldlr^{-/-}$ mice.

Table of Differentially Expressed genes

	Up reg, genes	Down reg. genes	Summary
CD vs. WD	5	27	32
WD vs. WD>CD	17	4	11
CD vs. WD>CD	379	646	1025

Furthermore, after an infection, the body's first line of defense are cytokines that are secreted by host cells by inducing the expression of interferon associated genes. Of all identified genes, 34% of down regulated and 46% of up regulated genes were interferon associated (Figure 3.8e). Additionally, the 646 down-regulated genes were mainly associated with proximal tubule bicarbonate reclamation, protein processing in endoplasmic reticulum and tight junctions, hippo signaling and bile secretion. On the other hand, the 379 up regulated genes are mainly involved in mRNA surveillance pathways, Influenza A, toll-like receptor signaling pathway, carbohydrate digestion and absorption, type II diabetes mellitus and NOD-like receptor signaling pathways (Figure 3.8d).

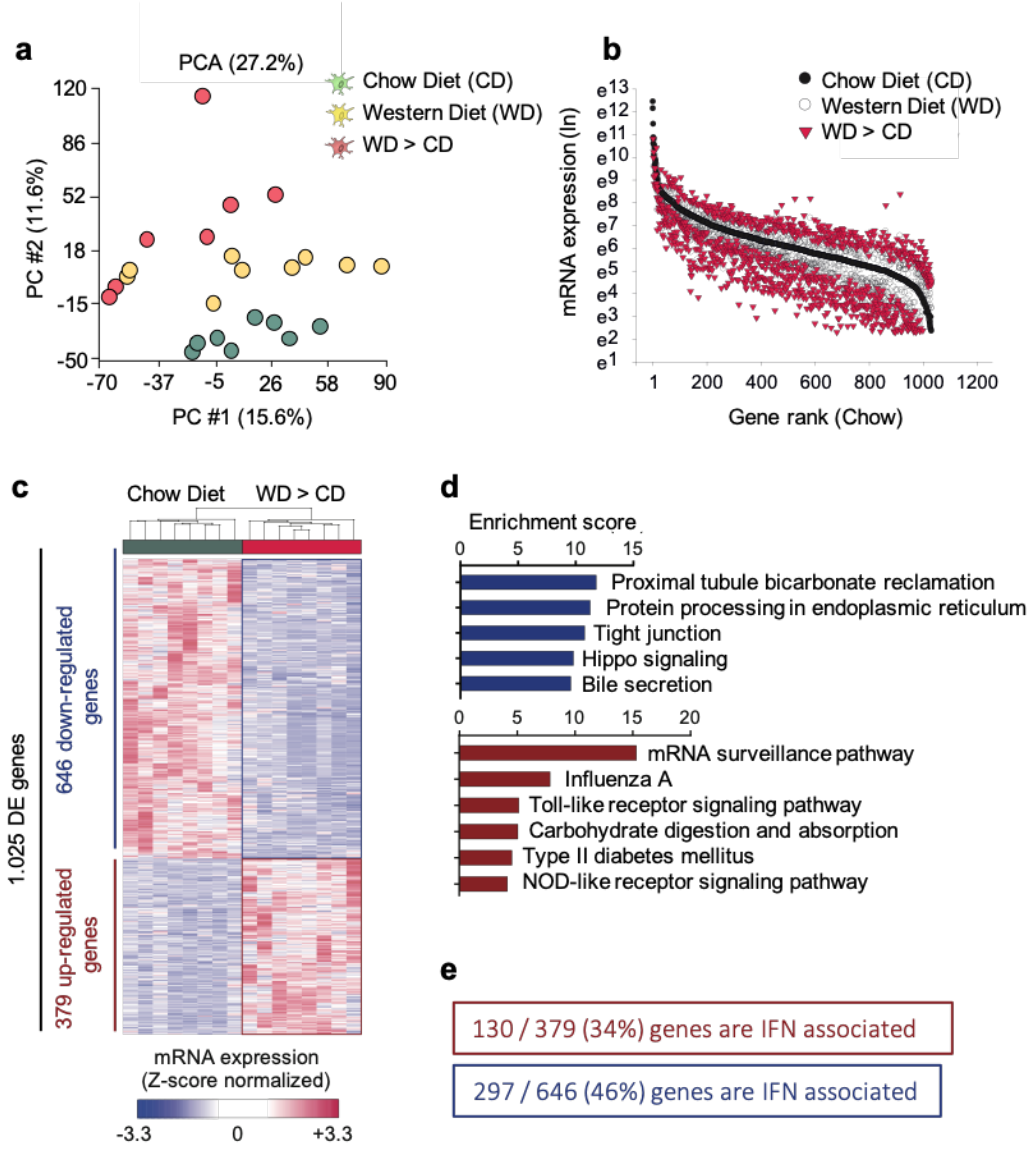

Figure 3.8.2 – Western diet induces variation in mRNA expression of microglia in the brain. Microglia of Ldl receptor knock out mice on CD, WD and WD>CD were isolated and mRNA sequenced. (**a**) Principal component analysis (PCA) displays independent clusters for each dietary plan. Each symbol represents one mouse (**b**) The switch from WD>CD to CD does not reprogram mRNA expression in microglia. Gene rankings confirm even a higher mRNA variation after the WD>CD switch. Hence, WD changes the long-term expression of genes. (**c**) Heat Map of 1025 differentially expressed (DE) genes. Comparing CD and WD>CD shows a majority of genes is down regulated and a specific gene cluster is up regulated. (**d**) Enrichment score of up (blue) and down (red) regulated genes indicate the associated function. (**e**) 34% of down regulated and 46% of up regulated genes are interferon associated.

4. Discussion

4.1 Almost no Nlrp6 Expression in the Brain of Mice

Inflammasomes are formed in various tissues and cell types. The first task of this thesis was to clarify where NLRP6 is expressed in mice. In house experiments and published data suggested that Nlrp6 is mainly expressed in the large intestine, liver and kidney, while NLRP6 expression in the brain is very low and almost considered as background. Hence, we assumed that any effects of knocking out the *NLRP6* gene apparent in the brain, would have to arise from the periphery, such as the microbiome or systemic inflammation. However, more recent studies had investigated NLRP6 also in the CNS and some findings indicated NLRP6 expression in the brain. For example, one study showed increased Nlrp6 expression in the brain of rats, which were used as a middle cerebral artery occlusion/reperfusion model. In this case, the upregulated brain expression of NLRP6 was considered to be neuroprotective because cerebral injury was aggravated and neurological functions worsened (Meng C. et al., 2019). Another finding, suggesting a neuroprotective role of NLRP6, was derived from downregulating Nlrp6 with micro RNA (miR-331-3p) in mice, which decreased the inflammatory response and restored neurological functions after intracerebral hemorrhage (Nie H. et al., 2020). In addition, NLRP6 inflammasome assembly was also recorded in vitro in astrocytes, which were oxygen-glucose deprived. The assembly triggered production of pro-inflammatory cytokines such as IL-1ß and IL-8, and was coupled with pyroptosis (Zhang J. et al., 2020). Taken all together, NLRP6 might have a more direct role in the CNS and during the development of neurodegenerative diseases, such as AD.

The NLRP6 in house experiments performed by Dr. Herzig included the comparison of NLRP6 expression in brain tissue from WT and NLRP6$^{-/-}$ mice by qPCR and immunohistochemistry. The results looked similar to the Tabula Muris data, suggesting barely any NLRP6 expression in the brain of mice. In addition, no NLRP6 was detected in any of the two microglia RNA data sets of this thesis. However, it would be of interest for this study to see whether Nlrp6 expression levels vary in the brain between the four

different genotypes, WT, Nlrp6$^{-/-}$, APP/PS1 and APP/PS1 / Nlrp6$^{-/-}$. In order to achieve maximum sensitivity, the protocols reported in the publications mentioned above should be tried. So far, no study has compared Nlrp6 expression in the brain when challenged with AD. To keep in mind, because Nlrp6 expression will always be relatively low, the impact of systemic factors warrants a continued thorough investigation when researching NLRP6 in the brain.

4.2 Contradicting Microbiome Results in NLRP6 Knock Out Mice

Studying the impact of host genes on the gut microbiome can be very complicated. Environmental factors influence the microbiome composition significantly (CS Chang et al., 2019). Translating this into a mouse study, different conditions need to be taken into consideration, e.g. food, medication, littermate effects and cage conditions. Because littermate and environmental factors can have such a strong impact on the gut's microbiome it could also mask any effects of the host's genotype. The impact of the host's genotype might also be masked if the diversity and quantity of microbes is too low. Hence, animal facilities that house mice for scientific purposes might not be the best environment to study changes of the microbiome caused by host genotypes. Animals research facilities are usually very clean with a significantly reduced micro-environment. In addition, the animal facility HET 1, animal facility for this study, works with the highest standards and should be considered even cleaner than other facilities. Another aspect is the time point when the microbiome is taken and compared. This can be crucial because of the microbiota's natural ability to change due to environmental changes.

4.2.1 NLRP6 Microbiome Phenotype

With that being said, the microbiome variation between all three analyzed cohorts might be explained by environmental factors. Cohort 1 showed signs of a NLRP6 phenotype in the gut microbiome, ranging from the age of 3 months to 9 months. Unfortunately,

only 5 mice per genotype were selected, reducing the statistical power. Also, all stool samples, which were collected from mice at an age of one year, were not sequenced. Even more relevant is that the microbiome of Cohort 1 was never sequenced after undergoing behavior testing in the Morris water maze (MWM) at the animal facility HET3.

Approximately one year after the first cohort, the second cohort reached an age of one year, went through behavior testing in the MWM at the HET3 and afterwards all stool samples of all animals were collected and sequenced. In contrast to cohort 1, the only stool samples sequenced were those which were collected after the MWM test. However, a NLRP6 phenotype was detected and the host genotype effect appeared to be reproducible.

The information on whether the samples were collected before or after the MWM test is relevant because the last cohort, number 3, never moved to the HET3 for the MWM test. The MWM test was closed due to COVID 19 restrictions in 2021. Hence, all stool samples of cohort 3 were collected from mice that never changed their location to the animal facility HET3. Eliminating this environmental factor seemed to result in the disappearance of a suspected NLRP6-related phenotype regarding the gut microbiome. In contrast, cohort 1 and 2 spent four weeks at the HET3 for adjustment purposes and the behavior test. Furthermore, within the HET3 the animals experienced various environmental changes such as: additional mice with various genotypes, lower hygiene regulations, a different light / dark cycle and more people with different tasks going in and out.

These findings seem to support the notion that a reduced microbiome can mask host genetic effects on the gut microbiome. The phenotype of Nlrp6 knockout WT and APP/PS1 mice was only significantly altered after moving the animals to a different location with a more diverse micro environment, such as the HET3, for 4 weeks. This might also suggest that the animals where not challenged by a NLRP6 loss-of-function-dependent dysbiosis while growing up in the HET1, because the micro environment seemed to be too restricted for any genetically induced changes in the gut microbiome.

With these contradicting microbiome results in all three analyzed cohorts, it is crucial for future studies investigating the role of NLRP6 in modulating the gut microbiome, to introduce proper environmental condition, exact time points and preferably additionally microbial-transfer strategies.

4.2.2 APP/PS1 Microbiome Phenotype

The focus of this thesis was to induce changes in the gut microbiome by NLRP6 deletion. However, some studies have shown that the APP/PS1 genotype can also cause shifts in microbiome composition during ageing (Bäuerl C. et al., 2018 & Harach T. et al., 2017). This APP/PS1 phenotype was not detectable within any cohort of this study. Again, the genetic impact of the host on the gut microbiome could have been masked by lacking or overwhelming environmental factors.

4.2.3 Alternatives of Influencing the gut Microbiome in Mice

The number of environmental factors capable to influence the gut microbiome of laboratory animals is overwhelming. Factors to be taken into consideration are e.g. the source of the animals (Ericsson et al., 2015), the diet (Ericsson et al., 2018), caging conditions, bedding (Ericsson et al., 2015), water treatment (Bidot et al., 2018), transportation (Montonye et al., 2018), housing density (Basson et al., 2020), sex (Kozik et al., 2017), genotype (Ericsson et al., 2015), or medications (Zhao et al., 2020). However, the impact of these factors also opens opportunities for research to determine how various microbes interact with the host. An example are microbial activators and inhibitors that possibly fine-tune the activation of the innate immune system and therefore influence gut homeostasis. Approaches to find such factors have been used at the Institute of Innate immunity with respect to the impact of nutrition. Mice were exposed to different high fat dietary plans. Other groups including the one led by our collaborator Prof. Dr. Eran Elinav at the Weizmann Institute of Science, Israel, takes it even further by housing germ free mice, performing microbial-transfer strategies and

antibiotic treatments. Because these strategies have a very strong impact on the gut microbiome, it would have been interesting to see potential effects in our APP/PS1 model and the development of AD. In medical therapy, manipulating the microbiome may in the future even be harnessed to control infectious, inflammatory and potentially metabolic diseases. However, the cellular and molecular level needs to be investigated in more depth to develop such therapeutic strategies.

4.3 Impact of NLRP6 on AD Development in APP/PS1 Mice

Until today, the best understood inflammasome within the CNS is the NLRP3 inflammasome. Heneka et al. showed in 2013 the important role of NLRP3 in the pathogenesis of AD, and suggested NLRP3 inhibition as a new therapeutic intervention for the disease. In the meantime, even more inflammasomes have been implicated in the progression of neurodegenerative diseases, such as NLRP1, NLRP2 and AIM2. All these inflammasomes are similar in structure and the activation of their sensors lead to oligomerization. This is followed by the formation of multiprotein complexes that serve as platform to activate inflammatory caspases. For Nlrp6, however, it was only recently shown that it can also assemble an inflammasome in vivo and during microbial infection. Also, while most of the NLRP6 research has been concentrated on the gut microbiome, the role of the molecule in neurodegeneration has only recently gained attention. New sensors and downstream signaling pathways of NLRP6 are constantly being elucidated. However, NLRP6 has not been investigated in a mouse model of AD.

In summary, this study did not show a clear NLRP6-dependent phenotypic change in the development of AD pathogenesis or neuroinflammation in APP/PS1 mice. The behavior MWM test showed no significant difference between APP/PS1 and APP/PS1 / Nlrp6$^{-/-}$ mice. Also, none of the other tests for neuroinflammation and AD pathogenicities indicated any NLRP6 influence. The only exception was the microglia FACS data which suggested an increased TLR2 expression in NLRP6 deficient APP/PS1 mice. Again, this result was not reproducible in all cohorts. However, here we need to take into consideration that some of the variation might have been introduced because the microglia isolation was performed on different days and with the help of

different scientists, especially for cohort 2. Handling the very delicate procedure of isolating and analyzing microglia cells can have a significant impact on the result.

Of course, the absence of a dysbiosis in the gut microbiome, due to environmental factors, could explain the negative data. While growing up, the animals might have been never challenged by a NLRP6-influenced microbiome at the animal facility HET 1. Moreover, the short time at the animal facility HET3 may have been insufficient to generate a more progressed state of AD pathogenesis in mice. However, the sampling scheme, i.e. the timing of sample collection, was based on known data for AD progression in APP mice. All MWM tests were performed and all brain samples were taken from mice at an age of one year. At this time point, all the available data sets suggest neuroinflammation and AD pathology in mice with APP/PS1 background. AD progression is usually at its maximum in APP/PS1 mice after one year. Therefore, it cannot be ruled out that differences between genotypes might be difficult to detect if the NLRP6 inflammasome accelerates neuroinflammation or the development of AD pathogenesis. Here, a younger age of mice should have been considered to compare AD progression, e.g. at 6 months of age. Initially, this age control was planned. However, the breeding process took too long to generate the needed additional cohorts.

4.4 NLRP6 deficiency does not Induce systemic Inflammation or Metabolomic Changes in APP/PS1 Mice

In the context of gut microbes inducing changes in the brain, it is necessary to consider the gut-brain link. Multiple studies in humans and mice have suggested that systemic inflammation may promote neurodegeneration, cognitive decline and AD pathology (Keenan A. et al., 2019). One readout to detect the manifestation of systemic inflammation is measuring pro-inflammatory cytokines. Their concentration may increase as a result of events such as infection, chronic diseases and physical stress. Pro-inflammatory cytokines within the body can increase the pro-inflammatory environment in the CNS through the gut-brain link (R. Daneman et al., 2015). As a

consequence, systemic inflammation is believed to induce pro-inflammatory phenotypes in microglia which can promote Aβ oligomerization. These potentially harmful bioactive metabolites can lead to progressive cognitive decline and AD pathology (Keenan A. et al., 2019).

Furthermore, downstream effects of the gut microbiome and NLRP6 inflammasome activation beyond the secretion of pro-inflammatory cytokines may be apparent in the organism's metabolism. Thus, it is important to search for possible changes in the metabolome of various host tissues. The brain requires a high amount of energy for all its processes, including synaptic activity and neurotransmitter production. Therefore, the brain requires about 20% of the body's total energy, measured in ATP (Jain et al., 2010). Although the brain only takes up 2% of the bodyweight, its energy demand is much higher compared to other tissues. Hence, systemic changes in metabolomes can have a strong impact on the brain (Joshi and Mochly-Rosen, 2018).

Experiments performed for this thesis did not detect any significant metabolic changes in the serum of NLRP6 deficient APP/PS1 mice compared to WT, NLRP6$^{-/-}$ and APP/PS1 mice. Possibly, this is again due to the lack of a microbial challenge in the gut. However, after being exposed to the MWM at the animal facility HET3, a shift in the gut microbiome occurred and a metabolomic adjustment could have been expected. In addition, no significant increase of pro-inflammatory cytokine levels were observed in any NLRP6 expressing organ including the kidney, liver and intestine, when comparing all four genotypes with each other. The intestine of APP/PS1 / NLRP6$^{-/-}$ mice did show signs of inflammation with increased, albeit not significantly, IL-12p70 and KC/GRO cytokine levels. This might be a reaction towards the environmental factors at the HET3. The results, suggest that no relevant systemic inflammation was induced by NLRP6 or the APP/PS1 genotype. This finding might also explain why all the data sets for neuroinflammation and AD pathology in the brain were negative regarding the NLRP6 phenotype. No pro-inflammatory signals were transmitted through the gut-brain link to induce additional neuroinflammation or prevent AD progression.

4.5 Dietary Impact on RNA Expression in Microglia

The availability of Ldl receptor knock out mice on different dietary plans, investigated in a parallel study led by Dr. Anette Christ, provided an opportunity to check if this environmental factor can change the gut microbiome in our animal facilities. Also, we were able to investigate changes in the brain occurring after different dietary plans. Previously, it had been shown that the western diet (WD) induced systemic inflammation in these Ldrl$^{-/-}$ mice (Christ A., et al. 2018).

The significant impact of a high fat diet on the composition of the gut microbiome has been demonstrated many times in mice and in humans (Carmody et al., 2015; David et al., 2014). Furthermore, the effect of a WD on the organism has been studied, even in context of NLRP6. For example, the gut microbiome composition, challenged by a high fat diet, can dictate metabolic condition, including diet induced obesity and non-alcoholic fatty liver disease (NAFLD). Apparently, the NLRP6 inflammasome can regulate and influence the progression of NAFLD and obesity by regulating the gut microbiota in mice (Henao-Mejia J. et al., 2012). Nevertheless, after experiencing the significant impact of environmental factors on the gut microbiota in our own NLRP6 study, it was interesting to see that we were able to challenge the gut microbiome by WD in Ldlr knock out mice and induce systemic inflammation.

It is widely accepted that a high fat diet can induce obesity-related metabolic disorders, combined with low-level systemic inflammation (Mollica et al., 2011). When the inflammatory state is prolonged, it can compromise cell functions in all organs, leading to altered metabolism and associated pathological conditions (Hernándes-Aguilera et al., 2013). As mentioned, this form of system inflammation can be an important risk factor for neurodegenerative diseases (Kumar, 2018). Indeed, studies show that a high fat diet can activate signalling pathways in several brain regions, such as the cortex and hippocampus (Chen et al., 2019). Similar to the hypotheses guiding this thesis, transcriptome changes in the brain have been assumed to be important in the regulation of metabolic diseases, linking nutritional influence, neuroinflammation and brain-related mechanisms together (Hanin et al., 2018; Haviv et al., 2018).

The microglia transcriptome, extracted from Ldlr$^{-/-}$ mice on different western dietary plans, showed a strong reaction to the altered nutrition and gut microbiome. Interesting was the unexpected big difference observed in the animals which were on a chow diet (CD) after being fed a WD (WD > CD), compared to the cow diet only. The dietary impact seemed to have a prolonged effect on mRNA expression in microglia. Dr. Anette Christ also saw epigenetic reprogramming of innate immune cells in response to microbes. Arguing, that the prolonged altered cellular functionality protects the organism from secondary infections. (Christ A. et al., 2018). The enrichment scores of the microglia mRNA sequence data presented in this thesis also suggests an innate immune response by indicating up regulated Toll-like and NOD-like receptor pathways.

The increased response amplitude of transcript abundance in microglia after switching from WD to a CD might be a hint why the microglia mRNA sequencing data derived from the NLRP6 in APP/PS1 study did not show any NLRP6 phenotype, even though the gut microbiome shifted after going through the MWM test. Possibly, microglia transcriptomes need more time to react. Harvesting all microglia samples right after the behaviour experiment might have been too early to see gut microbiome induced changes in microglia transcriptomics. This thought might also affect all the other experiments conducted in the brain.

Based on the observation discussed here, a very interesting experimental setting would be to challenge APP/PS1 mice with a high fat WD and see how this environmental factor changes the gut microbiome and consequently the progression of AD. In addition, NLRP6 knock out mice, in combination with APP/PS1, could be challenged with a WD too. This might force a gut microbiome shift and NLRP6 might cause an additional dysbiosis. The WT and NLRP6$^{-/-}$ control need to be included as well. Hence, this experimental setup could reveal how NLRP6 interacts with the gut microbiome, challenged by WD, and monitor changes in microorganisms and in the CNS.

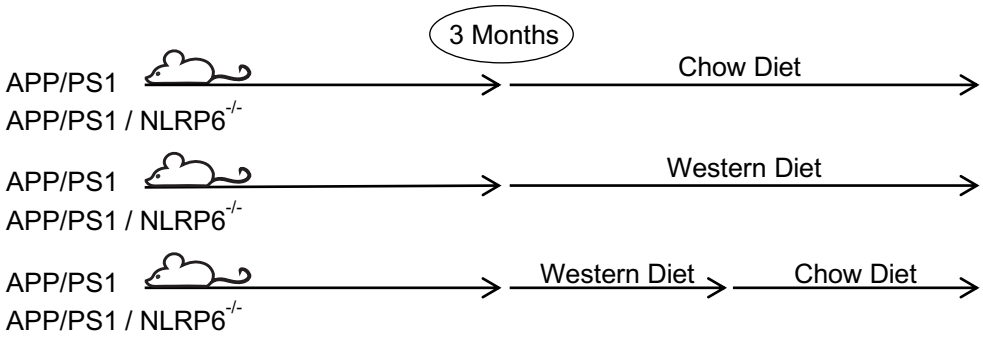

Proposed Experiment: At an age of 3 months, APP/PS1 and APP/PS1 / NLRP6 $^{-/-}$ mice are put on a CD, WD or WD>CD for 4 weeks, similar to the previous dietary plans. Thereafter, sequence the gut microbiome and check for systemic inflammation, neuroinflammation and AD pathology progression.

4.6 Conclusion

Since more and more evidence has shown strong association between inflammatory diseases and the gut microbiota, understanding the dynamic crosstalk of host and microbe interactions in the gut has become a rapidly developing field in the context of detection, prevention and therapy of neurodegenerative diseases. Alzheimer's disease has been associated with a wide variety of symptoms in the CNS and the periphery. To date, mainly the NLRP3 inflammasome has been recognized and applied as promising intervention in inflammatory diseases. However, given the intimate interaction of the NLRP6 inflammasome and the gut microbiome, similar therapeutic applications have been considered. How various microbial activators and inhibitors fine-tune the activation of NLRP6 and therefore influence gut homeostasis is yet to be determined. Unfortunately, this study cannot establish whether individual compositional and functional microbiota variants are associated with AD. The animal housing facilities, with their suspected lack of a micro environment resembling a natural situation were not adequate to address the question to our satisfaction. A more controlled and standardized micro environment would have been necessary to derive assumptions as to the NLRP6 inflammasome and the microbiome involvement in AD development. However, current knowledge and some insight suggested by this study might encourage future studies to develop strategies to decipher a cell-specific role of NLRP6 and decode NLRP6 modulated pathways.

5 Abstract

Alzheimer's disease (AD) is an irreversible, progressive neurodegenerative brain disorder. The progression of AD is characterized by the deposition of amyloid-β peptides and hyperphosphorylated Tau proteins, causing loss of memory and cognitive skills. It is the most common human dementia and as such confers a huge emotional and economic burden on patients, caregivers and society. Environmental influences are thought to be the main cause for disease development, manifestation, and progression. And inflammatory molecules in the brain, such as pro-inflammatory cytokines, were discovered to participate in perpetuating molecular pathways driving neurodegeneration. Inflammatory processes can be triggered by pathogen-associated molecules as well as endogenous danger signals. A source of pathogen-associated molecules is the microbiota, which also emerged as a major component of human physiology and pathology, integrating influences from host genetics and environmental impact. Alterations in the composition and function of the microbiota have been recently highlighted to dramatically affect a number of neurological diseases, yet the mechanisms linking microbiota changes in the gut to distal CNS disorders remain poorly understood.

The aim of this study was to use NLRP6-deficient mice as a dysbiosis model to characterize dysbiosis development during AD and how innate immune control of the microbiota impacts AD disease development. The hemizygous double transgenic mouse model APP/PS1 was used as a well-established model system for human Alzheimer's disease. However, microbiome sequencing data from stool samples of all mice revealed strong fluctuations between each independent cohort. Suggesting that environmental variations in microbiota diversity and quantity masked the host’s NLRP6 dysbiosis phenotype. Under the given circumstances a combination of cognitive analysis, metagenomics and different experimental set ups to compare neuro-inflammation and -degeneration in mice suggested almost no involvement of NLRP6 in AD development. The only statistical relevant finding was the increased expression of TLR2 on microglia, the immune cells of the brain, of NLRP6 deficient mice with APP/PS1 background compared to NLRP6 wild type mice with APP/PS1. The hypothesis that deciphering the inter-individual variability in microbiota composition and

its impact on inflammatory processes involved in AD may hold the key to better understanding is still valid. This was supported by feeding mice a high fat diet which lead to variations in the gut microbiome and also induced an astonishing effect on the RNA transcripts of microglia. Ongoing studies and findings of this thesis might encourage future studies to develop strategies to target the microbiome by NLRP6 deletion and decipher NLRP6 modulated pathways in AD development.

6 List of Figures

3.5.4	RNA sequencing of microglia shows no Nlrp6 phenotype
3.6.1	Microscopy reveals similar amount of Aβ plaques in brain slices of Nlrp6-/- and APP/PS1 mice
3.6.2	Amyloid-β concentrations in brains of APP/PS1 mice differing in Nlrp6 function
3.7	Nlrp6 has no impact on pro inflammatory cytokines in the brain
3.7.1	Nlrp6 deletion does not affect Caspase-1 in mice brains
3.8.1	Western diet induces transient changes in the gut microbiome
3.8.2	Western diet induces variation in mRNA expression of microglia in the brain

7 References

Akiyama H. Inflammation and Alzheimer's disease. Neurobiology of Aging 2000; 21: 383–421

Alasmari F, Alshammari MA, Alasmari AF, Alanazi WA, Alhazzani K. Neuroinflammatory Cytokines Induce Amyloid Beta Neurotoxicity through Modulating Amyloid Precursor Protein Levels/Metabolism. Biomed Res Int 2018; 2018: 3087475

Al-Haddad BJS, Jacobsson B, Chabra S, Modzelewska D, Olson EM, Bernier R, Enquobahrie DA, Hagberg H, Östling S, Rajagopal L, Adams Waldorf KM, Sengpiel V. Long-term Risk of Neuropsychiatric Disease After Exposure to Infection In Utero. JAMA Psychiatry 2019; 76: 594–602

Bäckhed F, Roswall J, Peng Y, Feng Q, Jia H, Kovatcheva-Datchary P, Li Y, Xia Y, Xie H, Zhong H, Khan MT, Zhang J, Li J, Xiao L, Al-Aama J, Zhang D, Lee YS, Kotowska D, Colding C, Tremaroli V, Yin Y, Bergman S, Xu X, Madsen L, Kristiansen K, Dahlgren J, Wang J, Jun W. Dynamics and Stabilization of the Human Gut Microbiome during the First Year of Life. Cell Host Microbe 2015; 17: 690–703

Baron R, Babcock AA, Nemirovsky A, Finsen B, Monsonego A. Accelerated microglial pathology is associated with Aβ plaques in mouse models of Alzheimer's disease. Aging Cell 2014; 13: 584–595

Basson AR, LaSalla A, Lam G, Kulpins D, Moen EL, Sundrud MS, Miyoshi J, Ilic S, Theriault BR, Cominelli F, Rodriguez-Palacios A. Artificial microbiome heterogeneity spurs six practical action themes and examples to increase study power-driven reproducibility. Sci Rep 2020; 10: 5039

Bäuerl C, Collado MC, Diaz Cuevas A, Viña J, Pérez Martínez G. Shifts in gut microbiota composition in an APP/PSS1 transgenic mouse model of Alzheimer's disease during lifespan. Lett Appl Microbiol 2018; 66: 464–471

Benson AK, Kelly SA, Legge R, Ma F, Low SJ, Kim J, Zhang M, Oh PL, Nehrenberg D, Hua K, Kachman SD, Moriyama EN, Walter J, Peterson DA, Pomp D. Individuality in gut microbiota composition is a complex polygenic trait shaped by multiple

environmental and host genetic factors. Proc Natl Acad Sci U S A 2010; 107: 18933–18938

Bidot WA, Ericsson AC, Franklin CL. Effects of water decontamination methods and bedding material on the gut microbiota. PLoS One 2018; 13: e0198305

Birchenough GMH, Nyström EEL, Johansson MEV, Hansson GC. A sentinel goblet cell guards the colonic crypt by triggering Nlrp6-dependent Muc2 secretion. Science 2016; 352: 1535–1542

Blacher E, Bashiardes S, Shapiro H, Rothschild D, Mor U, Dori-Bachash M, Kleimeyer C, Moresi C, Harnik Y, Zur M, Zabari M, Brik RB-Z, Kviatcovsky D, Zmora N, Cohen Y, Bar N, Levi I, Amar N, Mehlman T, Brandis A, Biton I, Kuperman Y, Tsoory M, Alfahel L, Harmelin A, Schwartz M, Israelson A, Arike L, Johansson MEV, Hansson GC, Gotkine M, Segal E, Elinav E. Potential roles of gut microbiome and metabolites in modulating ALS in mice. Nature 2019; 572: 474–480

Block ML, Zecca L, Hong J-S. Microglia-mediated neurotoxicity: uncovering the molecular mechanisms. Nat Rev Neurosci 2007; 8: 57–69

Bolmont T, Haiss F, Eicke D, Radde R, Mathis CA, Klunk WE, Kohsaka S, Jucker M, Calhoun ME. Dynamics of the microglial/amyloid interaction indicate a role in plaque maintenance. J Neurosci 2008; 28: 4283–4292

Brookmeyer R, Johnson E, Ziegler-Graham K, Arrighi HM. Forecasting the global burden of Alzheimer's disease. Alzheimers Dement 2007; 3: 186–191

Broz P, Dixit VM. Inflammasomes: mechanism of assembly, regulation and signalling. Nat Rev Immunol 2016; 16: 407–420

Caporaso JG, Kuczynski J, Stombaugh J, Bittinger K, Bushman FD, Costello EK, Fierer N, Peña AG, Goodrich JK, Gordon JI, Huttley GA, Kelley ST, Knights D, Koenig JE, Ley RE, Lozupone CA, McDonald D, Muegge BD, Pirrung M, Reeder J, Sevinsky JR, Turnbaugh PJ, Walters WA, Widmann J, Yatsunenko T, Zaneveld J, Knight R. QIIME allows analysis of high-throughput community sequencing data. Nat Methods 2010; 7: 335–336

Carmody RN, Gerber GK, Luevano JM, Gatti DM, Somes L, Svenson KL, Turnbaugh PJ. Diet dominates host genotype in shaping the murine gut microbiota. Cell Host Microbe 2015; 17: 72–84

Chang C-S, Kao C-Y. Current understanding of the gut microbiota shaping mechanisms. J Biomed Sci 2019; 26: 59

Chaplin DD. Overview of the immune response. J Allergy Clin Immunol 2010; 125: S3-23

Chen GY, Liu M, Wang F, Bertin J, Núñez G. A functional role for Nlrp6 in intestinal inflammation and tumorigenesis. J Immunol 2011; 186: 7187–7194

Chen Y, Wang T, Rogers KA, Rutt BK, Ronald JA. Close Association of Myeloperoxidase-Producing Activated Microglia with Amyloid Plaques in Hypercholesterolemic Rabbits. J Alzheimers Dis 2019; 67: 1221–1234

Christ A, Günther P, Lauterbach MAR, Duewell P, Biswas D, Pelka K, Scholz CJ, Oosting M, Haendler K, Baßler K, Klee K, Schulte-Schrepping J, Ulas T, Moorlag SJCFM, Kumar V, Park MH, Joosten LAB, Groh LA, Riksen NP, Espevik T, Schlitzer A, Li Y, Fitzgerald ML, Netea MG, Schultze JL, Latz E. Western Diet Triggers NLRP3-Dependent Innate Immune Reprogramming. Cell 2018; 172: 162-175.e14

Christensen K, Doblhammer G, Rau R, Vaupel JW. Ageing populations: the challenges ahead. The Lancet 2009; 374: 1196–1208

Chu H, Mazmanian SK. Innate immune recognition of the microbiota promotes host-microbial symbiosis. Nat Immunol 2013; 14: 668–675

Daneman R, Prat A. The blood-brain barrier. Cold Spring Harb Perspect Biol 2015; 7: a020412

Davalos D, Grutzendler J, Yang G, Kim JV, Zuo Y, Jung S, Littman DR, Dustin ML, Gan W-B. ATP mediates rapid microglial response to local brain injury in vivo. Nat Neurosci 2005; 8: 752–758

David LA, Maurice CF, Carmody RN, Gootenberg DB, Button JE, Wolfe BE, Ling AV, Devlin AS, Varma Y, Fischbach MA, Biddinger SB, Dutton RJ, Turnbaugh PJ. Diet rapidly and reproducibly alters the human gut microbiome. Nature 2014; 505: 559–563

d'Avila JC, Lam TI, Bingham D, Shi J, Won SJ, Kauppinen TM, Massa S, Liu J, Swanson RA. Microglial activation induced by brain trauma is suppressed by post-injury treatment with a PARP inhibitor. J Neuroinflammation 2012; 9: 31

Dethlefsen L, McFall-Ngai M, Relman DA. An ecological and evolutionary perspective on human-microbe mutualism and disease. Nature 2007; 449: 811–818

Dinarello CA. Interleukin-1. Cytokine & Growth Factor Reviews 1997; 8: 253–265

Dinarello CA. Immunological and inflammatory functions of the interleukin-1 family. Annu Rev Immunol 2009; 27: 519–550

Dodiya HB, Frith M, Sidebottom A, Cao Y, Koval J, Chang E, Sisodia SS. Synergistic depletion of gut microbial consortia, but not individual antibiotics, reduces amyloidosis in APPPS1-21 Alzheimer's transgenic mice. Sci Rep 2020; 10: 8183

Dona AC, Jiménez B, Schäfer H, Humpfer E, Spraul M, Lewis MR, Pearce JTM, Holmes E, Lindon JC, Nicholson JK. Precision high-throughput proton NMR spectroscopy of human urine, serum, and plasma for large-scale metabolic phenotyping. Anal Chem 2014; 86: 9887–9894

Elinav E, Strowig T, Kau AL, Henao-Mejia J, Thaiss CA, Booth CJ, Peaper DR, Bertin J, Eisenbarth SC, Gordon JI, Flavell RA. NLRP6 inflammasome regulates colonic microbial ecology and risk for colitis. Cell 2011; 145: 745–757

Ericsson AC, Davis JW, Spollen W, Bivens N, Givan S, Hagan CE, McIntosh M, Franklin CL. Effects of vendor and genetic background on the composition of the fecal microbiota of inbred mice. PLoS One 2015; 10: e0116704

Ericsson AC, Gagliardi J, Bouhan D, Spollen WG, Givan SA, Franklin CL. The influence of caging, bedding, and diet on the composition of the microbiota in different regions of the mouse gut. Sci Rep 2018; 8: 4065

Erion JR, Wosiski-Kuhn M, Dey A, Hao S, Davis CL, Pollock NK, Stranahan AM. Obesity elicits interleukin 1-mediated deficits in hippocampal synaptic plasticity. J Neurosci 2014; 34: 2618–2631

Erwin G. Zoetendal ADLA. The Host Genotype Affects the Bacterial Community in the Human Gastronintestinal Tract. Microbial Ecology in Health and Disease 2001; 13: 129–134

Filippo C de, Cavalieri D, Di Paola M, Ramazzotti M, Poullet JB, Massart S, Collini S, Pieraccini G, Lionetti P. Impact of diet in shaping gut microbiota revealed by a comparative study in children from Europe and rural Africa. Proc Natl Acad Sci U S A 2010; 107: 14691–14696

Fleshner M, Frank M, Maier SF. Danger Signals and Inflammasomes: Stress-Evoked Sterile Inflammation in Mood Disorders. Neuropsychopharmacology 2017; 42: 36–45

Ginhoux F, Greter M, Leboeuf M, Nandi S, See P, Gokhan S, Mehler MF, Conway SJ, Ng LG, Stanley ER, Samokhvalov IM, Merad M. Fate mapping analysis reveals that adult microglia derive from primitive macrophages. Science 2010; 330: 841–845

Goedert M, Spillantini MG. A century of Alzheimer's disease. Science 2006; 314: 777–781

Gong T, Liu L, Jiang W, Zhou R. DAMP-sensing receptors in sterile inflammation and inflammatory diseases. Nat Rev Immunol 2020; 20: 95–112

Goodrich JK, Davenport ER, Beaumont M, Jackson MA, Knight R, Ober C, Spector TD, Bell JT, Clark AG, Ley RE. Genetic Determinants of the Gut Microbiome in UK Twins. Cell Host Microbe 2016; 19: 731–743

Grosheva I, Zheng D, Levy M, Polansky O, Lichtenstein A, Golani O, Dori-Bachash M, Moresi C, Shapiro H, Del Mare-Roumani S, Valdes-Mas R, He Y, Karbi H, Chen M, Harmelin A, Straussman R, Yissachar N, Elinav E, Geiger B. High-Throughput Screen Identifies Host and Microbiota Regulators of Intestinal Barrier Function. Gastroenterology 2020; 159: 1807–1823

Gyoneva S, Davalos D, Biswas D, Swanger SA, Garnier-Amblard E, Loth F, Akassoglou K, Traynelis SF. Systemic inflammation regulates microglial responses to tissue damage in vivo. Glia 2014; 62: 1345–1360

Halle A, Hornung V, Petzold GC, Stewart CR, Monks BG, Reinheckel T, Fitzgerald KA, Latz E, Moore KJ, Golenbock DT. The NALP3 inflammasome is involved in the innate immune response to amyloid-beta. Nat Immunol 2008; 9: 857–865

Hara H, Seregin SS, Yang D, Fukase K, Chamaillard M, Alnemri ES, Inohara N, Chen GY, Núñez G. The NLRP6 Inflammasome Recognizes Lipoteichoic Acid and Regulates Gram-Positive Pathogen Infection. Cell 2018; 175: 1651-1664.e14

Harach T, Marungruang N, Duthilleul N, Cheatham V, Mc Coy KD, Frisoni G, Neher JJ, Fåk F, Jucker M, Lasser T, Bolmont T. Reduction of Abeta amyloid pathology in APPPS1 transgenic mice in the absence of gut microbiota. Sci Rep 2017; 7: 41802

Haviv R, Oz E, Soreq H. The Stress-Responding miR-132-3p Shows Evolutionarily Conserved Pathway Interactions. Cell Mol Neurobiol 2018; 38: 141–153

Henao-Mejia J, Elinav E, Jin C, Hao L, Mehal WZ, Strowig T, Thaiss CA, Kau AL, Eisenbarth SC, Jurczak MJ, Camporez J-P, Shulman GI, Gordon JI, Hoffman HM, Flavell RA. Inflammasome-mediated dysbiosis regulates progression of NAFLD and obesity. Nature 2012; 482: 179–185

Heneka MT, Carson MJ, Khoury JE, Landreth GE, Brosseron F, Feinstein DL, Jacobs AH, Wyss-Coray T, Vitorica J, Ransohoff RM, Herrup K, Frautschy SA, Finsen B, Brown GC, Verkhratsky A, Yamanaka K, Koistinaho J, Latz E, Halle A, Petzold GC, Town T, Morgan D, Shinohara ML, Perry VH, Holmes C, Bazan NG, Brooks DJ, Hunot S, Joseph B, Deigendesch N, Garaschuk O, Boddeke E, Dinarello CA, Breitner JC, Cole GM, Golenbock DT, Kummer MP. Neuroinflammation in Alzheimer's disease. The Lancet Neurology 2015; 14: 388–405

Heneka MT, Kummer MP, Latz E. Innate immune activation in neurodegenerative disease. Nat Rev Immunol 2014; 14: 463–477

Heneka MT, Kummer MP, Stutz A, Delekate A, Schwartz S, Vieira-Saecker A, Griep A, Axt D, Remus A, Tzeng T-C, Gelpi E, Halle A, Korte M, Latz E, Golenbock DT. NLRP3 is activated in Alzheimer's disease and contributes to pathology in APP/PS1 mice. Nature 2013; 493: 674–678

Hernández-Aguilera A, Rull A, Rodríguez-Gallego E, Riera-Borrull M, Luciano-Mateo F, Camps J, Menéndez JA, Joven J. Mitochondrial dysfunction: a basic mechanism in

inflammation-related non-communicable diseases and therapeutic opportunities. Mediators Inflamm 2013; 2013: 135698

Hickman SE, Kingery ND, Ohsumi TK, Borowsky ML, Wang L, Means TK, El Khoury J. The microglial sensome revealed by direct RNA sequencing. Nat Neurosci 2013; 16: 1896–1905

Hsiao EY, McBride SW, Hsien S, Sharon G, Hyde ER, McCue T, Codelli JA, Chow J, Reisman SE, Petrosino JF, Patterson PH, Mazmanian SK. Microbiota modulate behavioral and physiological abnormalities associated with neurodevelopmental disorders. Cell 2013; 155: 1451–1463

Hu B, Elinav E, Huber S, Strowig T, Hao L, Hafemann A, Jin C, Wunderlich C, Wunderlich T, Eisenbarth SC, Flavell RA. Microbiota-induced activation of epithelial IL-6 signaling links inflammasome-driven inflammation with transmissible cancer. Proc Natl Acad Sci U S A 2013; 110: 9862–9867

Hughes V. Microglia: The constant gardeners. Nature 2012; 485: 570–572

Jain V, Langham MC, Wehrli FW. MRI estimation of global brain oxygen consumption rate. J Cereb Blood Flow Metab 2010; 30: 1598–1607

Jakubzick CV, Randolph GJ, Henson PM. Monocyte differentiation and antigen-presenting functions. Nat Rev Immunol 2017; 17: 349–362

Janeway CA. Approaching the asymptote? Evolution and revolution in immunology. Cold Spring Harb Symp Quant Biol 1989; 54 Pt 1: 1–13

Jankowsky JL, Slunt HH, Ratovitski T, Jenkins NA, Copeland NG, Borchelt DR. Co-expression of multiple transgenes in mouse CNS: a comparison of strategies. Biomolecular Engineering 2001; 17: 157–165

Jarosz-Griffiths HH, Noble E, Rushworth JV, Hooper NM. Amyloid-β Receptors: The Good, the Bad, and the Prion Protein. J Biol Chem 2016; 291: 3174–3183

Joshi AU, Mochly-Rosen D. Mortal engines: Mitochondrial bioenergetics and dysfunction in neurodegenerative diseases. Pharmacol Res 2018; 138: 2–15

Kayagaki N, Warming S, Lamkanfi M, Vande Walle L, Louie S, Dong J, Newton K, Qu Y, Liu J, Heldens S, Zhang J, Lee WP, Roose-Girma M, Dixit VM. Non-canonical inflammasome activation targets caspase-11. Nature 2011; 479: 117–121

Kim S, Kwon S-H, Kam T-I, Panicker N, Karuppagounder SS, Lee S, Lee JH, Kim WR, Kook M, Foss CA, Shen C, Lee H, Kulkarni S, Pasricha PJ, Lee G, Pomper MG, Dawson VL, Dawson TM, Ko HS. Transneuronal Propagation of Pathologic α-Synuclein from the Gut to the Brain Models Parkinson's Disease. Neuron 2019; 103: 627-641.e7

Koch L. Metagenomics: Shaping the gut microbiome. Nat Rev Genet 2015; 16: 2

Kozik AJ, Nakatsu CH, Chun H, Jones-Hall YL. Age, sex, and TNF associated differences in the gut microbiota of mice and their impact on acute TNBS colitis. Exp Mol Pathol 2017; 103: 311–319

Kreutzberg GW. Microglia, the first line of defence in brain pathologies. Arzneimittelforschung 1995; 45: 357–360

Kumar S, Karthikeyan N, Mishra S, Padmanabhan P, Radda G, Gulyás B. Misfolded Protein Linked Strategies Toward Biomarker Development for Neurodegenerative Diseases. Mol Neurobiol 2019; 56: 2559–2578

Kurilshikov A, Medina-Gomez C, Bacigalupe R, Radjabzadeh D, Wang J, Demirkan A et al. Large-scale association analyses identify host factors influencing human gut microbiome composition. Nat Genet 2021; 53: 156–165

Lechtenberg BC, Mace PD, Riedl SJ. Structural mechanisms in NLR inflammasome signaling. Curr Opin Struct Biol 2014; 29: 17–25

Leng F, Yin H, Qin S, Zhang K, Guan Y, Fang R, Wang H, Li G, Jiang Z, Sun F, Wang D-C, Xie C. NLRP6 self-assembles into a linear molecular platform following LPS binding and ATP stimulation. Sci Rep 2020; 10: 198

Levy M, Thaiss CA, Zeevi D, Dohnalová L, Zilberman-Schapira G, Mahdi JA, David E, Savidor A, Korem T, Herzig Y, Pevsner-Fischer M, Shapiro H, Christ A, Harmelin A, Halpern Z, Latz E, Flavell RA, Amit I, Segal E, Elinav E. Microbiota-Modulated

Metabolites Shape the Intestinal Microenvironment by Regulating NLRP6 Inflammasome Signaling. Cell 2015; 163: 1428–1443

Liston A, Masters SL. Homeostasis-altering molecular processes as mechanisms of inflammasome activation. Nat Rev Immunol 2017; 17: 208–214

Lu WL, Zhang L, Song DZ, Yi XW, Xu WZ, Ye L, Huang DM. NLRP6 suppresses the inflammatory response of human periodontal ligament cells by inhibiting NF-κB and ERK signal pathways. Int Endod J 2019; 52: 999–1009

Lucin KM, O'Brien CE, Bieri G, Czirr E, Mosher KI, Abbey RJ, Mastroeni DF, Rogers J, Spencer B, Masliah E, Wyss-Coray T. Microglial beclin 1 regulates retromer trafficking and phagocytosis and is impaired in Alzheimer's disease. Neuron 2013; 79: 873–886

MacIntyre A, Abramov R, Hammond CJ, Hudson AP, Arking EJ, Little CS, Appelt DM, Balin BJ. Chlamydia pneumoniae infection promotes the transmigration of monocytes through human brain endothelial cells. J Neurosci Res 2003; 71: 740–750

Man SM, Karki R, Kanneganti T-D. Molecular mechanisms and functions of pyroptosis, inflammatory caspases and inflammasomes in infectious diseases. Immunol Rev 2017; 277: 61–75

Medzhitov R. Recognition of microorganisms and activation of the immune response. Nature 2007; 449: 819–826

Medzhitov R. Origin and physiological roles of inflammation. Nature 2008; 454: 428–435

Mélik-Parsadaniantz S, Rostène W. Chemokines and neuromodulation. J Neuroimmunol 2008; 198: 62–68

Meng C, Zhang J, Zhang L, Wang Y, Li Z, Zhao J. Effects of NLRP6 in Cerebral Ischemia/Reperfusion (I/R) Injury in Rats. J Mol Neurosci 2019; 69: 411–418

Méthot P-O, Alizon S. What is a pathogen? Toward a process view of host-parasite interactions. Virulence 2014; 5: 775–785

Meydan C, Bekenstein U, Soreq H. Molecular Regulatory Pathways Link Sepsis With Metabolic Syndrome: Non-coding RNA Elements Underlying the Sepsis/Metabolic Cross-Talk. Front Mol Neurosci 2018; 11: 189

Mollica MP, Lionetti L, Putti R, Cavaliere G, Gaita M, Barletta A. From chronic overfeeding to hepatic injury: role of endoplasmic reticulum stress and inflammation. Nutr Metab Cardiovasc Dis 2011; 21: 222–230

Montonye DR, Ericsson AC, Busi SB, Lutz C, Wardwell K, Franklin CL. Acclimation and Institutionalization of the Mouse Microbiota Following Transportation. Front Microbiol 2018; 9: 1085

Morales R, Moreno-Gonzalez I, Soto C. Cross-seeding of misfolded proteins: implications for etiology and pathogenesis of protein misfolding diseases. PLoS Pathog 2013; 9: e1003537

Morgan M, Much C, DiGiacomo M, Azzi C, Ivanova I, Vitsios DM, Pistolic J, Collier P, Moreira PN, Benes V, Enright AJ, O'Carroll D. mRNA 3' uridylation and poly(A) tail length sculpt the mammalian maternal transcriptome. Nature 2017; 548: 347–351

Nagpal R, Tsuji H, Takahashi T, Nomoto K, Kawashima K, Nagata S, Yamashiro Y. Gut dysbiosis following C-section instigates higher colonisation of toxigenic Clostridium perfringens in infants. Benef Microbes 2017; 8: 353–365

Netea MG, Balkwill F, Chonchol M, Cominelli F, Donath MY, Giamarellos-Bourboulis EJ, Golenbock D, Gresnigt MS, Heneka MT, Hoffman HM, Hotchkiss R, Joosten LAB, Kastner DL, Korte M, Latz E, Libby P, Mandrup-Poulsen T, Mantovani A, Mills KHG, Nowak KL, O'Neill LA, Pickkers P, van der Poll T, Ridker PM, Schalkwijk J, Schwartz DA, Siegmund B, Steer CJ, Tilg H, van der Meer JWM, van de Veerdonk FL, Dinarello CA. A guiding map for inflammation. Nat Immunol 2017; 18: 826–831

Neufeld K-AM, Kang N, Bienenstock J, Foster JA. Effects of intestinal microbiota on anxiety-like behavior. Commun Integr Biol 2011; 4: 492–494

Newton K, Dixit VM. Signaling in innate immunity and inflammation. Cold Spring Harb Perspect Biol 2012; 4

Nie H, Hu Y, Guo W, Wang W, Yang Q, Dong Q, Tang Y, Li Q, Tang Z. miR-331-3p Inhibits Inflammatory Response after Intracerebral Hemorrhage by Directly Targeting NLRP6. Biomed Res Int 2020; 2020: 6182464

Normand S, Delanoye-Crespin A, Bressenot A, Huot L, Grandjean T, Peyrin-Biroulet L, Lemoine Y, Hot D, Chamaillard M. Nod-like receptor pyrin domain-containing protein 6 (NLRP6) controls epithelial self-renewal and colorectal carcinogenesis upon injury. Proc Natl Acad Sci U S A 2011; 108: 9601–9606

Palop JJ, Chin J, Roberson ED, Wang J, Thwin MT, Bien-Ly N, Yoo J, Ho KO, Yu G-Q, Kreitzer A, Finkbeiner S, Noebels JL, Mucke L. Aberrant excitatory neuronal activity and compensatory remodeling of inhibitory hippocampal circuits in mouse models of Alzheimer's disease. Neuron 2007; 55: 697–711

Paludan SR, Pradeu T, Masters SL, Mogensen TH. Constitutive immune mechanisms: mediators of host defence and immune regulation. Nat Rev Immunol 2021; 21: 137–150

Parkhurst CN, Yang G, Ninan I, Savas JN, Yates JR, Lafaille JJ, Hempstead BL, Littman DR, Gan W-B. Microglia promote learning-dependent synapse formation through brain-derived neurotrophic factor. Cell 2013; 155: 1596–1609

Peterson LW, Artis D. Intestinal epithelial cells: regulators of barrier function and immune homeostasis. Nat Rev Immunol 2014; 14: 141–153

Pradeu T. Philosophy of Immunology 2020

Qin L, Wu X, Block ML, Liu Y, Breese GR, Hong J-S, Knapp DJ, Crews FT. Systemic LPS causes chronic neuroinflammation and progressive neurodegeneration. Glia 2007; 55: 453–462

Rivest S. Regulation of innate immune responses in the brain. Nat Rev Immunol 2009; 9: 429–439

Rosenblum MD, Remedios KA, Abbas AK. Mechanisms of human autoimmunity. J Clin Invest 2015; 125: 2228–2233

Rubio-Perez JM, Morillas-Ruiz JM. A review: inflammatory process in Alzheimer's disease, role of cytokines. ScientificWorldJournal 2012; 2012: 756357

Schett G, Neurath MF. Resolution of chronic inflammatory disease: universal and tissue-specific concepts. Nat Commun 2018; 9: 3261

Schmidt M, Rohou A, Lasker K, Yadav JK, Schiene-Fischer C, Fändrich M, Grigorieff N. Peptide dimer structure in an Aβ(1-42) fibril visualized with cryo-EM. Proc Natl Acad Sci U S A 2015; 112: 11858–11863

Selkoe DJ, Hardy J. The amyloid hypothesis of Alzheimer's disease at 25 years. EMBO Mol Med 2016; 8: 595–608

Seregin SS, Golovchenko N, Schaf B, Chen J, Pudlo NA, Mitchell J, Baxter NT, Zhao L, Schloss PD, Martens EC, Eaton KA, Chen GY. NLRP6 Protects Il10-/- Mice from Colitis by Limiting Colonization of Akkermansia muciniphila. Cell Rep 2017; 19: 733–745

Shen C, Lu A, Xie WJ, Ruan J, Negro R, Egelman EH, Fu T-M, Wu H. Molecular mechanism for NLRP6 inflammasome assembly and activation. Proc Natl Acad Sci U S A 2019; 116: 2052–2057

Shue EH, Carson-Walter EB, Liu Y, Winans BN, Ali ZS, Chen J, Walter KA. Plasmalemmal vesicle associated protein-1 (PV-1) is a marker of blood-brain barrier disruption in rodent models. BMC Neurosci 2008; 9: 29

Sims R, van der Lee SJ, Naj AC, Bellenguez C, Badarinarayan N, Jakobsdottir J et al. Rare coding variants in PLCG2, ABI3, and TREM2 implicate microglial-mediated innate immunity in Alzheimer's disease. Nat Genet 2017; 49: 1373–1384

Spadoni I, Fornasa G, Rescigno M. Organ-specific protection mediated by cooperation between vascular and epithelial barriers. Nat Rev Immunol 2017; 17: 761–773

Sveinbjornsdottir S. The clinical symptoms of Parkinson's disease. J Neurochem 2016; 139 Suppl 1: 318–324

Takeuchi O, Akira S. Pattern recognition receptors and inflammation. Cell 2010; 140: 805–820

The Tabula Muris Consortium., Overall coordination., Logistical coordination. et al. Single-cell transcriptomics of 20 mouse organs creates a Tabula Muris. Nature 2018; 562: 367–372

Tremblay M-È, Lowery RL, Majewska AK. Microglial interactions with synapses are modulated by visual experience. PLoS Biol 2010; 8: e1000527

Tung J, Barreiro LB, Burns MB, Grenier J-C, Lynch J, Grieneisen LE, Altmann J, Alberts SC, Blekhman R, Archie EA. Social networks predict gut microbiome composition in wild baboons. Elife 2015; 4

Turnbaugh PJ, Hamady M, Yatsunenko T, Cantarel BL, Duncan A, Ley RE, Sogin ML, Jones WJ, Roe BA, Affourtit JP, Egholm M, Henrissat B, Heath AC, Knight R, Gordon JI. A core gut microbiome in obese and lean twins. Nature 2009; 457: 480–484

Venegas C, Kumar S, Franklin BS, Dierkes T, Brinkschulte R, Tejera D, Vieira-Saecker A, Schwartz S, Santarelli F, Kummer MP, Griep A, Gelpi E, Beilharz M, Riedel D, Golenbock DT, Geyer M, Walter J, Latz E, Heneka MT. Microglia-derived ASC specks cross-seed amyloid-β in Alzheimer's disease. Nature 2017; 552: 355–361

Walker KA, Walston J, Gottesman RF, Kucharska-Newton A, Palta P, Windham BG. Midlife Systemic Inflammation Is Associated With Frailty in Later Life: The ARIC Study. J Gerontol A Biol Sci Med Sci 2019; 74: 343–349

Wang P, Zhu S, Yang L, Cui S, Pan W, Jackson R, Zheng Y, Rongvaux A, Sun Q, Yang G, Gao S, Lin R, You F, Flavell R, Fikrig E. Nlrp6 regulates intestinal antiviral innate immunity. Science 2015; 350: 826–830

Widmann CN, Heneka MT. Long-term cerebral consequences of sepsis. The Lancet Neurology 2014; 13: 630–636

Willyard C. How gut microbes could drive brain disorders. Nature 2021; 590: 22–25

Wlodarska M, Thaiss CA, Nowarski R, Henao-Mejia J, Zhang J-P, Brown EM, Frankel G, Levy M, Katz MN, Philbrick WM, Elinav E, Finlay BB, Flavell RA. NLRP6 inflammasome orchestrates the colonic host-microbial interface by regulating goblet cell mucus secretion. Cell 2014; 156: 1045–1059

Yang J, Zhao Y, Shao F. Non-canonical activation of inflammatory caspases by cytosolic LPS in innate immunity. Curr Opin Immunol 2015; 32: 78–83

Zhang J, Jiang N, Zhang L, Meng C, Zhao J, Wu J. NLRP6 expressed in astrocytes aggravates neurons injury after OGD/R through activating the inflammasome and inducing pyroptosis. Int Immunopharmacol 2020; 80: 106183

Zhao K, Hu Y. Microbiome harbored within tumors: a new chance to revisit our understanding of cancer pathogenesis and treatment. Signal Transduct Target Ther 2020; 5: 136

Zheng D, Kern L, Elinav E. The NLRP6 inflammasome. Immunology 2021; 162: 281–289

8 Acknowledgements

My time as a PhD student has come to an end. At this point I would like to thank Prof. Dr. Eicke Latz for his trust, patience and guidance during my PhD at the institute of Innate Immunity in Bonn, Germany. Eicke created a great work environment with fantastic people and endless opportunities. I am truly grateful to have him as my “Doktorvater” at work and beyond.

My PhD journey in Bonn started by applying to Prof. Dr. Michael T. Heneka and his department for Neuroimmunology. Thank you very much for accepting me as a PhD student and assigning me to this joint collaboration project with Prof. Dr. Eicke Latz and Prof. Dr. Eran Elinav. I am just as grateful for Prof. Dr. Michael T. Henekas supervision and support on numerous projects.

Prof. Dr. Eran Elinav and Dr. Timur Liwinski at the Weizmann Institute of Science, Israel, were resourceful collaborators and true experts in exploring interactions between mammalian hosts, their intestinal microbiota, the immune system and their effects on health and disease.

Also, I would like to thank Prof. Dr. Matthias Geyer and Prof. Dr. Michael Pankratz for agreeing to evaluate my research project, for their time and consideration.

It takes a village to raise a PhD student. I wouldn’t be where I am without the support of numerous exceptional colleagues. This animal-based study relied on the help of our mouse expert Maximilian Rothe, the bio-informatic expertise of Dr. Susanne Schmidt and hands on support of Miki Uchima. Also, the scientific guidance and help by Dr. Roisin McManus played a significant role in securing a successful PhD thesis. I would also like to mention and thank Dr. Tomasz Prochnicki, Dr. Pia Langhoff, Dr. Matthew Mangan, Angelika Griep, Stephanie Schwartz, Dr. Jan Niklas Hansen, Olivia van Ray, Dr. Anette Christ, Dr. Peter Düwell and Dr. Mario Lauterbach for being part of this study in one way or the other. To my office family: thank you for being my safe haven at work.

I couldn’t be more grateful for having the best dad, Prof. Dr. Stephan Clemens, with his scientific expertise and patience when it comes to supporting me. Further, I would like to thank Prof. Dr. Martin Korte for accompanying my scientific career with constant advice and help.

Last but definitely not least, I would like to thank my family and Sophia Tietjen for their endless love and encouraging support.